THE PHOTOLYSIS AND MASS SPECTROMETRY OF METHYL IODIDE, TRIFLUOROMETHYL IODIDE AND EQUIMOLAR MIXTURES OF METHYL IODIDE-TRIFLUOROMETHYL IODIDE IN THE GAS PHASE

BY

DAWIT TECLEMARIAM

A DISSERTATION PRESENTED TO THE GRADUATE COUNCIL OF
THE UNIVERSITY OF FLORIDA
IN PARTIAL FULFILLMENT OF THE REQUIREMENTS FOR THE
DEGREE OF DOCTOR OF PHILOSOPHY

UNIVERSITY OF FLORIDA

1984

Dedicated to

the memory of

Enatye Leteyesus Woldu Negassi

ACKNOWLEDGMENTS

The author expresses his sincere appreciation to Dr. R. J. Hanrahan for his uninterrupted encouragement, guidance, and patience throughout this work. Again, he thanks Dr. R. J. Hanrahan for help beyond his duty in the successful emigration of his family from the Sudan to the U.S.A. Equally he is thankful to M. L. Muga.

The author also thanks T. J. Buckley for the ICR work concerning the gas phase ion chemistry of the compounds used in this work. Also special thanks are extended to Dr. J. R. Eyler for providing access to the ICR instrument.

I greatly appreciate the friendship of F. K. St. Charles, Jorge E. Ramirez, Bob Doyle, A. Gupta, and R. K. Bera on and off this work.

Special thanks are given to Mr. Kallman, President of Kallman Publishing Company, for his friendship and kindness.

Above all, the author expresses his deepest love and gratitude to his wife, Mikela whose understanding and patience made this work possible. Also, special thanks are forewarded to their kids, Eden, Eri, Lula, and Yobial.

Thanks are extended to Frank Ramos for making many of the drawings in the text. Last but not least the author

forwards his deepest thanks to his sister, Abeba Teclemariam, his aunt, the late Lete Yesus Woldu and the late inspector Kidane Kifle, the late Dejazmatch Fessehaye Tesfamicael who helped him morally and finacially to finish his elementary, high school and undergraduate education.

The author also expresses his love and gratitude to his mother, Zigay Negusse(who stays in Ethiopia) and to all his brothers, Paulos, Foto, and Aeregai and his niece Letekidan who reside in the U.S.A. as well as those back home in Eritrea, Ethiopia.

TABLE OF CONTENTS

Page

ACKNOWLEDGMENTS.................................. iii

LIST OF TABLES................................... viii

LIST OF FIGURES.................................. ix

ABSTRACT... xiii

CHAPTER

I. INTRODUCTION................................... 1

- A. Foreward..................................... 1
- B. Review of Previous Work...................... 2
  - 1. Trifluoromethyl Iodide.................. 2
  - 2. Methyl Iodide........................... 5

II. EXPERIMENTAL PROCEDURES AND APPARATUS.......... 12

- A. Reagents and their Purification.............. 12
  - 1. Methyl Iodide........................... 12
  - 2. Trifluoromethyl Iodide.................. 12
  - 3. Hydrogen Iodide......................... 13
  - 4. Oxygen.................................. 14
  - 5. Chromatographic Calibration Standards.. 16

- B. Sample Preparation........................... 16
  - 1. Vacuum System........................... 16
  - 2. Treatment for Cleaning Photolysis Vessels.................................. 18
  - 3. Metering and Filling the Photolysis Vessels.................................. 18
  - 4. Experiments with Added Oxygen........... 19

- C. Sample Photolysis............................ 20
  - 1. Photolysis Lamp and Vessels............. 21
  - 2. Actinometry............................. 22

- D. Analytical Equipment and Product Analysis.. 26
  - 1. Gas Chromatograph Instrument............ 26
    - a. Product Non-Condensible at $-196^{\circ}C$.. 27
    - b. Product Condensible at $-196^{\circ}C$...... 27
  - 2. Gas Chromatograph-mass Spectrometer-Computer System....................... 28

Page

3. Spectrophotometer and Chemical Analysis of Iodine.............................. 29
4. Hydrogen Fluoride and Hydrogen Iodide Analysis.............................. 30
5. Equipment for Ion-Molecule Investigation.............................. 33
    a. High Pressure Mass Spectrometery... 33
    b. Ion Cyclotron Resonance Mass Spectrometry....................... 33

III. THE PHOTOLYSIS OF METHYL IODIDE IN THE GAS PHASE.............................. 45

A. Experimental Results...................... 45
B. Discussion.............................. 52
C. Summary.............................. 64

IV. THE PHOTOLYSIS OF TRIFLUOROMETHYL IODIDE IN THE GAS PHASE.............................. 66

A. Experimental Results...................... 66
B. Discussion.............................. 72
C. Summary.............................. 79

V. THE GAS PHASE PHOTOLYSIS OF EQUIMOLAR MIXTURES OF METHYL IODIDE-TRIFUOROMETHYL IODIDE......... 81

A. Experimental Results...................... 81
B. Discussion.............................. 93
C. Summary.............................. 104

VI. ION-MOLECULE REACTIONS IN THE SYSTEMS OF METHYL IODIDE, TRIFLUOROMETHYL IODIDE AND EQUIMOLAR MIXTURES OF METHYL-TRIFLUOROMETHYL IODIDE......... 106

A. INTRODUCTION.............................. 106

B. CH_3I System.............................. 107

1. Experimental Results.................... 107
2. Discussion.............................. 111

C. CF_3I System.............................. 121

1. Experimental Results.................... 121
2. Discussion.............................. 124

Page

D. CH_3I-CF_3I System.......................... 136

1. Experimental Results...................... 136
2. Time-of-Flight Results.................. 146
3. Discussion.............................. 162

E. Summary..................................... 167

APPENDIX I. IDENTIFICATION OF PHOTOLYSIS PRODUCTS... 169

APPENDIX II. IONIZATION POTENTIALS.................. 176

REFERENCES... 178

BIOGRAPHICAL SKETCH................................ 187

LIST OF TABLES

Table | Page
1. Quantum yields of products in CH_3I photolysis system.. 51
2. Photolysis mechanism in the CH_3I system......... 53
3. Quantum yields of products in CF_3I photolysis... 71
4. Photolysis mechanism in the CF_3I system......... 73
5. Quantum yields of photolysis products from methyl iodide-trifluoromethyl iodide equimolar mixtures at 50 torr total pressure.............. 92
6. Photolysis mechanism in the CH_3I-CF_3I system.... 94
7. Experimental rate constants and ion-molecule reactions in the CH_3I system.................... 108
8. Experimental rate constants and ion-molecule reactions in CF_3I system....................... 122
9. Experimental rate constants and ion-molecule reactions in the equimolar CH_3I-CF_3I system..... 147
10 Rate constants in the equimolar CH_3I-CF_3I system using the Time-of-Flight instrument............. 148
11. Ionization potentials.......................... 177

LIST OF FIGURES

Figure	Page
1. Photolysis vacuum system........................	15
2. Photolysis vessel..............................	17
3. Photolysis lamp................................	23
4. Gas sampling loops.............................	25
5. Potentiometric titration curve of hydrogen fluoride.......................................	31
6. Potentiometric titration curve of hydrogen iodide...	32
7. Schematic of Bendix high pressure ion-molecule studies..	34
8. Basic diagram of the Ion Cyclotron Resonance cell...	39
9. Production of HI and I_2 as a function of photolysis time...................................	46
10. Production of CH_2I_2 and C_4H_8 as a function of photolysis time..............................	47
11. Production of C_2H_4 and CH_4 as a function of photolysis time..............................	48
12. Production of C_2H_6 and n-C_4H_{10} as a function of photolysis time..............................	49
13. Production of n-C_5H_{12} and C_3H_6 as a function of photolysis time..............................	50
14. Production of iodine as a function of photolysis time...	67
15. Production of C_2F_6 and C_2F_4 as a function of photolysis time..............................	68
16. Production of CF_2I_2 and C_3F_8 as a function of photolysis time..............................	69
17. Production of $C_2F_4I_2$ as a function of photolysis time...................................	70

Page

18. Production of HI and I_2 as a function of photolysis time.............................. 83

19. Production of CH_2I_2 and C_2F_6 as a function of photolysis time.............................. 84

20. Production of CH_2I_2 as a function of photolysis time.............................. 85

21. Production of C_2F_6 as a function of photolysis time.............................. 86

22. Production of CH_4 and C_2H_6 as a function of photolysis time.............................. 87

23. production of C_2H_6 and CH_4 as a function of photolysis time.............................. 88

24. Production of C_2H_4, CF_3H, and 1,1,1-CF_3CH_3 as a function of photolysis time.................... 89

25. Production of CF_3H, 1,1,1-CF_3CH_3, and C_2H_4 as a function of photolysis time.................... 90

26. Production of HF, 1,1-CF_2CH_2, and C_2H_5I as a function of photolysis time.................... 91

27. Mass spectrum of I^+, CH_2I^+ and CH_3I^+ at a pressure of $1.8x10^{-6}$ torr...................... 114

28. Mass spectrum of pure CH_3I at $3.8x10^{-6}$ torr generated by electron impact with 70 eV electrons.............................. 115

29. Ion decay signal showing reaction of CH_3I^+ in pure CH_3I at a pressure of 8.8x10-6 torr..... 116

30. Ion decay signal showing reaction of $(CH_3)_2I^+$ in pure CH_3I at a pressure of $2.7x10^{-5}$ torr..... 117

31. Ion decay signal showing $CH_3I_2^+$ ions in pure CH_3I at $2.8x10^{-5}$torr generated by 5 ms electron impact of 70 eV electrons.............................. 118

32. Mass spectrum of pure CF_3I at a pressure of $1.5x10^{-5}$ torr.............................. 128

33. Ion decay signal showing reaction of CF_3I^+ ions in pure CF_3I at a pressure of $4.8x10^{-6}$torr..... 129

Page

34. Ion decay signal showing reaction of CF_3^+ in pure CF_3I at a pressure of $2.0x10^{-6}$ torr............ 130

35. Ion decay signal showing reaction of $(CF_3)_2I_2^+$ ions in pure CF_3I at a pressure of $1.4x10^{-5}$ torr...................................... 131

36. Ion decay signal showing reaction of $CF_3I_2^+$ ions in pure CF_3I at a pressure of $5.5x10^{-5}$ torr..... 132

37. Ion decay signal showing reaction of I_2^+ ions in pure CF_3I at a pressure of $9.2x10^{-6}$ torr........ 133

38. A mass spectrum of an equimolar mixture of CH_3I and CF_3I at a total pressure of $1.1x10^{-5}$ torr... 137

39. Ion decay signal showing reaction of pure CF_3I^+ (theplus sign) and in the equimolar mixture of CF_3I and CH_3I (the square signs)............... 138

40. Mass spectrum of CHICF+ and CF_2I^+ of the equimolar mixture of CH_3I and CF_3I.......... 139

41. Ion decay signal showing reaction of I^+ in the equimolar mixtures of CH_3I and CF_3I............ 140

42. Ion decay signal showing reaction of CH_3^+ in the equimolar mixture of CH_3I and CF_3I......... 141

43. Ion decay signal showing reaction of CF_2I^+ in an equimolar mixture of CH_3I and CF_3I......... 142

44. Normalized ion intensities as a function of delay time in the T.O.F. mass spectrometry of 1:1 mixture of CF_3I and CH_3I at 25°C........................ 149

45. Normalized ion intensities as a function of pressure in the T.O.F. mass spectrometry of a 1:1 mixtrue of CF_3I and CH_3I at 25°C........... 150

46. Normalized ion intensities as a function of pressure in the T.O.F. mass-spectrometry of a 1:1 mixtureof CF_3I and CH_3I at 25°C............... 151

47. Normalized ion intensities as a function of pressure in the T.O.F. mass spectrometry of a 1:1 mixture of CF_3I and CH_3I at 25°C................ 152

Page

48. Normalized ion intensities as a function of pressure in the T.O.F. mass-spectrometry of a 1:1 mixture of CF_3I and CH_3I at 25°C.............. 153

49. Normalizedion intensities as a function of pressure in the T.O.F. mass spectrometry of a 1:1 mixture of CF_3I and CH_3I at 25°C............... 154

50. Normalizedion intensities as a function of pressure in the T.O.F. mass spectrometry of a 1:1 mixture of CF_3I and CH_3I at 25°C............... 155

51. Normalizedion intensities as a function of pressure in the T.O.F. mass spectrometry of a 1:1 mixture of CF_3I at 25°C....................... 156

52. Normalizedion intensities as a function of pressure in the T.O.F. mass spectrometry of a 1:1 mixture of CF_3I and CH_3I at 25°C............... 157

53. Gas chromatogram of photolized CH_3I in the gas phase... 171

54. Gas chromatogram of photolized CF_3I in the gas phase... 173

55. Gas chromatogram of photolized CF_3I-CH_3I equimolar mixture in the gas phase.................. 175

Abstract of Dissertation Presented to the Graduate Council
of the University of Florida in Partial Fulfillment of the
Requirements for the Degree of Doctor of Philosophy

THE PHOTOLYSIS AND MASS SPECTROMETRY OF METHYL IODIDE, TRIFLUOROMETHYL IODIDE AND EQUIMOLAR MIXTURE OF METHYL IODIDE-TRIFLUOROMETHYL IODIDE

By

Dawit Teclemariam

April 1984

Chairman: Dr. Robert J. Hanrahan
Major Department: Chemistry

The gas phase ion chemistry of pure CH_3I and pure CF_3I was investigated using a Varian ICR Mass Spectrometer to study reaction channels and rate constants. Also, the ion-molecule reactions in the equimolar mixture of CH_3I-CF_3I were investigated using a Bendix TOF Mass Spectrometer as well as the ICR instrument. Several ion-molecule reactions were observed for fragment ions in the three systems. In the CF_3I system heavy ions were observed as a result of condensation reactions of the primary ions, CF_3I^+, I^+, and CF_3^+. The prominent product ions were $(CF_3)_2I^+$, $CF_3I_2^+$ and $(CF_3I)_2^+$.

In the pure CH_3I system, the condensation ion products $(CH_3)_2I^+$, $CH_3I_2{}^+$, and $(CH_3I)_2{}^+$ were detected. The ion-molecule chemistry in the CH_3I-CF_3I system was different from the pure systems for the reason that cross product ions were found such as $CH_3ICF_3{}^+$, $CH_2ICF_2{}^+$, $CH_3I_2CF_3{}^+$. These species were observed in the TOF instrument.

In the gas phase photolysis of pure CH_3I, eleven products were identified. These products and their respective quantum yields are CH_2I_2, 0.007; C_2H_6, 0.0039; I_2, 0.0032; CH_4, 0.0028; HI, 0.0017; C_4H_8, 3.4×10^{-4}; n-C_5H_{12}, 1.3×10^{-4}; C_3H_6, 8.1×10^{-6}; C_2H_4, 3.8×10^{-6}; i-C_5H_{12}, 1.8×10^{-6} and n-C_4H_{10}, 1.0×10^{-6}. In the presence of 10% added oxygen the quantum yield of I_2 was enhanced while other products yields decreased by more then 50%.

The gas phase photolysis of CF_3I was carried out at 35 torr pressure both pure and with 10% added oxygen. The identified products and their quantum yields are I_2, 0.021; C_2F_6, 0.0142; C_3F_8, 2.1×10^{-4}; C_2F_4, 1.1×10^{-4}; CF_2I_2, 4.0×10^{-5}; $C_2F_4I_2$, 3.5×10^{-5} and CF_4, 2.5×10^{-5}. The quantum yield of I_2 in the presence of 10% added O_2 was enhanced.

The gas phase photolysis of the equimolar mixture was studied at 50 torr total pressure both pure and with added oxygen. Thirteen products were identified and are as follows with their respective quantum yields: CH_2I_2, 0.0087; I_2, 0.0026; CH_4, 0.0022; 1,1-CH_2CF_2, 0.0022; C_2H_6,

0.0021; C_2F_6, 0.0018; CF_3H, 0.0011; HF, 2.7×10^{-4}; C_2H_4, 2.2×10^{-4}; C_2F_5I, 1.9×10^{-4}; 1,1,1-CH_3CF_3, 4.7×10^{-5}; CF_4, 2.1×10^{-5} and HI, 1.8×10^{-5}. Scavenging by the addition of oxygen enhanced quantum yield of I_2, while other product yields were decreased drastically with some yields being eliminated.

CHAPTER I
INTRODUCTION

A. Foreword

Investigations of the gas phase photolysis of methyl iodide, trifluoromethyl iodide and equimolar methyl iodide-trifluoromethyl iodide mixtures were undertaken to study the primary and secondary processes leading to decomposition of these compounds. In addition to the photolysis study, high pressure and ion cyclotron resonance mass spectrometry was carried out to study the ion-molecule chemistry in the equimolar mixtures as well as in the pure systems. In all of the photolysis cases oxygen was added as a scavenger to determine which species will decrease or increase or be eliminated from the products in the unscavenged system. An additional goal of this investigation was to compare the photochemistry of methyl iodide, trifluoromethyl iodide and their equimolar mixtures with that of other methyl halides since there are some studies on the chloride and bromide systems. This work was also undertaken for purpose of comparison with radiolysis (1, 2, 3, 4) and ion-molecule reaction studies (5, 6, 7, 8) of pure methyl iodide, trifluoromethyl iodide and other hydrocarbon analogs which were done in this laboratory and other laboratories. The study of the photodissociation of small halogenated polyatomic molecules is also important for practical and fundamental reasons. Knowledge of the dissociation products is necessary to give useful information in such diverse applications as atmospheric photochemistry and chemical lasers development. The interest in the laser area was initiated by the production of iodine atom laser action from photodissociation of methyl iodide and trifluoromethyl iodide (9, 10, 11, 12,13).

Although the photolysis of gaseous methyl iodide and trifluoromethyl iodide has been investigated in other laboratories, the earlier workers were looking for one or two photolysis products. No previous work has been reported on the photolysis or ion-molecule reaction chemistry of this mixture.

B. Review of Previous Work

1. Trifluoromethyl Iodide

About three decades ago, Dacey (14) studied the gas phase photolysis of trifluoromethyl iodide using a 253.7 nm mercury resonance lamp. At low pressure (above one torr) only hexafluoroethane (C_2F_6) and iodine molecules were formed, both with low quantum yields. However, at pressures above 10 torr, small amounts of polymer derived from C_2F_4 were also present. More recently, Skorobogatov and Simirnov (11) made mass spectrometric analyses of the volatile product residues after the pulsing of CF_3I and C_3F_7I lasers. From the result of these analyses, Skorobogatov and Simirnov concluded that, in the CF_3I system, the electronically excited $I\cdot(^2P_{1/2})$ atoms promote the conversion of CF_3I into CF_4.

The near ultraviolet absorption of CF_3I is continuous with a maximum at 265 nm in the region 248 nm to 281.5 nm (15). The photolysis of CF_3I in the near ultraviolet is represented by two primary processes.

$$CF_3I \dashrightarrow CF_3^{\cdot} + I\cdot(^2P_{1/2}) \qquad \text{I-1}$$

$$CF_3I \dashrightarrow CF_3^{\cdot} + I\cdot(^2P_{3/2}) \qquad \text{I-2}$$

The production of $I\cdot(^2P_{1/2})$ atoms in the near ultraviolet photolysis of CF_3I has been shown to occur by means of a mass spectrometer in conjunction with an inhomogeneous magnetic field (16). Donohue and Wiesenfield (17) had found experimentally that the fraction of $I\cdot(^2P_{1/2})$ production from CF_3I photolysis is 91% of the primary processes and behaves like that of CH_3I photolysis (18, 19).

$$CF_3^{\cdot} + I\cdot \dashrightarrow CF_3I \qquad \text{I-3}$$

$$CF_3^{\cdot} + I_2 \dashrightarrow CF_3I + I^{\cdot} \qquad \text{I-4}$$

Scavenging with NO and Ag increased the net yield for decomposition of CF_3I or CH_3I and it is apparently believed that it prevents the above reverse reactions (14).

There are also gas phase radiolysis studies done in the CF_3I system in this (20) and other laboratories (21, 22). All of these studies indicate that the chief primary event in the gas phase photolysis or radiolysis of CF_3I is the rupture of the C-I bond

$$CF_3I \dashrightarrow CF_3^{\cdot} + I^{\cdot *}(^2P_{1/2}) \qquad \text{I-1}$$

$$CF_3I \dashrightarrow CF_3^{\cdot} + I^{\cdot}(^2P_{3/2}) \qquad \text{I-2}$$

It is evident that one or both of the radicals $CF_3^{\cdot}$ and $I^{\cdot}$ may be excited (23, 24).

The mass spectrum of CF_3I shows that the most abundant ion is CF_3I^+ (100) followed by I^+ (95.6), CF_3^+ (77.4), and CF_2I^+ (31.2). Similarly the mass spectrum of CH_3I shows that the most abundant ion is CH_3I^+ (100) followed by I^+(53.0), CH_3^+ (28.0), and CH_2I^+ (14.0). Hsieh, Eyler, and Hanrahan (8) also did high pressure and ion cyclotron resonance mass spectrometry and observed the following reactions:

$$CF_3^+ + CF_3I \dashrightarrow CF_4 + CF_2I^+ \qquad \text{I-5}$$

$$I^+ + CF_3I \dashrightarrow I_2^+ + CF_3^{\cdot} \qquad \text{I-6}$$

$$CF_3I^+ + CF_3I \dashrightarrow CF_3I_2^+ + CF_3^{\cdot} \qquad \text{I-7}$$

$$CF_3I^+ + CF_3I \dashrightarrow (CF_3I)_2^+ \qquad \text{I-8}$$

but the product $(CF_3)_2I^+$ was not reported.

Based on the above evidence from photolysis and radiolysis studies, Hsieh (20) put forward a reaction mechanism which postulates the primary events as well as secondary reactions in the radiolysis of CF_3I.

To account for the formation of the several minor products in the CF_3I radiolysis system, it was suggested (20) that carbene (CF_2) insertion into the substrate, CF_3I, is important.

$$CF_3I + CF_2 \longrightarrow C_2F_5I^* \qquad \text{I-9}$$

$$C_2F_5I^* \longrightarrow C_2F_5^\cdot + I^\cdot \qquad \text{I-10}$$

$$\longrightarrow C_2F_4 + IF \qquad \text{I-11}$$

$$\longrightarrow CF_3^\cdot + CF_2I^\cdot \qquad \text{I-12}$$

$$C_2F_5^\cdot + CF_3I \longrightarrow C_3F_8 + I^\cdot \qquad \text{I-13}$$

$$C_2F_5^\cdot + I_2 \longrightarrow C_2F_5I + I^\cdot \qquad \text{I-14}$$

Since one bond is broken but two strong bonds are formed by the insertion of CF_2 into CF_3I, the resulting C_2F_5I should be excited to the extent of 75 kcal.

2. Methyl Iodide

Extensive work has been done on the photolysis of gas phase methyl iodide and only the most definitive studies are discussed here. The UV absorption of CH_3I from 360 nm to 200 nm had been investigated by Porret and Goodeve (25, 26) and Ito, Huang, and Kosower (27). Porret and Goodeve interpreted the spectrum in terms of two potentials, one dissociating to $^2P_{3/2}$ iodine atoms

$$CH_3I \longrightarrow CH_3^\cdot + I^\cdot(^2P_{3/2}) \qquad \text{I-15}$$

and the other dissociating to the excited $^2P_{1/2}$ state

$$CH_3I \text{ ---> } CH_3\cdot + I\cdot^*(^2P_{1/2}) \qquad \text{I-16}$$

Construction of an iodine atom laser from the photodissociation of CH_3I by Kasper and Pimentel (9) verified majority production of $I\cdot^*(^2P_{1/2})$. Using photofragment spectroscopy with a quadrupled YAG laser at 266 nm, Riley and Wilson (28) investigated the product energy distribution of the $CH_3\cdot$ and $I\cdot$ fragments. They determined $I\cdot^*/I\cdot$ yield ratio of 3.5/1 with an internal excitation of the $CH_3\cdot$ radical of 3.9 kcal/mole for the $I\cdot^*$ channel and 8.6 kcal/mole for the $I\cdot$ channel. Schultz and Taylor (29) concluded that all methane production came from the "hot" methyl radical abstraction reaction as shown in Reaction I-18 below. Also in the reaction

$$RI \text{ ---> } R\cdot + aI\cdot^* + (1-a)I\cdot \qquad \text{I-17}$$

the fraction a, of excited atoms produced is very high where a is 0.92 for CH_3I and 0.91 for CF_3I and greater than 0.99 for C_3F_7I (17). It was also concluded (30-36) that in the gas phase photolysis of CH_3I production of methane arose from an excited fraction of methyl radicals according to the reaction

$$CH_3\cdot^* + CH_3I \text{ ---> } CH_4 + CH_2I\cdot \qquad \text{I-18}$$

Efficient thermal methyl radical scavengers such as I_2 or

O_2 were present during photolysis. Thus, the conclusion of the above investigators was that some of the "hot" methyl radicals formed in the photodissociation of CH_3I undergo a hydrogen atom abstraction before they are moderated by collision. Also the product of the "hot" methyl radical reaction was seen to increase with an increase in photon energy (17, 28). It was also seen that the quantum yield of methane increases with a decrease in wavelengths from 0.12×10^{-3} (CD_3I) at 313 nm to 30.0×10^{-3} (CH_3I) at 184.9 nm (32, 35).

Harris and Willard investigated the gas phase photolysis of CH_3I (32) and reported the major products CH_4, CH_2I, and I_2 as well as minor yields of C_2H_4 and CHI_3; there was some evidence for the presence of C_2H_2. Since the technique of gas chromatography was not yet available at the time when thier work was done, it was very difficult to obtain detailed information on minor products.

The formation of ethane (C_2H_6) with a low probability in the photolysis of CH_3I may occur through the reaction (33, 35)

$$CH_3\cdot^{*} + CH_3I \text{ ---> } C_2H_6 + I\cdot \qquad \text{I-19}$$

In the presence of even small amount of iodine, the $CH_3\cdot$ radicals which are deactivated by collision will rapidly react to regenerate CH_3I (35)

$$CH_3\cdot + I_2 \text{ ---> } CH_3I + I\cdot \qquad \text{I-20}$$

C. C. Chou, R. Angelberger and F. S. Rowland (36) proved that when photolysis of CH_3I was carried out in the presence of metallic Ag a larger total yield of product was observed, consistent with the absence of the usual back Reaction I-20. R. D. Souffie, R. R. Williams, and W.H. Hamill (33) examined the photolysis of CH_3I vapor at 253.7 nm with a particular concern for the mode of production of CH_4 and C_2H_6 and have shown that the rate of CH_4 production is strictly linear with time, is independent of temperature, is unaffected by iodine added, and is decreased by addition of various unreactive gases supporting the postulate that methane is exclusively a "hot" radical reaction product. On the other hand, they found out that the rate of C_2H_6 production is initially comparable to that of CH_4 but decreases with extent of photolysis. Also, the rate decreased by addition of moderators as with methane leading to the conclusion that C_2H_6 is also the result of a "hot" radical reaction.

Even though, for many years, the primary photochemical process in CH_3I has been recognized to be rupture of the C-I bond (17, 35, 36)

$$CH_3I \dashrightarrow CH_3^{\cdot} + I\cdot(^2P_{1/2}) \qquad \text{I-15}$$

$$CH_3I \dashrightarrow CH_3^{\cdot} + I\cdot(^2P_{3/2}) \qquad \text{I-16}$$

at shorter wavelengths two new primary processes become energetically possible.

$$CH_3I \longrightarrow CHI: + H_2 \qquad \text{I-21}$$

$$CH_3I \longrightarrow CH_2: + HI \qquad \text{I-22}$$

Occurrence of Reaction I-21 is well known in alkanes. Mahan and Mandal (37) demonstrated the formation of H_2 in the vacuum ultraviolet photolysis of CH_4 and concluded that it was produced primarily from an intra-molecular process. Herzberg (38) suggested Reaction I-22 in CH_3Cl from a theoretical point of view.

In recent matrix isolation studies of the vacuum ultraviolet photolysis of CH_3Cl and CH_3F, the spectra of CHCl: and CHF: were identified (39, 40). It was suggested in the latter work that both CHCl: and CHF: resulted from primary processes such as Reaction I-22 but no attempts were made to detect the postulated molecular elimination of H_2.

The occurrence of Reaction I-21 at 228.8 nm has been verified recently in photolysis experiments with tritium labelled CH_3I (36). The singlet methylene was detected through the well known olefin addition and carbon-hydrogen insertion reactions.

T. F. Hunter and K. S. Kristjansson (41) examining the photolysis of alkyl iodides and especially methyl iodide at wavelengths greater or equal to 247.5 nm and following other suggestions by previous workers (42) proposed the following primary and secondary reactions.

$$I\cdot^{*}(^{2}P_{1/2}) + M \dashrightarrow I\cdot(^{2}P_{3/2}) + M \qquad \text{I-23}$$

$$CH_3\cdot^{*} + M \dashrightarrow CH_3\cdot + M \qquad \text{I-24}$$

The $CH_3\cdot^{*}$ is in an excited state and the iodine atom may be in its excited spin-orbit state ($^{2}P_{1/2}$) or the ground state ($^{2}P_{3/2}$). Due to availability of suitable collision partners, thermalization of excited fragments follows. The above processes are followed by iodine recombination reactions and by back reactions where the majority of methyl radicals and iodine atoms reform the parent CH_3I.

$$I\cdot + I\cdot + M \text{ (or Walls)} \dashrightarrow I_2 + M \text{ (or Walls)} \qquad \text{I-25}$$

$$CH_3\cdot + I\cdot + M \dashrightarrow CH_3I + M \qquad \text{I-26}$$

$$CH_3\cdot + I_2 \dashrightarrow CH_3I + I\cdot \qquad \text{I-20}$$

Minor reaction paths that may contribute to other products are

$$CH_3\cdot^{*} + CH_3I \dashrightarrow C_2H_6 + I\cdot \qquad \text{I-19}$$

$$CH_2I\cdot + I_2 \dashrightarrow CH_2I_2 + I\cdot \qquad \text{I-27}$$

$$CH_3\cdot + \text{Product} \dashrightarrow C_2H_4 + \text{Product} \qquad \text{I-28}$$

$$CH_3\cdot + CH_3\cdot \dashrightarrow C_2H_6 \qquad \text{I-29}$$

They concluded that the minor products resulting from minor reaction paths continuously bleed off the "hot" $CH_3\cdot$ radical and $I\cdot$ atoms. Since none of these products are sufficiently high in quantum yields they claimed none of them will give a flow of heat energy of any consequence in the optoacoustic measurement. Therefore, according to their predictions the potentially heat yielding processes are Reactions I-23 to I-26 and I-20.

CHAPTER II
EXPERIMENTAL PROCEDURES AND EQUIPMENT

A. Reagents and their Purification

1. Methyl Iodide

Eastman or Mallinckrodt Analytical Reagent grade methyl iodide was initially purified by removing I_2 with Fisher certified reagent grade sodium thiosulfate (43). It was distilled at room temperature into a vessel in a dry ice iso-propanol bath through a P_2O_5 drying tube. The sample was again distilled in vacuo into a storage vessel immersed in a dry ice iso-propanol bath. The storage vessel which was fitted with a Teflon stopcock was kept in the dark and the sample was always degassed in a freeze-pump-thaw cycle before use.

2. Trifluoromethyl Iodide

Colombia Organic Chemicals Company (COC) trifluoromethyl iodide was tested by chromatography and no trace of impurity was detected. It was transferred to a storage vessel via P_2O_5 as a drying agent. It was degassed in several freeze-pump-thaw cycles and kept in a vessel in the dark at liquid nitrogen temperature.

3. Hydrogen Iodide

Hydrogen iodide was obtained from the Matheson Company (98.0% min.) and was passed through P_2O_5 into a storage vessel on the vacuum line and degassed by the freeze-pump-thaw method. The hydrogen iodide was then bled into the sub-manifold which was open to the photolysis vessel until the desired pressure was indicated by the Wallace and Tiernan differential pressure gauge. Then the valve to the photolysis vessel was closed and the remaining material condensed back to the storage vessel. The hydrogen iodide in the storage vessel was kept in the dark at liquid nitrogen temperature. While the valve to the photolysis vessel was closed, the HI was kept under liquid nitrogen and sealed off with the torch. All actinometry experiments were carried out at a pressure of 95.8 torr of HI, using any one of several photolysis vessels with somewhat different volumes. Product yields were normalized with respect to the amount of reactant photolyzed.

4. Oxygen

Matheson Company research grade oxygen was bled into the vacuum system through a P_2O_5 on glass wool drying tube into a storage vessel.

Fig. 1. Photolysis vacuum system

1. Main manifold
2. Photolysis vessel
3. Wallace and Tiernan differential pressure gauge
4. Storage reservoir for sample
5,6. Cryo traps (liq. N_2 or dry ice)
7. Oil diffusion pump

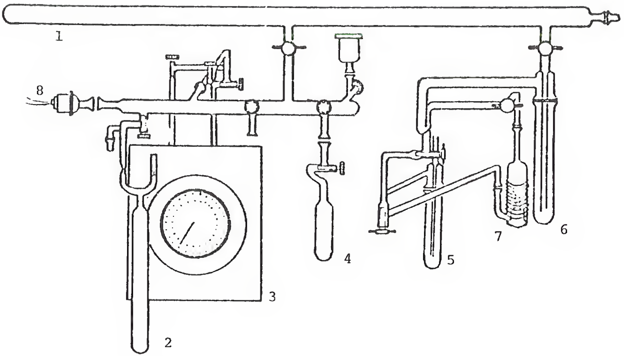

Fig. 1. Photolysis vacuum system

5. Chromatographic Calibration Standards

The gas and liquid calibration standards were used as received from the producers.

B. Sample Preparation Vacuum System

1. Vacuum System

To avoid mercury sensitized reactions in photolysis experiments, a mercury-free system was used for sample preparations (Fig. 1). The pumping system consisted of the Labglass LG-10980 two stage oil diffusion pump, heated by a 50 ml Glass-Col heating mantle, backed by a Welch Duo-Seal model 1400 B forepump, and two liquid nitrogen traps. The oil diffusion pump and the traps were attached to the vacuum line by O-ring joints.

Preparation of samples for photolysis was conducted on the sub-manifold. All pressure measurements were determined with a Wallace and Tierman Model 62-075 series differential pressure gauge. The extent of vacuum was monitored through a thermocouple vacuum gauge. The vessels used in photolysis experiments had volumes of 101, 92.6, 68.5, 50 and 43.8 cc, respectively. They were constructed of 18 mm ID GE type 204 clean fused quartz and were equipped with a glass break seal and side arm as shown in Fig. 2. Also attached to the main manifold were storage vessels for trifluoromethyl iodide, methyl iodide, oxygen and hydrogen iodide.

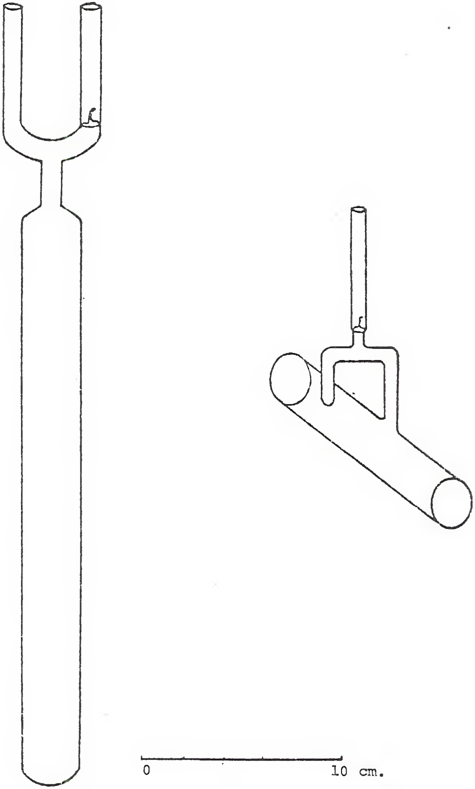

Fig. 2. Photolysis vessel

2. Treatment for Cleaning Photolysis Vessels

The vessels used for photolysis were rinsed with water and then with isopropyl alcohol to remove any iodine formed during photolysis. After all this was done, a glass break seal was blown on one of the side arms. The vessels were then annealed at 550°C to pyrolyze any organic materials on the wall. All these cleaning routines were done between photolysis experiments.

3. Metering and Filling the Photolysis Vessels

Before sample preparation, trifluoromethyl iodide and methyl iodide were deaerated by repeated cycles of freezing, pumping and melting until the thermocouple vacuum gauge indicated the absence of air. Also before any sample preparation the manifold was isolated from the pumps. In the case of the photolysis of unscavenged methyl iodide - trifluoromethyl iodide systems, samples were measured into the photolysis vessel while the desired pressure was monitored on the Wallace and Tiernan gauge. When the desired pressure was reached, the valve to the photolysis vessel was closed and the vessel was kept under liquid nitrogen. After the excess material was condensed back, the manifold was opened to the vacuum line and pumped until the vacuum came back to the position on the vacuum gauge noted before sample transfer. Then the frozen sample in the photolysis vessel was pumped for about 3 to 4 minutes. Finally, the vessel was sealed with an oxygen-methane torch and then allowed to warm to room temperature after the heated glass had cooled. The photolysis vessel was sealed at a reproducible position to minimize the deviation from its original calibrated volume. For photolysis of the equimolar mixtures the desired pressure of one sample was measured and stored in a standard metered volume and then transferred to the photolysis vessel under liquid nitrogen; any excess was condensed back into the storage vessel. The same amount of the other sample was metered similarly. Then the two samples were mixed in the sub-manifold and condensed back into the photolysis vessel followed by the same treatment as for the pure ones.

Pressures of 35 torr for pure trifluoromethyl iodide, 89 torr for pure methyl iodide and a pressure of 50 torr total pressure of the equimolar mixtures were used in all photolyses. The reason for using three different pressures in the three systems is given below under the subtitle actinometry.

4. Experiments with Added Oxygen

In all photolyses experiments the pressures of pure trifluoromethyl iodide, pure methyl iodide and equimolar mixtures were kept as mentioned above and that of the oxygen was 10% of the total pressure.

C. Sample Photolysis

1. Photolysis Lamp and Vessels

The photolysis lamp employed in this study was a General Electric 15 watt germicidal lamp which is illustrated in Fig. 3. The lamp is essentially a low pressure mercury lamp in a quartz envelope.

In the spectral range of 170 nm to 450 nm, the principal lines are 253.7 nm, 296.7 nm, 313.0 nm, 404.6 nm and 435.8 nm. It should be noted that the output of the lamp is rich in 253.7 nm resonance line and that the 184.9 nm is not observed (44). Figure 2 shows the two types of photolysis vessels used in these experiments. The smaller vessel was essentially a 10 cm path length quartz spectrophotometer cuevette attached to a Pyrex cold finger. The long cylinderical vessels were constructed of 20 mm O.D. and 18 mm I.D. General Electric Type 204 clear fused quartz with a Pyrex break seal. The General Electric quartz was later found to be inferior to several other brands, for instance that of the American Quartz Company. A number of pieces of quartz from G.E. had striations that marred their optical quality, and so care had to be exercised in the selection of the pieces used. Also glass blowing on this material proved difficult because slight over-heating of the glass caused bubbles to form on it.

The smaller vessel was used only for spectrophotometric analysis of iodine products. All other product yields were determined using the longer vessels. The volumes of the vessels used the in photolysis are listed below.

Vessel No.	Volume (cc)
1	43.8
2	50.0
3	68.5
4	92.6
5	101.0

The lamp fixture was a standard desk lamp designed to hold two two watt fluorescent lamps. One of the lamps was removed and replaced by a stack of Pyrex tubes that aided in providing reproducible positioning of the photolysis vessel. The vessel was positioned longitudinally and parallel to the single lamp and marks on the glass tubing allowed the vessels to be positioned reproducibly. The photolysis arrangement was covered with a wooden eye shield and air was passed between the vessel and the lamp to avoid thermal effects and to remove any ozone possibly formed. The latter has a strong absorption band at 253.7 (45). In addition, to minimize voltage fluctuations from the power line, a Sola transformer was employed. The geometry of the arrangement and the lamp's output allowed the photolysis to be carried out in periods of less than 20 minutes.

2. Actinometry

Gaseous hydrogen iodide was employed for actinometry with the germicidal lamp. The near ultraviolet absorption spectrum of hydrogen iodide resembles that of methyl iodide and trifluoromethyl iodide as would be expected if the electron originates from an orbital on the iodine atom. The hydrogen iodide absorption band is rather broad with a maximum at 221.5 nm and a long wavelength tail extending to 300 nm (46), while the absorption band of methyl iodide reaches a maximum at about 253.7 nm tailing approximately to 400 nm (25, 47, 48) and trifluoromethyl iodide reaches maximum around 260.0 nm and tails to approximately 400 nm (14). Therefore, the main contributing emission line from the germicidal lamp should be the one at 253.7 nm and it may be concluded that hydrogen iodide was an excellent choice for actinometry in this investigation.

Hydrogen iodide was photolyzed at a pressure of 95.8 torr and a temperature of 24°C for actinometry in the photolysis of 35, 89 and 50 torr of CF_3I, CH_3I and equimolar mixtures of CH_3I-CF_3I respectively, in a mercury-free system. The quantum yield for hydrogen production has been taken as unity in the photolysis of HI (49, 50). The hydrogen yields corresponded to an absorbed intensity of $0.81x10^{15}$ quanta/cc/sec for the I_2 analyzing cell and $2.680x10^{15}$ quanta/cc/sec for the other photolysis cells.

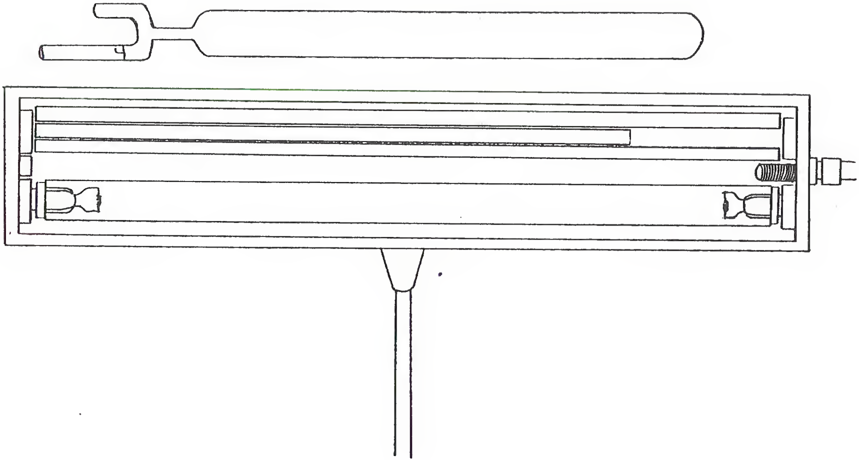

Fig. 3. Photolysis lamp

The experimental conditions were designed so that the absorbance of the hydrogen iodide actinometer was the same as that of pure CF_3I, CH_3I and CH_3I-CF_3I equimolar mixtures. Combination of the ideal gas law with the Beer-Lambert law for equal absorbance of the hydrogen iodide and methyl iodide, trifluoromethyl iodide, and methyl iodide - trifluoromethyl iodide equimolar mixtures yields the following equations:

$$P(HI) = \frac{a(CF_3I)P(CF_3I) + a(CH_3I)P(CH_3I)}{a(HI)} \qquad \text{II-1}$$

a = Extinction Coefficient P = pressure in torr

Since $P(CH_3I) = P(CF_3I) = 25$ torr

$$(HI) = \frac{25[295 \text{ torr}^{-1}\text{cm}^{-1} + 115 \text{ torr}^{-1}\text{cm}^{-1}]}{107 \text{ torr}^{-1}\text{cm}^{-1}} = 95.75 \text{ torr}$$

Similarly

$$P(CF_3I) = \frac{P(HI)a(HI)}{a(CF_3I)} = \frac{95.79 \times 107}{295} = 34.74 \text{ torr}$$

$$P(CH_3I) = \frac{95.79 \times 107}{115} = 89.13 \text{ torr}$$

where the extinction coefficients at 253.7 nm for hydrogen iodide, methyl iodide, trifluoromethyl iodide, and equimolar mixtures of methyl iodide-trifluoromethyl iodide were

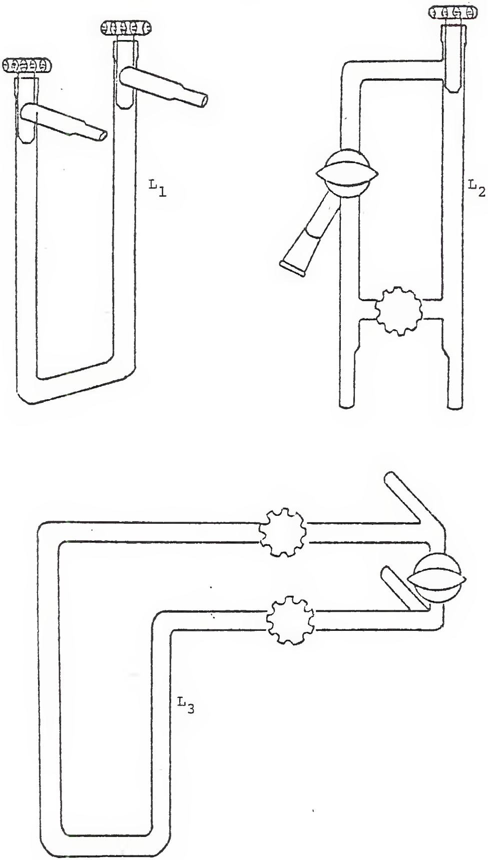

Fig. 4. Gas sampling loops

interpolated from the graphical data of B. J. Huebet and R. M. Martin (46), Porret and Goodeve (25) and J. R. Dacey (14) and the pressures of the CH_3I-CF_3I, pure CH_3I and pure CF_3I, were those employed in this study.

D. Analytical Equipment and Product Analysis

1. Gas Chromatograph Instrument

A Tracor Model 550 research gas chromatograph equipped with flame ionization and thermal conductivity detec-tors was used for the quantitative analysis of organic products. In this instrument, the gas chromatographic column is enclosed in an oven whose temperature is controlled by a multifunction temperature programmer. The output of the gas chromatographic detector system was fed to a 1 mv recorder for the flame ionization detector and to a 10 mv recorder for the thermal conductivity detector. All products were transferred on the vacuum line sub-manifold to one of the sample loops shown in Fig. 4 for subsequent injection into the gas chromatograph.

Also, a MicroTek Model 2000 research gas chromatograph equipped with a flame ionization and a thermal conductivity detectors was used for the quantitative analysis of organic products from the photolysis of pure methyl iodide in the gas phase.

a. Product Non-Condensible at -196°C

In the determination of non-condensibles, the photolysis vessel was attached to a sub-manifold leading to a Toepler Pump-McLeod gauge apparatus through a break-seal. The vessel was immediately immersed in a Dewar of liquid nitrogen to reduce the possibility of post-photochemical effects and pumped on until a good vacuum was reached. Then, the system was isolated from the vacuum pumps and the break-seal was broken. The products were passed through a liquid nitrogen U-trap. The non-condensible fraction was collected and transferred in 12 Toepler pump cycles to the McLeod gauge for measurement. It was then transferred to a sample loop (shown in Fig. 4) for flame ionization gas chromatographic analysis. This procedure allowed determination of small quantities of methane and ethylene that contribute to the pressure measurement.

b. Organic Products Condensible at -196°C

Depending on whether the Tracor Model 550 or the MicroTek Model 2000 gas chromatograph was to be used, the organic products were transferred to sample loops L1 or L3 on the sub-manifold by breaking the break seal. All products were separated on a 9.5 ft, 0.25" x 0.20" wall stainless steel column packed with 60/200 mesh silica gel, with helium carrier gas flow rate of 30 cc/min. The column was operated at 30°C in the Tracor and 45°C in the MicroTek until the low boiling gases were separated. Twenty minutes after injection, temperature programming was started at the rate of 5°C/min to 250°C in the Tracor G.C. oven and 215°C in the MicroTek oven. In the case of the equimolar mixtures of CH_3I-CF_3I, a longer column was used as there were products with very close retention time such as C_2F_6 and C_2H_6.

Prior to each analysis the relative response of the flame ionization detector to a typical organic compound was determined by using perfluoropropane in the case of pure trifluoromethyl iodide photolysis, and by using propane, in the case of photolysis of pure methyl iodide and equimolar mixture of CH_3I-CF_3I.

Since tetrafluoromethane has an extremely small molar response in a flame ionization detector, it was measured using a thermal conductivity detector.

2.Gas Chromatograph-Mass Spectrometer-Computer System

A detailed description of the gas chromatograph - Bendix Model 14-107 mass spectrometer - General Automation SPC-12 minicomputer system has been given elsewhere (44, 51). The gas chromatograph was equipped with a stream splitter at the column exit. A Hoke "Milli-Mite" metering valve diverted approximately 1/3 of the column effluent to the detector of the gas chromatograph and the remaining fraction to the ion source of the Bendix mass spectrometer through a single stage jet molecular separator. The effluent splitter system allows the gas chromatograph to operate at atmospheric pressure while running the mass spectrometer under vacuum (10^{-6} Torr). Helium was used as a carrier gas since it is easily skimmed off by the molecular separator; furthermore, it provides minimum interference with the mass spectra of other species. The mass spectral data acquisition was accomplished by a General Automation SPC-12 minicomputer. During a gas chromatograph-mass spectrometer run or mass spectrometry run, data are stored on magnetic tape (PEC 9 - track magnetic tape unit) and are retrieved and analyzed at a later time.

3. Spectrophotometric and Chemical Analysis of Iodine

The determination of iodine in the pure and scavenged sample was made spectrophotometrically at room temperature in the vapor phase. Absorbance measurements at 520 nm were carried out between successive photolysis processes on a Beckman DU Spectrophotometer with a Gilford Model 222 Photometer and power supply. In a typical analysis the cell absorbance with the unphotolysed sample was determined and an optical measurement was then made of the photolysed product and the difference in the optical density was taken to be proportional to the concentration of iodine. The amount of iodine present was determined using an extinction coefficient of 820 liter $mole^{-1}cm^{-1}$ (52,53) at 520 nm. The uncertainty in measurement may be as large as 20%.

4. Hydrogen Fluoride and Hydrogen Iodide Analysis

After the sample had been photolyzed, the photolysis vessel was cooled to liquid nitrogen temperature. Slightly acidified water was then added to the solid sample through the break seal fittings on the HI analysis cell; 2 ml of 95% ethanol was added instead of water to carry out HF analysis. The break seal was opened with a rod introduced through a piece of rubber tubing used as a gland. This procedure was necessary to avoid condensation of oxygen inside the vessel. While the sample was warming up to room temperature, it was shaken for 20 minutes to help recover hydrogen fluoride or hydrogen iodide absorbed on the walls of the vessel. In the case of HF, the ethanolic solution was transferred into a 5 ml polyethylene beaker, but in HI analysis the content of the photolysis vessel was emptied into a 5 ml glass beaker. The photolysis vessel was then rinsed out with another 2 ml of solvent (in both HF and HI analysis). The determination of HF was based on a procedure described by E. Heckel and P. E. Marsh (54). A solution of 1×10^{-3} M lanthanum nitrate, $La(NO_3)_3 \cdot 6H_2O$ (Fisher Scientific Company) in a 100 microliter gas tight Hamilton Syringe was used as a titrant. The electrode potential of the Orion model 96-09 combination fluoride ion selective electrode was monitored by the Orion Model 801A digital pH/mv meter. During the titration, the solution was stirred with a Teflon coated magnetic stirrer.

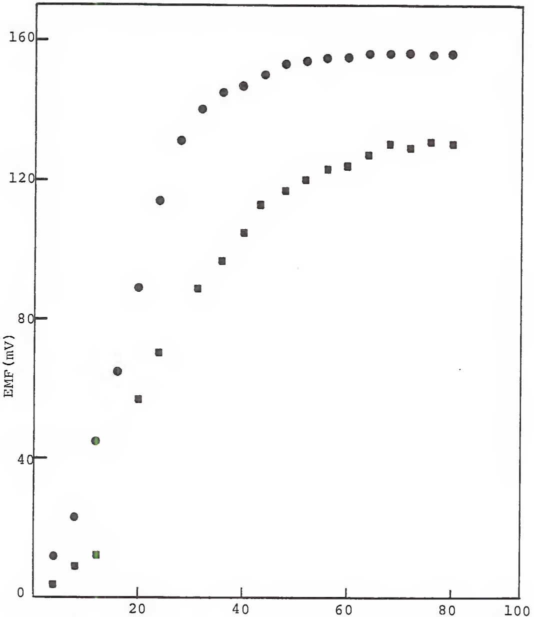

Volume in microliters of 1.0×10^{-3} M $La(NO_3)_2 \cdot 6H_2O$

Fig. 5. Titration curves for quantitative analysis of F^-; 40 microliters of NaF, ■ ; photolysis, ● .

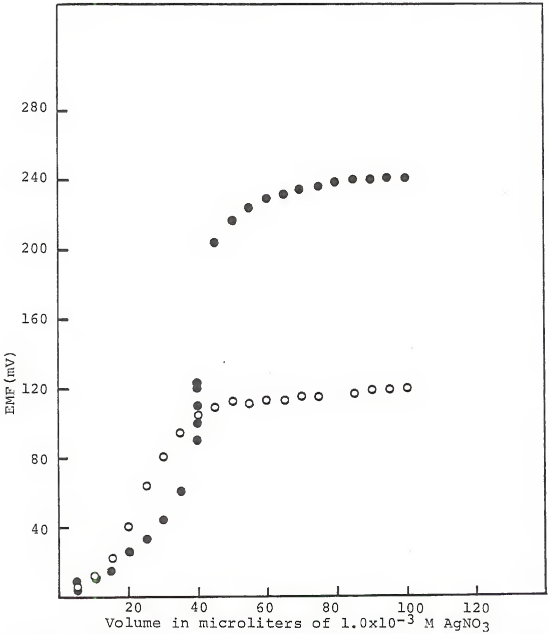

Fig. 6. Titration curves for quantitative analysis of I^-; 40 microliters of KI, ●; photolysis, ○.

The HI was determined in the same way as HF except that a solution of 1x10^{-3} M silver nitrate, $AgNO_3$ (Fisher Scientific Co.) was used as a titrant, and measurements were made with a Lazar model Is-146 iodine ion selective electrode.

Titration curves for standardization of the electrodes and typical titration curves for an irradiated sample are shown in Figs. 5 and 6.

5. Equipment for Ion-Molecule Investigation

a. High Pressure Mass Spectrometry

The Bendix Time of Flight mass spectrometer (Model 14-107) was modified as described by Futrell et al. (55). It could easily be changed from the analytical to the ion-molecule mode (56). The electron energy was 100 eV. Ion grid No. 1 was at +18 v and the repeller grid at +20 v with respect to ground. Distance from the repeller grid to the exit orifice was 0.533 cm, and the drift distance from the electron beam position to the exit orifice was 0.267 cm. A circuit for pulse generation for ion grid number 1 that can provide for the variation of the pulse height from 1 to 25 v and the width from 2 to 6 microsec while maintaining a very fast rise time (ca. 2 nsec) and very short delay (<1 nsec) relative to the ion focus was installed (57). All other ion source potentials were identical to those reported by Futrell et al. (55). Further details about setting up and adjusting the instrument were described by Heckel

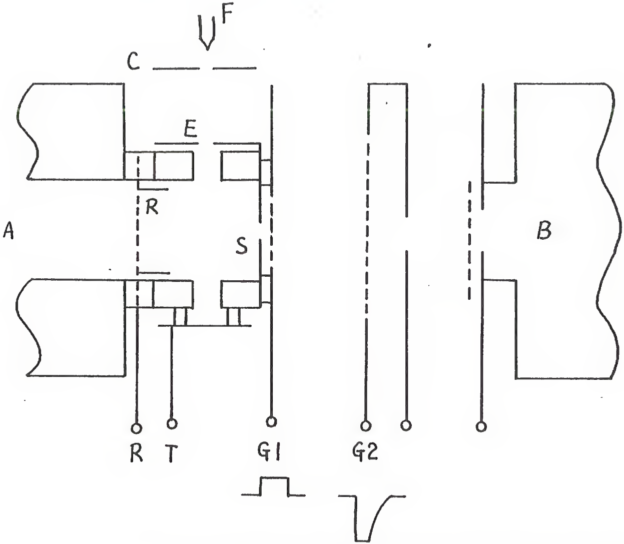

A. Gas inlet
B. Flight tube
C. Electron control grid
E. Electron beam inlet
F. Filament
G1. Blocking pulse
G2. Ion focus pulse
R. Backing plate
S. Ion outlet slit
T. Electron trap

Fig. 7. Schematic of Bendix high pressure ion-molecule studies

and Hanrahan (58). Similar procedures were employed in the present work.

The ion source (Fig. 7) is housed inside a stainless steel "cross" which is connected directly to the drift tube of the mass spectrometer. Besides the regular pumping system supplied with the instrument, a CVC Type D4 oil diffusion pump backed by a Welch Duo-Seal forepump, acting as an auxiliary gas pumping system was used. This system was attached directly to the ion source by means of a metallic bellows in order to maintain a pressure differential of about 1000:1 between the interior of the source and its surroundings inside the "cross." With this set up, ion-molecule reactions could be studied at a pressure as high as 0.5 Torr. Figure 5 shows a schematic diagram of the ion-molecule reaction source. The ion-molecule reaction chamber is a rectangular block with a length of 0.222 inch in the direction parallel to the flight tube, 0.25 inch in the direction parallel to the electron beam and 1 inch in the vertical direction.

Mass Spectrometer data acquisition and reduction were carried out using a General Automation SPC-12 minicomputer as described in a previous report (59).

The ion source was operated at 50°C. The reactant (CH_3I-CF_3I equimolar mixtures) was leaked into the ion source through a gold leak from a five liter reservoir. Variation of the reservoir's pressure allowed adjustment of the pressure in the ion source, which was monitored using an MKS Baratron Capacitive micromanometer Model 77 equipped with a 3 mm head.

The point to be considered at this stage is the relationship of the ion concentrations as sampled by the analysis system to the concentrations emerging from the source. The ion draw out pulse only extracts those ions residing between grids G1 and G2. At this point a discrimination in favor of heavy ions starts to take place. Each ion species will have had a residence time in the sampling region inversely proportional to its average velocity across the region. If it is assumed that the ions have equal energy in this region, then an equation proposed by Futrell et al. (55) is obtained

$$n_1/n_2 = (M_1/M_2)^{1/2} N'_1/N'_2 \qquad \text{II-2}$$

where n_1/n_2 is the desired ratio of concentrations of ion 1 and 2 within the source, N'_1/N'_2 is the measured intensity ratio, and M_1 and M_2 are the masses of ion 1 and ion 2 respectively. This equation has been applied to all intensities data taken from the TOF.

A semiquantitative treatment of ion-molecule reaction rates in the TOF ion source was carried out by viewing the the reaction process as a quasi-first order reaction. Since the concentration of neutral reactant gas is in large excess compared to the concentration of the ions, the rate of reaction with substrate can be formulated as

$$-d[I^+]/dt = k_{app.}[I^+] \qquad \text{II-3}$$

where the apparent first order rate constant, $k_{app.} = k'_{true}[M] = k_{abs}[n/v]$, where k_{abs} is the absolute bimolecular rate constant in units of $cm^3\ molec^{-1}\ s^{-1}$. This equation is integrated to give

$$\ln[I^+]/[I_o^+] = -k_{abs}[n/v]t \qquad \text{II-4}$$

where I^+ is the intensity of a reactant ion at any given pressure, I_o^+ is the intensity at low background gas pressure, and t is the residence time of the ion in the reaction source. The product k[n/v] can be evaluated from the slope of a plot of $\ln[I^+]$ versus pressure (or number density [n/v]), but determination of the bimolecular rate constant requires a knowledge of the residence time and the ion source, t.

The residence time can be evaluated approximately using a free flight model, according to which ions move in a straight line from point of origin through the exit slit, without collisions. The relevant equation is

$$\text{velocity} = dx/dt = qVt/ml. \qquad \text{II-5}$$

Integrating x from 0 to l (the distance from the electron beam to the exit slit) and time from 0 to t(residence time) gives an equation which can readily be solved for t

$$t = (2ml^2/qV)^{1/2} \qquad \text{II-6}$$

In this expression, m is the ion mass, q the charge, V the potential on the repeller grid in the ion source, and l the length of the ion flight path (2.67 mm in the TOF instrument). The resulting residence times are a weak function of the ion mass, but generally have values around 1.5 microseconds. (It will be seen in Chapter VI that the above calculation underestimates actual ion residence times in the TOF source.)

b. Ion Cyclotron Resonance Mass Spectrometry

Ion Cyclotron Resonance (ICR) mass spectrometry is a very important technique for the study of ion-molecule reactions (60). Even though its use by analytical chemists is not widespread due to its limited mass range, it is one of the best tools in use by the physical chemist in the field of ion-molecule reactions. Due to advances in detection theory, electronics and computers, it is intensively used in many chemistry research labs.

A comprehensive survey of ICR work has been presented by Hartmann (61) and Buckley (62). Hartmann (61) and Wanczek (63) recently reviewed the instrumentation and theory from its early stage to the present. In 1971 Beauchamp presented a description of the application of ICR spectrometry in the determination of ion-molecule collision

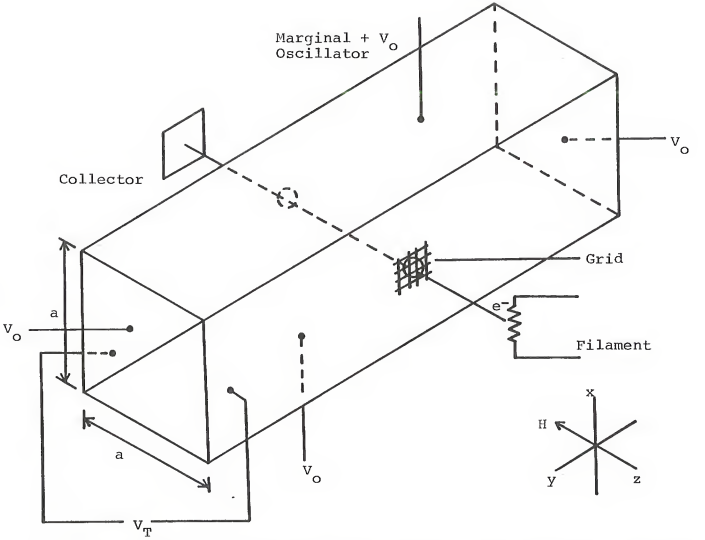

Fig. 8. Basic diagram of the trapped ion ICR cell showing the connections for the marginal oscillator, the ionizing electron source, and the various plate potentials (V's).

frequencies, reaction rate constants, reaction pathways and product distributions, energy dependence of rate constants and thermochemical properties such as gas phase acidities and proton affinities (64).

A Varian V-5900 ICR instrument with improved hardware (62) and equipped with a trapping ion cell, a marginal oscillator, and electron impact ion source was used as shown in Fig. 8. The marginal oscillator is a tuned detector; thus one ion only can be seen at a time. Mass sweeps are usually accomplished by a slow magnetic field scans which bring the ions into resonance at the frequency of the marginal oscillator detector (65). An ion in crossed electric and magnetic fields, as shown in Fig. 8, is governed by the Lorentz equation

$$\mathbf{F} = q(\mathbf{E} + \mathbf{V} \times \mathbf{B}) \qquad \text{II-7}$$

where **F** is the force exerted on the ion, q is the ion's charge V is the velocity, and E and B are the electric and magnetic field vectors, respectively (66). The magnetic field causes the ion to move in a circular orbit in a plane perpendicular to the magnetic field with a characteristic angular frequency, w_c ,

$$w_c = \frac{qB}{m} \qquad \text{II-8}$$

for an ion of mass m. The electric field experienced by an ion in a trapped ion cell with flat rectangular sides, as shown in Fig. 8, has been numerically calculated to correspond closely to a three dimensional quadrupole field (66). The ion oscillates back and forth in a region between the two trapping plates at a frequency, w_T, given by

$$w_T = \{4q(V_T - V_o)/ma^2\}^{1/2} \qquad \text{II-9}$$

Here, a is the distance between the plate pairs and V_T and V_o are the trapping and side plate potentials respectively (67). The observed cyclotron frequency of the ion, w, is

$$w = (w_c{}^2 - w_T{}^2)^{1/2} \qquad \text{II-10}$$

but since $w_T << w_c$ for practical experiments, $w = w_c$ to a first approximation.

If the ion is probed by a radio frequency electric field in a plane perpendicular to the magnetic field, it can absorb energy from the radio frequency field for frequencies near w. The ions are accelerated to an average kinetic energy, T give by

$$T = (qEt)^2/8m + (M/2)V_o{}^2 \qquad \text{II-11}$$

where t is the duration of the r.f. pulse of amplitude, E, and V_o is the initial velocity of the ion (67). The first term is the energy absorbed by the ion from the r.f. field, while the second term corresponds to the initial kinetic energy of the ion.

As the ion accelerates, the size of the cyclotron orbit increases. The radius, r, of the orbit can be calculated from

$$r = (2T/mw^2)^{1/2} \qquad \text{II-12}$$

The maximum orbital radius attainable is limited by the physical dimensions of the cell and is equal to one half of the separation between the upper and lower plate.

The ICR instrument performed at pressures from 1×10^{-4} to 10^{-7} torr. Ions were formed by electron impact with 20 to 70 ev electrons and trapped in the ICR cell. The signal was monitored as a function of the electric pulse delay time.

The cyclotron frequency for most experiments was set for ion resonance at a magnetic field of 1.2T. For a typical experiment the cell trapping plate was at + 1v, the upper, lower and end plates were at -1v, the grid was pulsed for 5ms, and a 4ms detect pulse gated the 30 mv peak-to-peak marginal oscillator irradiating frequency. After each experiment, ions were removed from the cell with a 5ms quench pulse. Ion signals were averaged from 10 to 25 times at each detect pulse delay time, then stored on disk. Gaseous samples in glass bulbs were routinely purified by repeated freeze-pump-thaw cycles in this experiment.

Another important technique using the ICR mass spectrometer is double resonance. It was accomplished by sweeping the probe frequency w_2 while the analyzer was set at the magnetic field required to observe a secondary ion of interest with the marginal oscillator set at w_1. The change in product ion intensity caused by changing the kinetic energy of the primary ion was thus directly observed. The double-resonance radio frequency field was applied to the source region and the irradiating field strength was kept as low as possible to prevent sweep-out effect (68). The double resonance method is very important to identify reaction channels.

Due to the low gas densities involved in ICR studies, the most difficult quantity to measure, if accurate ion-molecule rate constants are to be determined, is pressure. Pressure was measured using an ionization gauge. Since this transducer works by ionizing the gas and then measuring the resulting ion current, the gauge sensitivity depends upon gas characteristics, particularly the cross-section for ionization. Since the sensitivity is not directly related to some known quantity such as the ionization potential or polarizability of the gas, the gauge must be calibrated against a single-sided capicitance manometer (69) in the mid 10^{-6} to 10^{-7} torr range. To aid in reading the manometer, a digital voltmeter was connected to the analog output of the manometer control unit.

Experiments were performed by first pumping out the vacuum chamber to reach background pressure, then reading both pressure gauges. Next, a sample gas was leaked into the vacuum system followed immediately by the reading of both gauges. When the pressure had stabilized the gauges were again read. This procedure was repeated for several different sample pressures in the range specified above.

CHAPTER III
THE PHOTOLYSIS OF METHYL IODIDE IN THE GAS PHASE

A. Experimental Result

The photolysis of methyl iodide in the gas phase was investigated at 89 torr pressure and 24°C using 253.7 nm radiation emitted by a 15 watt General Electric germicidal lamp for periods ranging form 10 seconds to 30 minutes. The number of quanta absorbed per second per cc at this pressure corresponded to 2.68 x 10^{15} for the regular photolysis vessels and 0.81 x 10^{15} for the iodine analyzing cell. A summarry of the quantum yields is shown in Table 1.

In the gas phase photolysis of pure methyl iodide, five major and six minor products were identified. The major and minor products and their respective quantum yields are as follows: diiodomethane, 0.007; ethane, 0.0039; iodine, 0.0032; methane, 0.0028; hydrogen iodide, 0.0017; butene, 3.4×10^{-4}; n-pentane, 1.3×10^{-4} ; propene, 8.1×10^{-6} ; ethylene, 3.8×10^{-6}; iso-pentane, 1.8×10^{-6}, and n-butane, 1.0×10^{-6}. When 10% oxygen was added the quantum yields became the following: iodine, 0.014; diiodomethane 0.0024; ethane, 2.3×10^{-4}; methane, 0.0016; butene, 1.2×10^{-4}; n-pentane, 6.4×10^{-5}; and propene, 1.4×10^{-6}. The quantum yields were calculated using the least squares

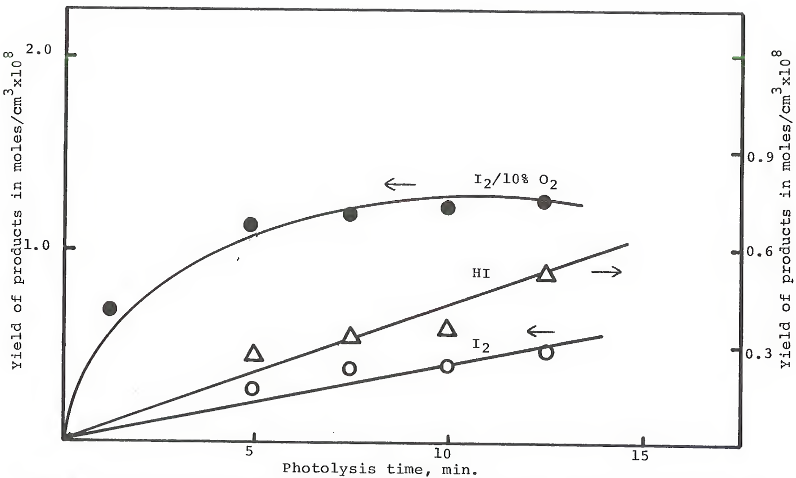

Fig. 9. Production of I_2 (pure,○ ; 10% O_2,●) and HI (pure, △) as a function of photolysis time.

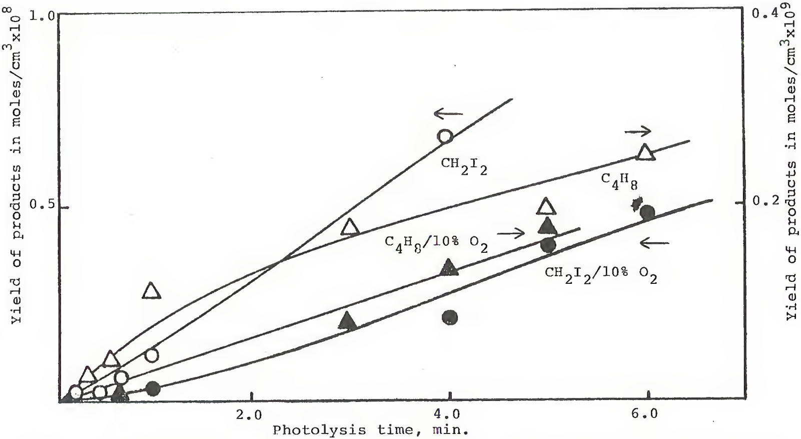

Fig. 10. Production of CH_2I_2 (pure, ○; 10% O_2, ●), C_4H_8 (pure, △; 10% O_2, ▲) as a function of photolysis time.

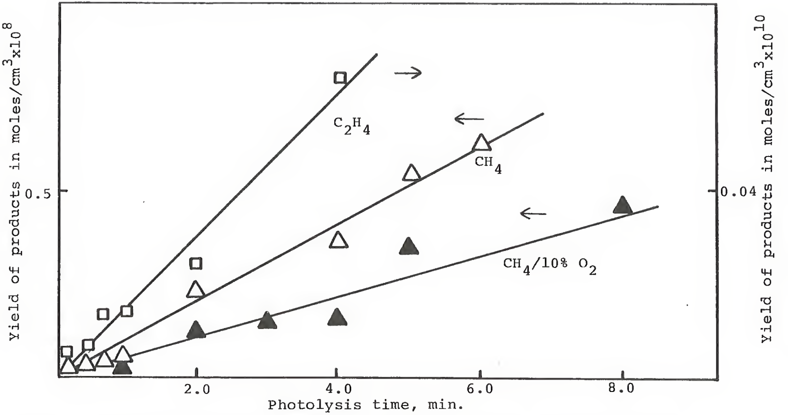

Fig. 11. Production of C_2H_4 (pure, □) and CH_4 (pure, △ ; 10% O_2 ▲) as a function of photolysis time.

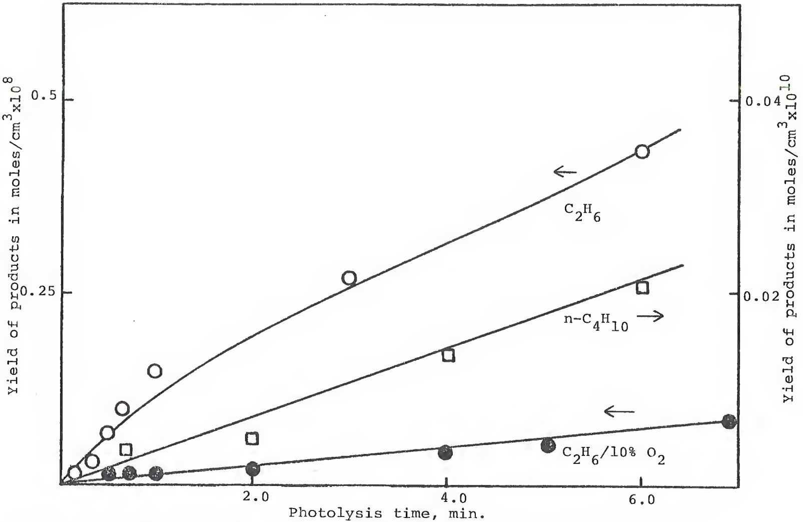

Fig. 12. Production of C_2H_6 (pure, ○ ; 10% O_2, ●), n-C_4H_{10} (pure, □) as a function of photolysis time.

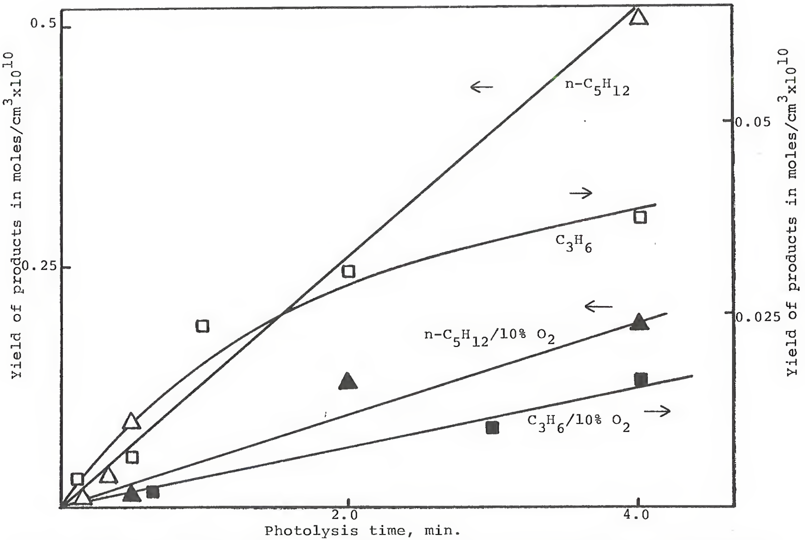

Fig. 13. Production of n-C_5H_{12} (pure,△ ; 10% O_2,▲) and C_3H_6 (pure,□ ; 10% O_2,■) as a function of photolysis time.

Table 1

Quantum yields in pure CH_3I photolysis

Compound	Quantum Yield	Relative Yield	Quantum Yield With 10% O_2 Added	Relative Yield
CH_2I_2	0.007	1.0	0.0024	0.17
C_2H_6	0.0039	0.56	0.00023	0.016
I_2	0.0032	0.46	0.014	1.0
CH_4	0.0028	0.4	0.0016	0.11
HI	0.0017	0.24	a	
C_4H_8	3.4×10^{-4}	0.049	1.2×10^{-4}	0.0086
n-C_5H_{12}	1.3×10^{-4}	0.019	6.4×10^{-5}	0.0046
C_3H_6	8.1×10^{-6}	0.0012	1.4×10^{-6}	1.0×10^{-4}
C_2H_4	3.8×10^{-6}	5.4×10^{-4}	b	
i-C_5H_{12}	1.8×10^{-6}	2.6×10^{-4}	b	
n-C_4H_{10}	1.0×10^{-6}	0.00014	b	

a. Not analyzed.
b. Not seen.

determined slopes of the curves in Fig. 9 through Fig. 13. Quantum yields for photolysis with and without oxygen are summarized in Table 1.

All products' yields were plotted as a function of photolysis time in Figs. 9 through 13. Overall material balance is very good in this system, with a ratio of C/H/I = 1/3.0/1.1 There is no surplus of hydrogen or iodine containing compounds. A brief description of these results follows.

B. Discussion

The previous photolysis (9,19,32,33,35) and radiolysis (1) studies of the gas phase of methyl iodide indicate that the main primary event is the rupture of the C-I bond, which can be represented as follows.

$$CH_3I \dashrightarrow CH_3^{\cdot} + I^{\cdot}\ (^2P_{1/2}) \qquad \text{III-1}$$

$$CH_3I \dashrightarrow CH_3^{\cdot} + I^{\cdot}\ (^2P_{3/2}). \qquad \text{III-2}$$

The formation of excited $^2P_{1/2}$ iodine atoms as well as the $^2P_{3/2}$ ground state is critical to the operation of the photochemical iodine laser (9), as discussed in the Introduction.

A mechanism which accounts qualitatively for the results in the methyl iodide photolysis system is presented in Table 2. As shown in Reactions III-1 of Table 2, the excited iodine atoms in the $^2P_{1/2}$ state mainly

Table 2

Photolysis mechanism in the CH_3I system

PRIMARY PROCESSES

$$CH_3I \longrightarrow CH_3\cdot + I\cdot\ (^2P_{1/2}) \tag{III-1}$$

$$CH_3I \longrightarrow CH_3\cdot + I\cdot(^2P_{3/2}) \tag{III-2}$$

$$CH_3I \longrightarrow CH_2: + HI \tag{III-3}$$

SECONDARY PROCESSES

$$I\cdot^*\ (^2P_{1/2}) + M \longrightarrow I\cdot(^2P_{3/2}) + M \tag{III-4}$$

$$I\cdot + I\cdot + M \longrightarrow I_2 + M \tag{III-5}$$

$$CH_3\cdot + I_2 \longrightarrow CH_3I + I\cdot \tag{III-6}$$

$$CH_3\cdot + CH_3I \longrightarrow CH_4 + CH_2I\cdot \tag{III-7}$$

$$CH_2I\cdot + I_2 \longrightarrow CH_2I_2 + I\cdot \tag{III-8}$$

$$CH_3\cdot + CH_3I \longrightarrow C_2H_6^* + I\cdot \tag{III-9}$$

$$C_2H_6^* + M \longrightarrow C_2H_6 + M \tag{III-10}$$

$$CH_3\cdot + CH_3\cdot \longrightarrow C_2H_6 \tag{III-11}$$

$$CH_2: + CH_3I \longrightarrow C_2H_5I^* \tag{III-12}$$

$$C_2H_5I^* + M \longrightarrow C_2H_5I + M \tag{III-13}$$

$$C_2H_5I^* \longrightarrow C_2H_5\cdot + I\cdot \tag{III-14}$$

$$C_2H_5I^* \longrightarrow C_2H_4 + HI \tag{III-15}$$

$$R_1 + C_2H_4 \longrightarrow R_1C_2H_4\cdot \tag{III-16}$$

$$R_1C_2H_4\cdot + I_2 \longrightarrow R_1C_2H_4I\cdot + I \tag{III-17}$$

$$R_1C_2H_4\cdot + R_2\cdot \longrightarrow R_1C_2H_4R_2 \tag{III-18}$$

---

a. Where R_1 and R_2 = $CH_2I\cdot$, $CH_3\cdot$, or $C_2H_5\cdot$

become deactivated by collision with the substrate.

$$I\cdot^{*}\ (^{2}P_{1/2}) + M \longrightarrow I\cdot\ (^{2}P_{3/2}) + M \qquad \text{III-4}$$

The ground state iodine atom combine to form I_2 in a 3-body process as shown below

$$I^{\cdot} + I^{\cdot} + M \longrightarrow I_2 + M \qquad \text{III-5}$$

A large majority (approximately 99%) of the methyl radicals formed in Reaction III-1 and III-2 back react with product I_2 to form CH_3I.

$$CH_3{}^{\cdot} + I_2 \longrightarrow CH_3I + I^{\cdot} \qquad \text{III-6}$$

In consequence, all net products in methyl iodide photolysis arise from relatively minor side reactions. The most important of these minor processes forms methane and ethane.

Reactions III-7 is the main route for the yield of CH_4

$$CH_3{}^{\cdot} + CH_3I \longrightarrow CH_4 + CH_2I^{\cdot} \qquad \text{III-7}$$

It is similar to the process suggested by Young and Willard (70) in the radiolysis and photolysis of CCl_3Br. They reported that the main products of the analogous reaction are CCl_4 and the $CCl_3{}^{\cdot}$ radical, which could be either thermal or "hot." Reaction III-7 has an activation energy of less than 8 kcal/mole (37). A second reaction channel competing with Reaction III-7 and involving the same reactants is proposed as the main process for ethane formation.

$$CH_3^{\cdot} + CH_3I \dashrightarrow C_2H_6 + I^{\cdot} \qquad \text{III-9}$$

As discussed in the Introduction, this process is also thought to play a role in the photochemical iodine laser (9,10). In the presence of oxygen in the system, the yields of methane and ethane were reduced substantially, where methane is decreased by 42%, ethane by 94%. These observations suggest that Reactions III-7 and III-9 are the only major routes to methane and ethane formation. Since the C-C bond formation process in Reaction III-9 provides ca. 90 kcal of energy, whereas the C-I rupture takes only 55 kcals, the product C_2H_6 may contain substantial internal energy, subsequently lost in collisions with the substrate. These details are shown in Reactions III-9 and III-10 of Table 1.

Souffie, William and Hamill (33) have found in the gas phase photolysis of CH_3I that the yield of methane decreased upon the addition of either unreactive or scavenging gases and also discovered the rate of methane formation to be independent of temperature and I_2 concentration. These observations supported their conclusion that in the photolysis of methyl iodide in the gas phase, methane is the product of "hot" methyl radical reaction. Similarly it was concluded that ethane was produced mostly through "hot" methyl radicals. These conclusions are in agreement with the results of the present work.

In an important earlier paper using classical analytical methods, West and Schlessinger (71) reported formation of methane with low quantum efficiency, along with even smaller yields of ethane and ethylene. They also found a non-condensible product, identified as CH_2I_2 by its melting point. They reported that one-third of the net methyl iodide decomposed appeared as CH_2I_2.

Diiodomethane was also found to be an important product in the present work. Formation of this product via reaction with I_2 is a major fate of the iodomethyl radical formed along with methane in Reaction III-7.

$$CH_2I\cdot + I_2 \longrightarrow CH_2I_2 + I\cdot \qquad \text{III-8}$$

In the present work, hydrogen iodide was found to be a product of moderate importance, with a quantum yield of 0.0017 in the oxygen-free system. Its concentration was followed using an iodide selective electrode, a technique which was not available at the time when most of the earlier research on this system was done. Although HI was not detected by previous workers, its role in CH_3I photolysis was postulated by Benson (72), who suggested a route of formation involving excited ethyl iodide as shown below and in Table 2.

$$CH_3^{\cdot} + CH_2I^{\cdot} \longrightarrow C_2H_5I^{*} \qquad \text{III-19}$$

$$C_2H_5I^* + M \text{ -----> } C_2H_5I + M \qquad \text{III-13}$$

$$C_2H_5I^* \text{ -----> } C_2H_5\cdot + I\cdot \qquad \text{III-14}$$

$$C_2H_5I^* \text{ -----> } C_2H_4 + HI \qquad \text{III-15}$$

There appear to be several other routes to HI formation in this system, including a possible minor branching pathway in the primary photolysis step

$$CH_3I \text{ -----> } CH_2: + HI \qquad \text{III-3}$$

Since this process requires only 80 kcal of energy compared to 112 kcal available from a 253.7 nm photon, it appears difficult to rule out entirely. It is not necessary, however, that the above reaction represents an independent primary photochemical event. It would suffice if as much as 0.2% of the yields of Reactions III-1 and III-2 was diverted to follow the stoichiometry of the above reaction due to collisions with the wall or other molecules. (Discussion of the time between collisions versus dissociation time of CH_3I^* following photon absorption is not necessarily relevant. The reactant CH_3I molecule could be bound in a "sticky-collision" complex to another CH_3I molecule, to I_2, or to the wall at the time of photon absorption.) A second plausible reaction pathway involves a disproportionation process between $CH_3\cdot$ radical and iodine atom, as originally postulated by Bonhoeffer and Farcas (73) and supported by Bates and Spence (74) as presented below

$$CH_3\cdot + I\cdot \longrightarrow CH_2: + HI \qquad \text{III-20}$$

Although this process is ca. 20 kcal/mole endoergic, a portion of the $CH_3\cdot$ population in this system is born "hot" and could undergo such a reaction. An additional pathway to HI formation involving two $CH_2I\cdot$ radicals as precursors was proposed by Maines and Lewis (75)

$$2CH_2I\cdot \longrightarrow C_2H_2 + 2HI \qquad \text{III-21}$$

These authors also suggested a two step analog proceeding via a $CH_2I\cdot-I_2$ complex. Since this reaction involves the square of the concentration of a rather minor intermediate, however, it appears incapable of explaining an HI yield which is about 10% as large as the predominant products in this system.

Several minor hydrocarbon products were observed in this investgation, having quantum yields in the range from 3×10^{-4} to 2×10^{-6}. It is not possible that any of these species contain iodine, since they all elute prior to the parent CH_3I. Several possible minor iodine containing products such as C_2H_5I and C_3H_7I could be masked by the parent CH_3I peak, which overloads the column and tails for 15 to 20 minutes. The only measurable product subsequent to CH_3I is CH_2I_2, which elutes 25 to 30 minutes after the parent.

Benson (72) suggested a route towards several minor products starting with a combination reaction between $CH_3^{\cdot}$ and $CH_2I^{\cdot}$ radicals, as discussed above. His scheme predicts formation of excited $C_2H_5I^*$ which can be collisionally stablized to give C_2H_5I or fragment to give C_2H_4 plus HI or $I^{\cdot}$ plus $C_2H_5^{\cdot}$. The latter can serve as a precursor to very minor yields of propane and butane. Since the system is heavily self-scavenged by product I_2, however, it is suggested below that the excited $C_2H_5I^*$ is probably formed via carbene insertion rather than by radical-radical combination.

Several of the reactions postulated earlier in connection with formation of HI also produce methylene, CH_2:. The most probable fate of this intermediate is insertion into the substrate as shown below.

$$CH_2: + CH_3I \longrightarrow C_2H_5I^* \qquad \text{III-12}$$

$$C_2H_5I^* \longrightarrow C_2H_5^{\cdot} + I^{\cdot} \qquad \text{III-14}$$

$$\longrightarrow C_2H_4 + HI \qquad \text{III-15}$$

$$\longrightarrow CH_2I^{\cdot} + CH_3^{\cdot} \qquad \text{III-22}$$

The possible role of methylene in methyl iodide photolysis has been discussed by several authors including Schultz and Taylor(29), Rowland et al. (36) and Schmitt and Comer(76).

The reaction pathways described above lead to formation of $CH_2I^{\cdot}$, $CH_3^{\cdot}$, and $C_2H_5^{\cdot}$ radicals, which could only account for small yields of C_3 and C_4 products, but nothing higher. In addition, the C_4 product predicted would be C_4H_{10} rather than C_4H_8 as observed. It thus appears that some aspect of the mechanism is still missing.

It is suggested that the main clue to the "hidden" reaction pathways is revealed by the fact that C_2H_4 is found with the small quantum yield of 3.8×10^{-6}, whereas it is formed via at least two reaction sequences (CH_2 insertion into substrate and reactions of $CH_2I^\cdot$ with itself or with $CH_3^\cdot$) of rather good efficiency. It is suggested accordingly that C_2H_4 is a steady-state species, and that most of this substance formed is consumed by reactions with radicals

$$CH_3^\cdot + C_2H_4 \text{ -----> } C_3H_7^\cdot \qquad \text{III-23}$$

$$CH_2I^\cdot + C_2H_4 \text{ -----> } C_3H_6I^\cdot \qquad \text{III-24}$$

$$C_2H_5^\cdot + C_2H_4 \text{ -----> } C_4H_9^\cdot \qquad \text{III-25}$$

Formation of these intermediates would open reaction routes to several additional C_4, C_5, and C_6 products. Although $CH_3^\cdot$ radicals are formed initally in larger yield than $CH_2I^\cdot$, it is very likely to be much more reactive, and hence to exist at lower steady-state concentrations. Particularly relevant in this connection is reaction with the substrate,

$$CH_3^\cdot + CH_3I \text{ ---> } CH_4 + CH_2I^\cdot \qquad \text{III-7}$$

The corresponding reaction of $CH_2I^\cdot$ simply reforms the reactants. It is suggested that the steady-state radical concentrations are in the order $CH_2I^{\cdot} > CH_3^{\cdot} > C_2H_5^{\cdot}$, and that Reaction III-24 occurs to a greater extent than III-23 or III-25. Each of the product species of these Reactions could also react with $CH_2I^{\cdot}$, $CH_3^{\cdot}$, or $C_2H_5^{\cdot}$. Reactions among themselves could occur, but would be much less important. These predicted higher products would be formed according to

$$C_3H_6I^{\cdot} + CH_2I^{\cdot} \longrightarrow C_4H_8I_2^{*} \tag{III-26}$$

$$\longrightarrow C_4H_8 + I_2 \tag{III-27}$$

$$C_3H_6I^{\cdot} + CH_3^{\cdot} \longrightarrow C_4H_9I^{*} \tag{III-28}$$

$$\longrightarrow C_4H_8 + HI \tag{III-29}$$

$$C_3H_6I + C_2H_5^{\cdot} \longrightarrow C_5H_{11}I^{*} \tag{III-30}$$

$$\longrightarrow C_5H_{10} + HI \tag{III-31}$$

where the latter process is of least importance. Following the species $C_3H_7^{\cdot}$ it was predicted

$$C_3H_7^{\cdot} + CH_2I^{\cdot} \longrightarrow C_4H_9I^{*} \tag{III-32}$$

$$\longrightarrow C_4H_8 + HI \tag{III-33}$$

$$C_3H_7^{\cdot} + CH_3^{\cdot} \longrightarrow C_4H_{10} \tag{III-34}$$

$$C_3H_7^{\cdot} + C_2H_5^{\cdot} \longrightarrow C_5H_{12} \tag{III-35}$$

Finally following the intermediate C_4H_9 it was predicted

$$C_4H_9 + CH_2I^{\cdot} \longrightarrow C_5H_{11}I^{*} \tag{III-36}$$

$$\longrightarrow C_5H_{10} + HI \tag{III-37}$$

$$C_4H_9 + CH_3^{\cdot} \longrightarrow C_5H_{12} \tag{III-38}$$

$C_4H_9\cdot + C_2H_5\cdot \dashrightarrow C_6H_{14}$ III-39

These are very minor pathways; and the species C_5H_{10} and C_6H_{14} may well be formed but escape detection. The products of reaction of the postulated C_3 and C_4 radical with I_2 would not be detected, due to experimental difficulties explained earlier. It is likely that C_3H_6 is also a steady-state intermediate similar to C_2H_4, but these are no major pathways leading to its formation. It is apparently less reactive than C_2H_4, since it is found among the products in larger yield. The predominant radicals $CH_3\cdot$, $CH_2I\cdot$, and $C_2H_5\cdot$ are more likely to react with C_2H_4 (present at "finite" concentration) rather than with themselves, since their steady-state concentrations are ca. 10^{-8} molar or less. To the extent that such reactions do occur, resulting products would be C_2H_6, C_2H_5I, C_3H_8, $C_2H_4I_2$, C_3H_7I, and C_4H_{10}.

Although the presence of higher hydrocarbon radicals such as $C_2H_5\cdot$ and $C_3H_7\cdot$ in methyl iodide photolysis is speculative, Gevantman and Williams (77) used radio iodine tracers to demonstrate the presence of these species in the radiolysis of CH_3I, along with the more important intermediates $CH_3\cdot$ and $H\cdot$. While routes to the C_2 and C_3 radicals might be similar under photolysis and radiolysis conditions, the latter conditions can involve ionic pathways not possible in the photolysis experiment.

In the case of methane the reduction of yield with added oxygen is not drastic when compared to that of ethane, implying that "hot" methyl radicals formed in the photolysis of methyl iodide can undergo hydrogen abstraction before they are moderated by collision. Also, the "hot" methyl radical reaction and the quantum yield of methane was seen to increase with an increase in photon energy (28,29,33,35). P. T. McTigue and A. S. Buchanan (78) also observed an increase in the quantum yield of ethane in the presence of silver metal and have attributed this to the blocking and enhancement of the following reactions, respectively.

$$CH_3^{\cdot} + I_2 \longrightarrow CH_3I + I^{\cdot} \qquad \text{III-6}$$

$$CH_3^{\cdot} + CH_3^{\cdot} \longrightarrow C_2H_6 \qquad \text{III-11}$$

The reason for the enhancment was ascribed to the iodine atoms reacting with the silver metal surface, blocking the first of the two above reactions.

An enhanced yield of iodine in the presence of added oxygen was seen in the present work on CH_3I. This effect was also reported by other workers in the methyl iodide system, and is observed in the work on pure CF_3I and CF_3I-CH_3I mixtures as described in Chapters IV and V of this work. The increased iodine yield in the presence of 10% oxygen scavenger implies that in the pure CH_3I system the $CH_3^{\cdot}$ radicals are scavenged efficiently by iodine. Thus the higher yield with added oxygen is due to the reduction of the back reaction

$$CH_3^{\cdot} + I_2 \longrightarrow CH_3I + I^{\cdot} \qquad \text{III-6}$$

by oxygen scavenging the methyl radicals. Similarly, T. Iredale and E.R. McCartney (79) and other workers found that the I_2 quantum yield is increased with the addition of scavengers such as NO and O_2.

In the presence of oxygen, the yields of butane, n-pentane and propene were reduced substantially, but those of C_2H_4, i-C_5H_{12}, and n-C_4H_{10} were completely eliminated.

Although hydrogen was not seen as a product in the photolysis of methyl iodide, trace amounts could be formed through secondary processes such as photolysis of HI, or by molecular elimination from excited higher hydrocarbon intermediates.

C. Summary

The gas phase photolysis of methyl iodide was carried out at 89 torr and 24°C in both pure form and with 10% added oxygen. In the pure system at an absorbed light intensity of 2.68×10^{15} quanta/cc/sec for the regular photolysis vessel and 0.81x10^{15} quant/cc/sec for the I_2 analysis vessel, the products and their respected quantum yields are as follows: diiodo methane, 0.007; ethane, 0.0039; iodine, 0.0032; methane, 0.0028; hydrogen iodide, 0.0017; butene, 3.4x10^{-4}; n-pentane, 1.3x10^{-4}; propene, 8.1x10^{-6}; ethylene, 3.8x10^{-6}; iso-pentane, 1.8x10^{-6} and n-butane, 1.0x10^{-6}. When 10% oxygen is added the quantum yields become the following: iodine, 0.014; diiodomethane, 0.0024; ethane, 2.3x10^{-4}; methane, 0.0016; butene, 1.2x10^{-4}; n-pentane, 6.4x10^{-5}; propene, 1.4x10^{-6}. The results are discussed in terms of both primary and secondary processes.

CHAPTER IV
GAS PHASE PHOTOLYSIS OF TRIFLUOROMETHYL IODIDE

A. Experimental Results

The photolysis of CF_3I was studied at 35 torr pressure and 24°C using radiation of 253.7 nm emitted by a 15 Watt General Electric germicidal lamp for periods between 10 seconds and 10 minutes. As discussed previously the number of quanta absorbed per second per cc at this pressure corresponded to 2.680×10^{15} for the regular photolysis vessels and 0.81×10^{15} for the I_2 analyzing system.

In the photolysis of pure CF_3I, there are two major and five minor products of the decomposition. The major products are I_2 and C_2F_6, with quantum yields of 0.021 and 0.0142, respectively. The minor products and their quantum yields are C_3F_8, $2.1\text{x}10^{-4}$; C_2F_4, $1.1\text{x}10^{-4}$; CF_2I_2, $4.0\text{x}10^{-5}$; $C_2F_4I_2$, $3.5\text{x}10^{-5}$; and CF_4, $2.5\text{x}10^{-5}$. When 10% oxygen was added the quantum yields became the following: I_2, 0.202; C_2F_6, 0.0073; C_3F_8, $1.0\text{x}10^{-4}$; and $C_2F_4I_2$, $7.6\text{x}10^{-6}$. Table 3 presents the summary of quantum yields, the number of molecules formed per quanta of light absorbed. The quantum yields were calculated using the least squares determined slopes of the curves in Figs. 14 through 17. The CF_4 quantum yield was determined by photolysing

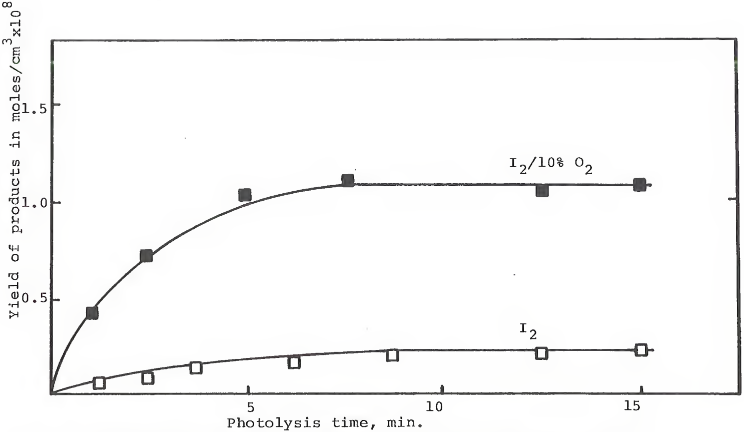

Fig. 14. Production of iodine (pure,□ ; 10% O_2,■) as afunction of photolysis time.

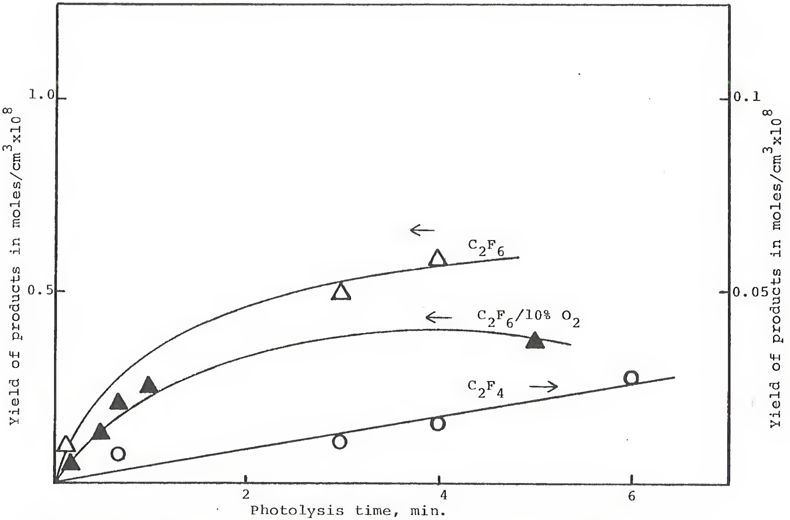

Fig. 15. Production of C_2F_6 (pure, △; 10% O_2, ▲) and C_2F_4 (pure, ○) as a function of photolysis time.

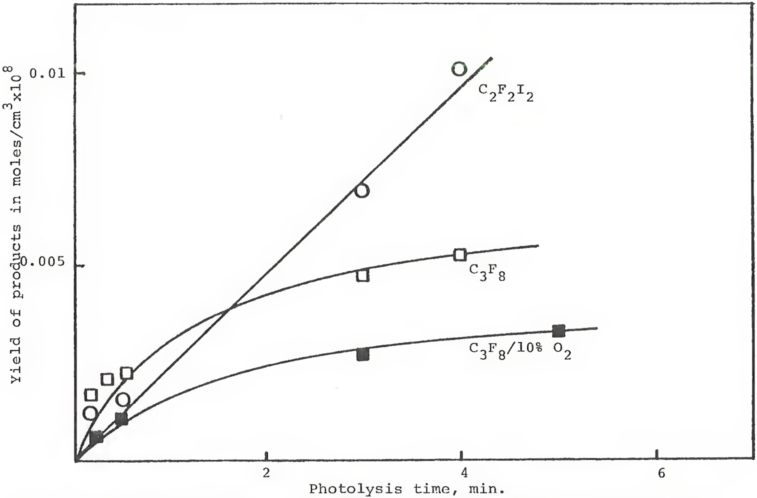

Fig. 16. Production of $C_2F_4I_2$ (pure, ○) and C_3F_8 (pure, □ ; 10% O_2, ■) as a function of photolysis time.

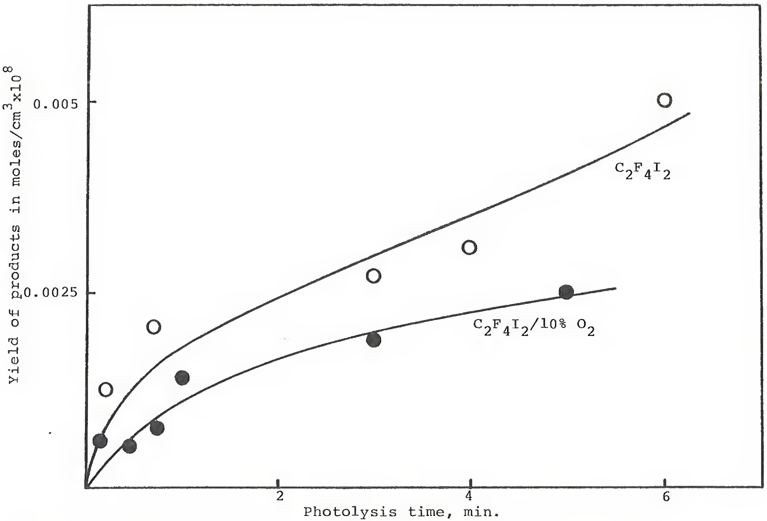

Fig. 17. Production of $C_2F_4I_2$ (pure, ○ ; 10% O_2, ●) as a function of photolysis time.

Table 3

Quantum yields of products formed in the pure CF_3I photolysis system

Product	Quantum Yield	Relative Yield	Quantum Yield with 10% O_2 Added	Relative Yield
I_2	0.021	1.0	0.202	1.0
C_2F_6	0.0142	0.68	0.0073	0.036
C_3F_8	2.1×10^{-4}	0.01	1.0×10^{-4}	5.0×10^{-4}
C_2F_4	1.1×10^{-4}	0.005	a	
CF_2I_2	4.0×10^{-5}	0.0019	a	
$C_2F_4I_2$	3.5×10^{-5}	0.0017	7.6×10^{-6}	3.8×10^{-5}
CF_4	2.5×10^{-5}	3.6×10^{-4}	b	

a. Not seen under this experimental condition.
b. Not measured.

pure CF_3I at a relatively high pressure, 695 torr and a relatively long time, 25 minutes. At the 35 pressure in torr where the other product yields were measured, CF_4 could not be detected because the sensitivity of the flame ionization detector to this compound is extremely poor. Therefore it was analyzed with a thermal conductivity detector.

All product yields were plotted verses photolysis time in Figs. 14 through 17. Overall material balance is only fair in this system with a ratio of C/F/I = 1/3.0/1.4. There is a surplus of I_2 containing compounds, although the ratio of fluorine to carbon in the products is satisfactory. A brief description of these products follows.

B. Discussion

The previous photolysis (14) and radiolysis (20,21,22) studies indicate that the main primary event in the gas phase photolysis of pure CF_3I is the rupture of the C-I bond. This event can be represented by two primary processes.

$$CF_3I \text{ ---> } CF_3^{\cdot} + I^{\cdot}\ (^2P_{1/2}) \qquad \text{IV-1}$$

$$CF_3I \text{ ---> } CF_3^{\cdot} + I^{\cdot}\ (^2P_{3/2}) \qquad \text{IV-2}$$

The production of I $(^2P_{1/2})$ atoms has been shown to occur by Talroze et al. (16) and by Donohue and Wiesenfield (17);

Table 4

Photolysis mechanism in the CF_3I system

PRIMARY PROCESS

$CF_3I \longrightarrow CF_3^{\bullet} + I^{\bullet}(^2P_{1/2})$ IV-1

$CF_3I \longrightarrow CF_3^{\bullet} + I^{\bullet}(^2P_{3/2})$ IV-2

$CF_3I \longrightarrow CF_2{:} + IF$ IV-3

SECONDARY PROCESSES

$I^{*\bullet} + M \longrightarrow I^{\bullet} + M$ IV-4

$I^{\bullet} + I^{\bullet} + M \longrightarrow I_2 + M$ IV-5

$CF_3^{\bullet} + I_2 \longrightarrow CF_3I + I^{\bullet}$ IV-6

$CF_3^{\bullet} + CF_3I \longrightarrow C_2F_6^{*} + I^{\bullet}$ IV-7a

$CF_3^{*\bullet} + CF_3I \longrightarrow C_2F_6 + I^{\bullet}$ IV-7b

$M + C_2F_6^{*} \longrightarrow C_2F_6 + M$ IV-8

$CF_3^{\bullet} + CF_3^{\bullet} + M \longrightarrow C_2F_6 + M$ IV-9

$CF_2I^{\bullet} + I_2 \longrightarrow CF_2I_2 + I^{\bullet}$ IV-10

$CF_3^{\bullet} + CF_3I \longrightarrow CF_4 + CF_2I^{\bullet}$ IV-11 the fraction of $I(^2P_{1/2})$ production is 91% of the total iodine yield in the CF_3I system. It is possible that some or all of the $CF_3^{\bullet}$ radicals may also be excited (23).

The low overall yields in the pure systems indicate that the back Reaction IV-6 plays a significant role in the photolysis of pure CF_3I. The higher yields of iodine observed in the presence of radical scavengers are due to blocking of the back reaction via reaction of the $CF_3^{\bullet}$ radicals with the added scavengers. It has been reported previously (80, 81) that there is no activation energy for Reaction IV-6 and that the corresponding rate constant is 4.32×10^{-12} cm^3 molec.$^{-1}$ s^{-1}. These observations indicate that the gas phase photolysis of pure CF_3I is similar to the photolysis of other alkyl iodides in the gas phase. Unless there is a process to consume $CF_3^{\bullet}$ radicals, the following reactions will occur efficiently.

$$CF_3I \text{ ---> } CF_3^{\bullet} + I^{\bullet}(^2P_{1/2}) \qquad \text{IV-1}$$

$$CF_3I \text{ ---> } CF_3^{\bullet} + I^{\bullet}(^2P_{3/2}) \qquad \text{IV-2}$$

$$I^{*\bullet} + M \text{ ---> } I_{\bullet} + M \qquad \text{IV-4}$$

$$I^{\bullet} + I^{\bullet} + M \text{ ---> } I_2 + M \qquad \text{IV-5}$$

$$CF_3^{\bullet} + I_2 \text{ ---> } CF_3I + I^{\bullet} \qquad \text{IV-6}$$

Although $I(^2P_{1/2})$ can combine with the $I(^2P_{3/2})$ ground state in a reasonably fast 3-body process (82), the majority of the excited iodine atoms are deactivated by collision with the substrate prior to recombination.

It is proposed that reaction of CF_3 radicals with the substrate is the major route to formation of C_2F_6 during steady-state photolysis of CF_3I. Since only 47% of the initial C_2F_6 yield is scavenged by 10% added O_2, it is suggested that a considerable fraction of the $CF_3^{\bullet}$ radical population is born "hot". Along with thermalization, a further minor fate of the "hot" methyl radicals is abstraction of F• from the substrate to give CF_4 and the $CF_2I^{\bullet}$ free radical.

$$CF_3I \text{ ----> } CF_3^* + I(^2P_{1/2}) \qquad \text{IV-1}$$

$$CF_3^{\bullet} + I_2 \text{ ----> } CF_3I + I \qquad \text{IV-6}$$

$$CF_3^{*\bullet} + CF_3I \text{ ----> } C_2F_6^* + I \qquad \text{IV-7a}$$

$$CF_3^{\bullet} + CF_3I \text{ ----> } C_2F_6 + I^{\bullet} \qquad \text{IV-7b}$$

$$CF_3^{*\bullet} + CF_3I \text{ ----> } CF_4 + CF_2I^{\bullet} \qquad \text{IV-11}$$

$$CF_3^{*\bullet} + M \text{ ----> } CF_3^{\bullet} + M \qquad \text{IV-12}$$

The great majority of $CF_3^{\bullet}$ radicals back-react with I_2 in any event, since the primary quantum yield for C-I bond rupture is thought to be unity (as it is for other alkyl halides) whereas the C_2F_6 quantum yield in the unscavenged system is only 0.0142. The marked fall of I_2 and C_2F_6 production rates with increasing dose, as seen in Figs. 14 and 15 is attributed to increasing interference of Reaction IV-6 with Reaction IV-7 as I_2 concentration builds up. The I_2 yield-dose graph reacts a plateau, while the C_2F_6

production rate appears to have a small residual value to beyond 5 minutes photolysis time. The somewhat different behavior of the I_2 yield reflects the fact that it is coupled to several other processes beside Reaction IV-6 and IV-7.

Judging from the quantum yield of 2.7×10^{-5} for CF_4 formation, the efficiency of Reaction IV-11 is very small. The $CF_2I^\cdot$ radicals formed by Reaction IV-11 (or by an alternate route shown below) react with I_2 in the pure system, but are lost via reaction with O_2 in the oxygen scavenged system.

$$CF_2I^\cdot + I_2 \text{ ----> } CF_2I_2 + I^\cdot \qquad \text{IV-10}$$

$$CF_2I^\cdot + O_2 \text{ ----> products} \qquad \text{IV-13}$$

Since CF_2I_2 arises from CF_3^* (or from CF_2: as discussed below) its yield is linear in the unscavenged system, although the reaction sequence is teminated by Reaction IV-13 when oxygen is present.

Additional reactions are considered to describe the minor products in the CF_3I photolysis system. It has been known (83, 84) that $C_2H_5^\cdot$ radicals are produced in small yield in the radiolysis of liquid CH_3I. The precursor to this species could easily be the simple carbene, CH_2. The formation of excited $C_2Cl_6^*$ due to direct insertion of CCl_2 into CCl_4 appears to be an efficient process in the photolysis of CCl_4 (85). Similarly insertion of CF_2 into CF_3I

may account for formation of several minor products, including C_2F_4, C_3F_8 and C_2F_5I.

The most plausible route to formation of CF_2 in this system appears to be a direct photochemical process (of very small yield).

$$CF_3I \text{ ----> } CF_2\!: + IF \qquad \text{IV-3}$$

This process is energetically possible since the energy requirement computed by bonds broken-bonds formed is ca. 105 + 54 - 67 = 92 kcal, whereas 254 nm photons have 112.7 kcal/mole energy (86). As suggested in Chapter IV above for CH_3I photolysis, Reaction IV-3 may not represent an independent primary process of isolated CF_3I molecules; it might occur only if the reactant is in collision with or bound to another molecule or the vessel walls. The total quantum yield of all detected products thought to arise via this species is only 2×10^{-4}.

Starting with the difluoro carbene intermediate, a straightforward reaction sequence leads to most of the minor products in the CF_3I photolysis system.

$$CF_2 + CF_3I \text{ ----> } C_2F_5I^* \qquad \text{IV-14}$$

$$C_2F_5I^* \text{ ----> } C_2F_5^{\cdot} + I^{\cdot} \qquad \text{IV-15}$$

$$C_2F_5I^* \text{ ----> } CF_3^{\cdot} + CF_2I^{\cdot} \qquad \text{IV-16}$$

$$\text{ ----> } C_2F_4 + IF \qquad \text{IV-17}$$

$$C_2F_5^{\cdot} + CF_3I \text{ ----> } C_3F_8 + I^{\cdot} \qquad \text{IV-18}$$

$C_2F_5^{\bullet} + I_2 \longrightarrow C_2F_5I + I^{\bullet}$ IV-19

Since one bond is broken but two strong bonds are formed by the insertion of CF_2 into CF_3I, Reaction IV-14, the resulting C_2F_5I should be excited to the extent of approximately 75 kcal. Reaction IV-17 gives an account for the production of the minor product C_2F_4. Reactions IV-18 and IV-19 may be the only source accounting for production of C_3F_8 and a small (undetected) yield of C_2F_5I.

Formation of $C_2F_4I_2$ can arise from reaction of iodine atoms with C_2F_4

$I^{\bullet} + C_2F_4 \rightleftarrows C_2F_4I^{\bullet}$ IV-20

$C_2F_4I^{\bullet} + I_2 \longrightarrow C_2F_4I_2 + I$ IV-21

This reaction scheme would suggest that the $C_2F_4I_2$ yield curve would parallel the C_2F_4 graph, which is linear. It is possible that $C_2F_4I_2$ is attacked by $CF_3^{\bullet}$ radicals, since the C-I bonds in the former are probably very weak

$CF_3^{\bullet} + C_2F_4I_2 \longrightarrow CF_3I + C_2F_4I^{\bullet}$ IV-22

The yield of $C_2F_4I_2$ is so small that this reaction would have an imperceptible influence on other product yields. If Reactions IV-20 and 21 correctly account for $C_2F_4I_2$ formation, it follows that at least a small yield of C_2F_4 must persist when O_2 is added. Since the C_2F_4 chromatographic peak falls on the tail of the C_2F_6 peak, a yield in the O_2 scavenged system which was 10% of the scavenged value would be hard to detect. A lower steady state concentration of $C_2F_4I\cdot$ in the quasi-equilibrium Reaction IV-20 would be counterbalanced by a much higher I_2 concentration, so that the rate of Reaction IV-21 would show only a moderate fall-off.

In the present work all the photolysis was done for relatively short times to avoid photolysis of products. The maximum product conversion at 6 minutes photolysis time was about 1%.

The photolysis of CF_3I was investigated three decades ago by Dacey (14) using a 253.7 nm mercury resonance lamp. Formation of C_2F_6 and I_2 was reported with low quantum yields at lower pressure than employed in the present work. However, at pressures above 10 torr, small amounts of polymer were seen, presumably formed from C_2F_4.

C. Summary

The photolysis of gas phase CF_3I was investigated at 35 torr pressure and 24°C, in both pure form and with added oxygen as a scavenger. For the pure system seven products were identified and their quantum yields were determined. The major products are I_2 and C_2F_6, respectively, and the minor products are C_3F_8, C_2F_4, CF_2I_2, $C_2F_4I_2$ and CF_4. The addition of 10% O_2 reduced or completely scavenged all products, except that the I_2 production is enhanced. The results are discussed in terms of primary and secondary processes involving rupture of the C-I bond to form $CF_3^{\cdot}$ radicals and iodine atoms, which are precursors to major product yields, as well as small yields of CF_4 and CF_2I_2. It is suggested that difluorocarbene is formed along with IF in a very minor primary process. Difluorocarbene is the precursor of small yields of several products including C_2F_4, C_3F_8, and $C_2F_4I_2$.

CHAPTER V
PHOTOLYSIS OF EQUIMOLAR MIXTURES OF METHYL IODIDE-TRIFLUOROMETHYL IODIDE

A. Experimental Result

The photolysis of equimolar mixtures of methyl iodide and trifluoromethyl iodide was studied at 50 torr pressure and at room temperature (24°C) using radiation of 253.7 nm wavelength emitted by a 15 watt General Electric germicidal lamp for periods between 10 seconds (0.17 minutes) and 20 minutes. As discussed in section C, part 2 of chapter II, the number of quanta absorbed per second per cc at this pressure corresponds to 2.680×10^{15} for the regular photolysis vessels and 0.81×10^{15} for the I_2 analyzing vessel.

Thirteen compounds were identified in the photolysis of methyl iodide-trifluoromethyl iodide equimolar mixtures as seen in Figs. 18 to 26. The major and minor products with their respective initial quantum yields are CH_2I_2, 0.0087; I_2, 0.0026; CH_4, 0.0022; 1,1-CH_2CF_2, 0.0022; C_2H_6, 0.0021; C_2F_6, 0.0018; CF_3H, 0.0011; HF, 2.7×10^{-4}; C_2H_4, 2.2×10^{-4}; C_2F_5I, 1.9×10^{-4}; 1,1,1-CF_3CH_3, 4.7×10^{-5}; CF_4, 2.06×10^{-5} and HI, 1.8×10^{-5}. (Quantum yields of CH_4 and

C_2H_4 show an induction period; see below.) The yield of CF_4 was determined by photolysing the equimolar mixture at a total pressure of 300 torr and a relatively longer photolysis time of 35 minutes, using a thermal conductivity detector, since CF_4 has an extremely poor sensitivity in the flame ionization detector. It could not be detected at 50 torr total pressure where the other products were determined. In the presence of 10% added oxygen as a scavenger-iodine was formed in substantial yield. The I_2 quantum yield increased from 0.0026 to 0.024. The other product yields decreased substantially. Table 5 presents a summary of quantum yields, the number of molecules formed per quantum of light absorbed. The quantum yields were calculated using the least squares determined slopes of the curves in Figs. 18 through 26 except for the I_2 yield in Fig. 18, the CH_4 yield in Fig. 22, and the C_2H_4 yield in Fig. 24. The CH_4 yield shows an initial slow-production regime with a quantum yield of 0.0022 up to about 20 seconds, and a more rapid linear production with a quantum yield of 0.0052 from 20 seconds to beyond 60 seconds. The C_2H_4 yield is very small at times less than 10 seconds with a quantum yield of 8.0×10^{-6} , increases to about a quantum yield of 1.7×10^{-5} from 10 to 40 seconds, and falls off at longer times. Iodine yields are maximum at short photolysis time; the yields decrease at longer times, with I_2 concentration eventually reaching a steady-state. (It was

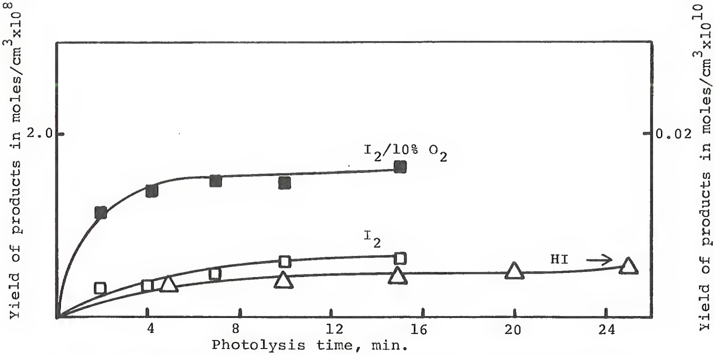

Fig. 18. Production of HI (pure, △), I_2 (pure, □; 10% O_2, ■) as a function of photolysis time.

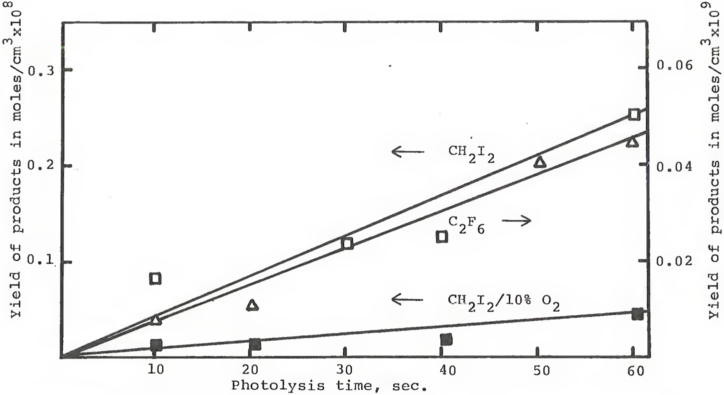

Fig. 19. Production of CH$_2$I$_2$ (pure, □; 10% O$_2$, ■) and C$_2$F$_6$ (pure, △) as a function of photolysis time.

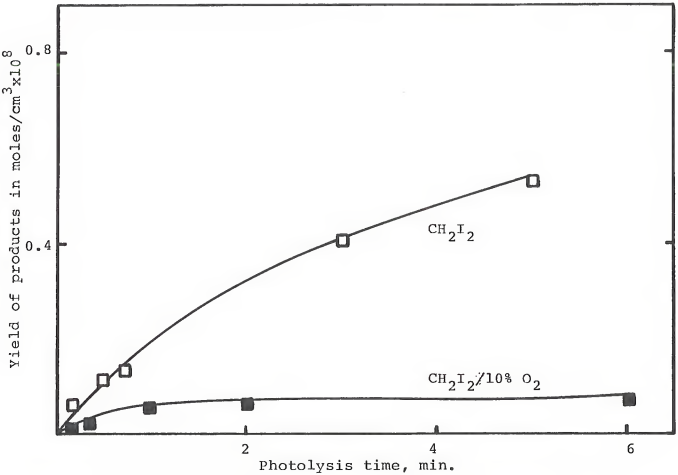

Fig. 20. Production of CH_2I_2 (pure, □; 10% O_2, ■) as a function of photolysis time.

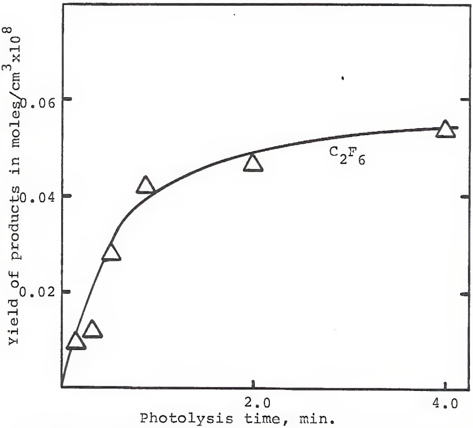

Fig. 21. Production of C_2F_6 (pure, △) as a function of photolysis time.

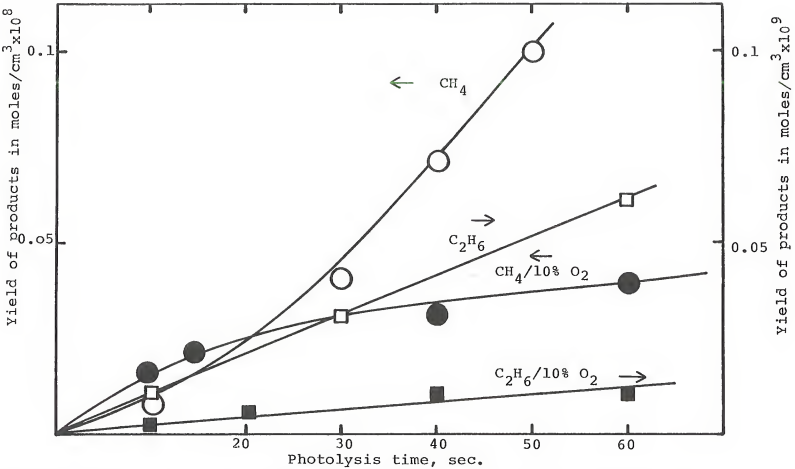

Fig. 22.Production of CH_4 (pure, ○ ; 10% O_2, ●) and C_2H_6 (pure, □; 10% O_2, ■) as a function of photolysis time.

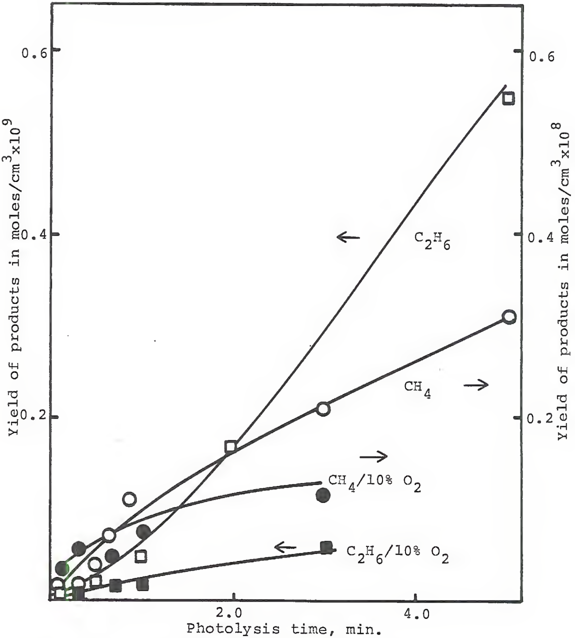

Fig. 23. Production of CH_4 (pure,○ ; 10% O_2,●) and C_2H_6 (pure,□ ; 10% O_2,■) as a function of photolysis time.

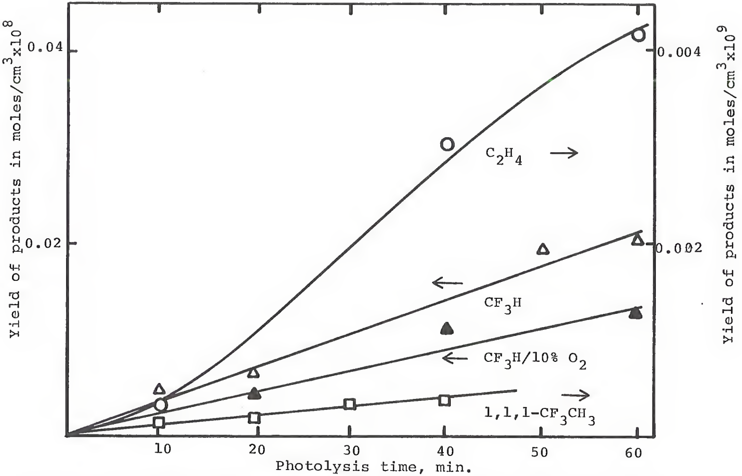

Fig. 24. Production of C_2H_4 (pure, ○), CF_3H (pure, △; 10% O_2, ▲) and 1,1,1-CF_3CH_3 as a function of photolysis time.

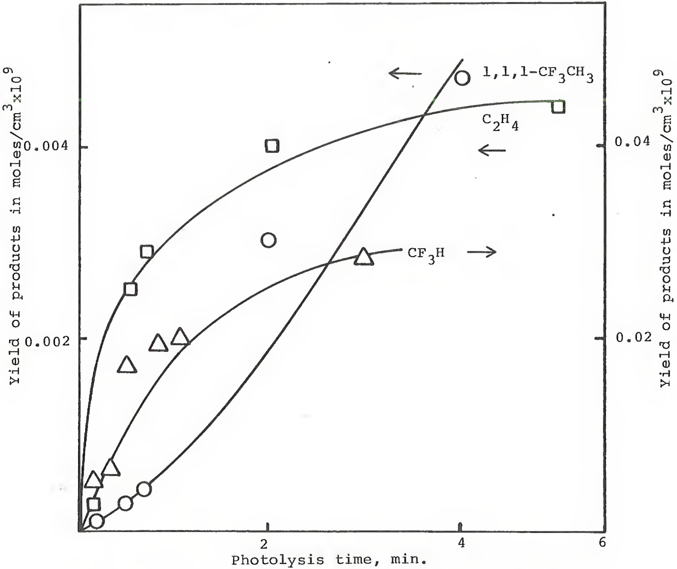

Fig. 25. Production of CF_3H (pure, △), 1,1,1-CF_3CH_3 (pure, ○) and C_2H_4 (pure, □) as a function of photolysis time.

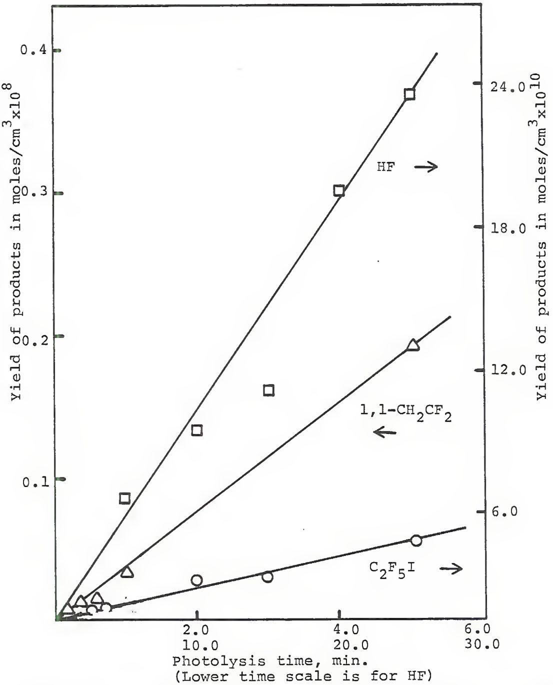

Fig. 26. Production of HF (pure, □), 1,1-CH_2CF_2 (pure, △) and C_2F_5I (pure, ○) as a function of photolysis time.

Table 5

Quantum yields[a] of photolysis products from methyl iodide - trifluoromethyl iodide equimolar mixtures at 50 Torr total pressure

Product	Quantum Yield	Relative Yield	Quantum Yield With 10% O_2 Added	Relative Yield
CH_2I_2	0.0087	1.0	0.0011	0.045
I_2[b]	0.0026	0.29	0.024[c]	1.0
CH_4	0.0022[d]	0.25	0.0033	0.14
1,1-CH_2CF_2	0.0022	0.25	e	-
C_2H_6	0.0021	0.24	$3.7\mathrm{x}10^{-4}$	0.015
C_2F_6	0.0018	0.24	e	-
CF_3H	0.0011	0.13	$3.1\mathrm{x}10^{-4}$	0.013
HF[b]	$2.7\mathrm{x}10^{-4}$	0.03	f	-
C_2F_5I	$1.9\mathrm{x}10^{-4}$	0.022	$2.8\mathrm{x}10^{-5}$	0.0012
1,1,1-CF_3CH_3	$4.7\mathrm{x}10^{-5}$	0.0054	e	-
CF_4[b]	$2.1\mathrm{x}10^{-5}$	0.0021	e	-
HI[b]	$1.8\mathrm{x}10^{-5}$	0.0021	f	-
C_2H_4	$8.0\mathrm{x}10^{-6}$[g]	$9.2\mathrm{x}10^{-4}$	e	-

a Quantum yields are least-square fits to essentially straight- line yield graphs measured from 0 to 60 sec., unless otherwise indicated.
b Photolysis was carried out at a relativily longer time.
c This value is from 0 to 2 min. of photolysis time.
d This value was measured from 0 to 20 secs of photolysis time and increased to 0.0052 from 20 to 60 s. Value given for added oxygen measured from 0 to 20 s.
e Not seen under this condition.
f Not measured.
g This value measured from 0 to 10 s.and $1.7\mathrm{x}10^{-5}$ from 10 to 60 s.

difficult experimentally to measure I_2 concentrations at time shorter than two minutes.) Yields for CH_4, C_2H_4, and I_2 (in the presence of added O_2) were obtained by best visual fit of tangents to the yield-time curves. All product yields were plotted as a function of time of photolysis in Figs. 18 through 26.

Overall material balance is fairly satisfactory in this system, with a ratio of C/(H + F)/I = 1.04 / (2.58 + 0.83) / 1.00 or 1.04/3.41/1.00. There is a small excess of fluorine plus hydrogen as compared to carbon and iodine. Considerably larger yields of hydrogen-containing products were found, as compared to fluorine-containing products, probably due to difference in reactivity with respect to secondary reactions rather than to difference in primary quantum yields. A brief description of these results follows.

B. Discussion

With the exception of the formation of cross-products containing both fluorine and hydrogen, the pattern of product yields, yield-dose behavior, and response to added oxygen in the photolysis of CF_3I - CH_3I mixtures all show a marked resemblance to the corresponding aspects of the photolysis of the two pure compounds, as described in Chapters III and IV of this Dissertation. Accordingly, the mechanism presented below (and summarized in Table 6) is

Table 6
Photolysis mechanism in the CH_3I–CF_3I system

PRIMARY PROCESSES

$$CH_3I \longrightarrow CH_3^{\bullet} + I^{\bullet}(^2P_{1/2}) \tag{V-1}$$

$$CH_3I \longrightarrow CH_3^{\bullet} + I^{\bullet}(^2P_{3/2}) \tag{V-2}$$

$$CF_3I \longrightarrow CF_3^{\bullet} + I^{\bullet}(^2P_{1/2}) \tag{V-3}$$

$$CF_3I \longrightarrow CF_3^{\bullet} + I^{\bullet}(^2P_{3/2}) \tag{V-4}$$

SECONDARY PROCESSES

$$I^{*\bullet} + M \longrightarrow I^{\bullet} + M \tag{V-5}$$

$$I^{\bullet} + I^{\bullet} + M \longrightarrow I_2 + M \tag{V-6}$$

$$CH_3^{\bullet} + CH_3I \longrightarrow CH_4 + CH_2I^{\bullet} \tag{V-7}$$

$$CH_2I^{\bullet} + I_2 \longrightarrow CH_2I_2 + I^{\bullet} \tag{V-8}$$

$$CH_3^{*\bullet} + CH_3I \longrightarrow C_2H_6^{*} + I^{\bullet} \tag{V-9}$$

$$C_2H_6^{*} + M \longrightarrow C_2H_6 + M \tag{V-10}$$

$$CF_3^{\bullet} + CH_3I \longrightarrow CF_3H + CH_2I^{\bullet} \tag{V-11}$$

$$CF_3^{*\bullet} + CF_3I \longrightarrow C_2F_6^{*} + I^{\bullet} \tag{V-12}$$

$$C_2F_6^{*} + M \longrightarrow C_2F_6 + M \tag{V-13}$$

$$CH_3^{\bullet} + CF_3I \longrightarrow CF_3CH_3^{*} + I \tag{V-14}$$

$$CF_3^{\bullet} + CH_3I \longrightarrow CH_3CF_3^{*} + I \tag{V-15}$$

$$CF_3CH_3^{*} + M \longrightarrow CH_3CF_3 + M \tag{V-16}$$

$$CF_3CH_3^{*} \longrightarrow CH_2CF_2 + HF \tag{V-17}$$

$$CH_3^{\bullet} + CH_3^{\bullet} \longrightarrow C_2H_6 \tag{V-18}$$

$$CF_3^{\bullet} + CF_3^{\bullet} \longrightarrow C_2F_6 \tag{V-19}$$

$$CF_3^{\bullet} + CF_3I \longrightarrow CF_4 + CF_2I^{\bullet} \tag{V-20}$$

largely similar to those presented for the two pure systems. Cross-reactions which yield fluoro-hydrocarbon products will be emphasized in the discussion.

The previous studies on the photolysis (14, 28, 31, 32, 34) and radiolysis (41,42-46) of pure methyl iodide and pure trifluoromethyl iodide in the gas phase as well as other iodides (40) indicate the primary process to be the rupture of the C-I bond, as presented below.

$$CH_3I \dashrightarrow CH_3^{\bullet} + I^{\bullet}(^2P_{1/2}) \qquad \text{V-1}$$

$$CH_3I \dashrightarrow CH_3^{\bullet} + I^{\bullet}(^2P_{3/2}) \qquad \text{V-2}$$

$$CF_3I \dashrightarrow CF_3^{\bullet} + I^{\bullet}(^2P_{1/2}) \qquad \text{V-3}$$

$$CF_3I \dashrightarrow CF_3^{\bullet} + I^{\bullet}(^2P_{3/2}) \qquad \text{V-4}$$

It is possible (23,24) that a major proportion of the radicals $CH_3^{\bullet}$, $CF_3^{\bullet}$ and $I^{\bullet}$ may be excited.

As shown in Reactions V-5 and V-6 of Table 6, the excited iodine atoms in the $^2P_{1/2}$ state mainly become deactivated by collisions with the substrates.

$$I^{*}\cdot(^2P_{1/2}) + M \dashrightarrow I^{\bullet}(^2P_{1/2}) + M \qquad \text{V-5}$$

Then these deactivated iodine atoms combine to form I_2 as a product.

$$I^{\bullet} + I^{\bullet} + M \dashrightarrow I_2 + M \qquad \text{V-6}$$

Most of the I_2 product will back react with methyl and trifluoromethyl radicals to form the substrates as presented below

$CH_3^{\bullet} + I_2 \longrightarrow CH_3I + I^{\bullet}$ V-21

$CF_3^{\bullet} + I_2 \longrightarrow CF_3I + I^{\bullet}$ V-22

Since the amount of iodine accumulated in a few seconds (or even less) will be sufficient to completely inhibit radical-radical routes to organic products due to Reactions V-21 and V-22, it follows that other routes such as radical-substate or carbene insertion processes must account for formation of most final products. The nature of the product spectrum indicates that the former processes are more important at short photolysis times. In the mixed system, hydrocarbon radical-hydrocarbon substrate and fluorocarbon radical-fluorocarbon substrate processes will occur, as in the pure systems. Fluorocarbon radical-hydrocarbon substrate processes are also expected, and are confirmed by the observed products. Hydrocarbon radical abstraction on fluorocarbon substrate is thought to be unimportant, due to the greater stability of the latter substrate, but iodine displacement upon reaction of $CH_3^{\bullet}$ radical with CF_3I should be favorable. Postulated abstraction and displacement processes are as follows.

$CH_3^{*}{\bullet} + CH_3I \longrightarrow CH_4 + CH_2I^{\bullet}$ V-7

$CH_3^{*}{\bullet} + CH_3I \longrightarrow C_2H_6^{*} + I^{\bullet}$ V-9

$C_2H_6^{*} + M \longrightarrow C_2H_6 + M$ V-10

$CF_3^{\cdot} + CH_3I \rightarrow CF_3H + CH_2I^{\cdot}$ V-11

$CF_3^{\cdot} + CF_3I \rightarrow C_2F_6^{*} + I^{\cdot}$ V-12

$C_2F_6^{*} + M \rightarrow C_2F_6 + M$ V-13

$CH_3^{\cdot} + CF_3I \rightarrow CH_3CF_3^{*} + I^{\cdot}$ V-14

$CF_3^{\cdot} + CH_3I \rightarrow CF_3CH_3^{*} + I^{\cdot}$ V-15

$CF_3CH_3^{*} + M \rightarrow CF_3CH_3 + M$ V-16

$CF_3CH_3^{*} \rightarrow CF_2CH_3^{*} + HF$ V-17

$CF_3^{\cdot} + CF_3I \rightarrow CF_4 + CF_2I^{\cdot}$ V-20

The ethanes produced in Reactions V-9, V-10, V-12 and V-13 are shown to be excited because the C-C bonds formed are ca. 30 kcal stronger than the C-I bonds broken, aside from the fact that the reactant methyl radicals may contain energy in excess of the thermal expectation. The fate of the three excited ethanes is considered further below.

Diiodomethane was found to be a prominent product in the equimolar mixture as it was in pure methyl iodide photolysis. Its formation could be explained through the reaction of I_2 with $CH_2I^{\cdot}$ as shown in Reaction V-8.

$CH_2I^{\cdot} + I_2 \rightarrow CH_2I_2 + I^{\cdot}$ V-8

The corresponding product CF_2I_2 expected through the reaction of $CF_2I^{\cdot}$ with I_2 was not observed in the present work. Even in the photolysis of pure CF_3I as described in Chapter IV of this dissertation, CF_2I_2 was reported as one of the minor products.

Reaction V-7 which is the main route for CH_4 formation has an activation energy of less than 8 kcal/mole (29).

$$CH_3{}^{\bullet} + CH_3I \dashrightarrow CH_4 + CH_2I^{\bullet} \qquad V\text{-}7$$

The yield of methane upon addition of oxygen increases up to 20 seconds of photolysis time and thereafter decreases compared to the unscavenged methane product.

The yield of CF_4, which is hardly more than a trace, can be accounted for by a reaction analogous to the process which forms methane.

$$CF_3{}^{\bullet} + CF_3I \dashrightarrow CF_4 + CF_2I^{\bullet} \qquad V\text{-}20$$

The activation energy for Reaction V-20 has been estimated (48) to be less than 3 kcal/mole on the assumption that 88-90% of the energy of the bond formed is available to aid the bond breakage processes (87). The reaction may have a low steric factor due to the presence of so many electronegative substituents, however.

Young and Willard (70) suggested for the photolysis and radiolysis of CCl_3Br a reaction similar to Reactions V-7 and V-20 to account for the formation of CCl_4 and CCl_2Br_2, the main products observed in thier system.

Other reaction pathways competing with Reactions V-7 and V-20 involving the same reacting species are proposed as the main processes for ethane and hexafluoroethane formation.

$$CH_3^{\bullet} + CH_3I \dashrightarrow C_2H_6^{*} + I^{\bullet} \qquad \text{V-9}$$

$$CF_3^{\bullet} + CF_3I \dashrightarrow C_2F_6^{*} + I^{\bullet} \qquad \text{V-12}$$

The excited ethanes are presumably deactivated by collision with substrate.

The other important product observed in the equimolar mixture is 1,1-CF_2CH_2 and its route of formation is described below along with the products HF and 1,1,1-CF_3CH_3, since their origins are interelated. The "hot" $CF_3^{\bullet}$ and $CH_3^{\bullet}$ radicals can attack the substrates CH_3I and CF_3I as shown in Reactions V-14 and V-15 to form excited 1,1,1-$CF_3CH_3^{*}$ which becomes stabilized collisionally to form CF_3CH_3 as indicated in Reaction V-16 or decompose to form CH_2CF_2 and HF as in Reaction V-17.

$$CH_3^{\bullet} + CF_3I \dashrightarrow CH_3CF_3^{*} + I^{\bullet} \qquad \text{V-14}$$

$$CF_3^{\bullet} + CH_3I \dashrightarrow CH_3CF_3^{*} + I^{\bullet} \qquad \text{V-15}$$

$$CH_3CF_3^{*} + M \dashrightarrow CH_3CF_3 + M \qquad \text{V-16}$$

$$CH_3CF_3^{*} \dashrightarrow CH_2CF_2 + HF \qquad \text{V-17}$$

Decomposition of CH_3CF_3 to CH_2CF_2 and HF was observed by Alcok and Whittle (88) in 1965 in the photolysis of hexafluoroacetone in the presence of methyl iodide at 300 nm wavelength. Since then has been observed by other investigators (89,90).

Concerning the route of formation of CF_3H in the equimolar mixture, it is possible for CF_3 radical to abstract hydrogen from CH_3I as follows:

$$CF_3^{\cdot} + CH_3I \dashrightarrow CF_3H + CH_2I^{\cdot} \qquad \text{V-11}$$

This reaction is nearly thermoneutral or slightly exothermic for thermal $CF_3^{\cdot}$ radicals, and may have an activation energy of ca. 10 kcal/mole. It would occur more rapidly with "hot" $CF_3^{\cdot}$ radicals.

R.A. Fass and J.E. Willard (23) observed low quantum yields of CF_3H ($\leq 0.05 \times 10^{-4}$) from photolysis of CF_3I in the presence of methane at 253.7 nm. The above reaction should be more favorable as compared with the photolysis of CF_3I in the presence of CH_4, since the C-H bond in CH_3I is weaker than in CH_4. The photolysis of CF_3I at 253.7 nm in the presence of two or three carbon containing hydrocarbon molecules increases the quantum yield of CF_3H. This is because abstraction by the "hot" or thermal CF_3 radical is "easier" for tertiary than for secondary and for secondary than primary hydrogen atoms.

Similarly, C. L. Kibby and R. E. Weston (91) found the quantum yield of CF_3H $< 5 \times 10^{-6}$ in the photolysis of CF_3I in the presence of CH_3I at 253.7 nm and room temperature where the mixture's concentration was 0.15×10^{-3} moles for CF_3I and 0.27×10^{-3} moles for CH_3I. The yield of CF_3H was decreased by 72% in the presence of 10% added oxygen.

Even though hydrogen was not seen as a product, a trace amount could be accounted for through photolysis of products such as HI, or via elimination from higher carbon-number hydrocarbon compounds that contain residual excitation energy.

The formation of HF should occure through reactions of $CH_3\cdot$ and $CF_3\cdot$ with CF_3I or CH_3I followed by elimination.

$$CF_3CH_3^* \text{ --> } C_2H_2F_2 + HF \qquad \text{V-17}$$

Even though the yield of HI is small compared to that in pure CH_3I photolysis, its formation would be through one of the several routes suggested in the photolysis of pure CH_3I in the gas phase as described in chapter III of this work.

Molecular iodine has only one major route of formation as shown below.

$$I\cdot + I\cdot + M \text{ --> } I_2 + M \qquad \text{V-6}$$

As described above and in the Introduction of Chapter I, it is obvious that much of I_2 will back react with $CF_3\cdot$ and $CH_3\cdot$ radicals.

Additional reaction schemes are suggested for the minor products in this system. It has been reported (73,74) that $C_2H_5\cdot$ radicals are produced in small yield in the radiolysis of liquid methyl iodide. The precursor to this species could be the simple carbene, CH_2. The formation of excited C_2Cl_6 due to the direct insertion of $CCl_2\cdot$ into CCl_4 appears to be an efficient route in the photolysis of CCl_4 (85). It is proposed that insertion of CH_2 and CF_2 carbenes into the substrates account for formation of several minor products in this system.

$$CF_2 + CF_3I \dashrightarrow C_2F_5I^* \qquad V\text{-}23$$

$$C_2F_5I^* + M \dashrightarrow C_2F_5I + M \qquad V\text{-}24$$

$$C_2F_5I^* \dashrightarrow C_2F_4 + IF \qquad V\text{-}25$$

$$C_2F_5I^* \dashrightarrow CF_3\cdot + CF_2I\cdot \qquad V\text{-}26$$

Similarly for CH_2:

$$CH_2\!: + CH_3I \dashrightarrow C_2H_5I^* \qquad V\text{-}27$$

$$C_2H_5I^* + M \dashrightarrow C_2H_5I + M \qquad V\text{-}28$$

$$C_2H_5I^* \dashrightarrow C_2H_4 + HI \qquad V\text{-}29$$

There is ample evidence that methylene reacts with methane (92,93) to form excited ethane.

$$CH_2 + CH_4 \dashrightarrow C_2H_6^* \qquad V\text{-}30$$

This activated molecule is either stablized by collision or dissociates to give free radical fragments or two neutral molecules, C_2H_4 and H_2.

Although the several alkyl radicals present in the system are certainly capable of reacting with iodine atoms,

$$R\cdot + I\cdot \dashrightarrow RI \qquad V\text{-}31$$

such reactions are not expected in the present system. A small fraction of the radicals present interact with the reactive CF_3I and CH_3I substrates, and those which escape this fate will react with molecular iodine.

As postulated originally by Benson, formation of C_2H_4 most likely occurs via elimination of HI from excited $C_2H_5I^*$ as in the photolysis of pure CH_3I. However, the excited ethyl iodide is thought to arise via carbene insertion into substrate rather than by radical-radical combination. An additional route is suggested by the reaction below

$$CH_3^* + CH_3I \dashrightarrow C_2H_6^* + I\cdot \qquad \text{V-9}$$

The ethane formed by this reaction could easily have sufficient energy for decomposing to form C_2H_4 and H_2 (87). As from the considering energy carried by the "hot" methyl radical, the process is 30 kcal/mole exoergic due to the difference in energy for the C-I bond broken and the C-C bond formed. Ethylene had been reported in CH_3I photolysis (29,32) in other laboratories as well as in this work. It was also seen in the radiolysis of CH_3I (1), in the photolysis of CH_3I in the gas phase in the present work as well as in the radiolysis of mixtures of CH_3I-CF_3I (94).

The yield of I_2 in the presence of oxygen was enhanced substantially, suggesting that the two back reactions with $CF_3\cdot$ and $CH_3\cdot$ were blocked due to the reactions of O_2 with

$CH_3\cdot$ and $CF_3\cdot$ radicals.

$$CH_3\cdot + O_2 \dashrightarrow CH_3O_2 \qquad \text{V-32}$$

$$CF_3\cdot + O_2 \dashrightarrow CF_3O_2 \qquad \text{V-33}$$

I. Mcalpine and H. Sutcliffe (21) reported that the iodine yield in the presence of scavenger was much higher than in the unscavenged radiolysis of gas phase CF_3I. They suggested that $CF_3\cdot$ radicals are scavenged by I_2 effectively in the CF_3I system. Therefore, the high yields of I_2 in the CH_3I - CF_3I scavenged system means the back reactions represented by Reactions V-21 and V-22 are reduced by the oxygen scavenging the $CF_3\cdot$ and $CH_3\cdot$ radicals. Under conditions where radical-radical reactions are significant, addition of O_2 would also block the direct back reaction between $I\cdot$ and $CF_3\cdot$ or $CH_3\cdot$.

The product yield of C_2H_6 was greatly reduced in the presence of oxygen in the system and C_2F_6 was completely eliminated, suggesting that Reactions V-9 and V-12 are the only important routes leading to their formation. The yields of CH_3CF_3 and CH_2CF_2 were also eliminated in the presence of added oxygen, implying that these products are formed exclusively from radical reactions.

C. Summary

The gas phase photolysis of an equimolar mixture of methyl iodide and trifluoromethyl iodide was studied at 50

Torr total pressure (25 Torr of each) both pure and with 10% added oxygen. For the pure system, thirteen products were identified and their quantum yields have been determined. The products identified were CH_2I_2 I_2, CH_4, 1,1-CH_2CF_2, C_2H_6, C_2F_6, CF_3H, HF, C_2H_4, C_2F_5I, 1,1,1-CF_3CH_3, CF_4 and HI. The addition of 10% oxygen reduced the products yields significantly except the I_2 yield which was enhanced. The results are discussed in terms of bond breaking primary processes and secondary abstraction and displacement reaction processes. The C-I bonds in CF_3I and CH_3I have almost the same strength, so that primary C-I bond rupture of both compounds is comparably efficient. The yields of hydrocarbon products exceed the yields of perfluorocarbon products. It is concluded that attack of perfluoro intermediates on the CH_3I substrate is considerably more likely than the inverse situation.

CHAPTER VI

ION-MOLECULE REACTIONS IN THE SYSTEMS OF METHYL IODIDE, TRIFLUOROMETHYL IODIDE AND EQUIMOLAR MIXTURES OF METHYL IODIDE-TRIFLUOROMETHYL IODIDE

A. Introduction

The primary processes which lead to formation of reactive intermediates in the gamma radiolysis of organic compounds include excitation and ionization steps. Thus insight on the primary event in radiation chemistry may be obtained by studying the photochemistry and mass spectrometry of the reactant molecules. As described in Chapter I of this Dissertation, the present research was undertaken to provide background information relevant to studies of the radiation chemistry of gas phase CF_3I-CH_3I mixtures. Chapter III, IV, and V of this work described the photolysis of pure CH_3I, pure CF_3I and equimolar CF_3I-CH_3I mixtures, respectively, as well as reviewing the relevant literature (11-16, 29-36). This chapter describes investigations of the gas phase ion chemistry of pure CH_3I, pure CF_3I and CF_3I-CH_3I equimolar mixtures.

Gas phase ion-chemistry of pure CH_3I (5,7,95) and pure CF_3I (62,96) was the subject of several previous investigations. Much of the work was done with hardware possessing limited capabilities, however, and was mostly of a qualitative nature. One of the previous report on the ion-molecule reaction chemistry of CF_3I was done in this laboratory (8), but the ICR instrument has been considerably improved since that work was completed, and a reinvestigation of the subject appeared in order. No previous work on gas phase ion chemistry of CF_3I-CH_3I mixtures has been reported.

The section below described investigations which were done on pure CF_3I, pure CH_3I and equimolar CF_3I-CH_3I mixtures, respectively. The studies on the two pure compounds were done in the Ion Cyclotron Resonance (ICR) mass spectrometer, while the work on eqimolar mixtures utilized both the ICR and Time-of-Flight (TOF) instruments.

Now, the discussion which follows will be classified into systems of pure CF_3I, pure CH_3I and the equimolar mixtures of CH_3I-CF_3I.

B. CH_3I System

1. Experimental Results

Ion-molecule reactions in gas phase CH_3I were reinvestigated using a modified ICR mass spectrometer. Figures 27 and 28 display, respectively, a partial mass spectrum taken at a relatively low pressure and short reaction time,

Table 7

Experimental rate constants and ion-molecule reactions in the CH_3I system

Reaction	k(exp)[a]	Comments
$CH_3^+ + CH_3I \longrightarrow$ product	19.9 ± 1.2	
$CH_3^+ + CH_3I \longrightarrow CH_4 + CH_2I^+$	< 0.2	
$CH_3^+ + CH_3I \longrightarrow CH_3I^+ + CH_3\cdot$	~ 19	
$I^+ + CH_3I \longrightarrow I\cdot + CH_3I^+$	9.7 ± 2.8	
$CH_3I^+ + CH_3I \longrightarrow$ Products	0.34 ± 0.12	
$\longrightarrow I + CH_3ICH_3^+$	0.24	ICDR[b,c]
$\longrightarrow CH_3\cdot + CH_3I_2^+$	0.15	ICDR[b]
$CH_3ICH_3^+ \longrightarrow$ Products	0.09 ± 0.02	

[a] All k's are in cm^3 $molec.^{-1}$ s^{-1} $x10^{+10}$.

[b] ICDR means the reactions was verified by ICR double resonance experiments.

[c] Literature value 0.237 ± 0.005 (97).

showing some of the primary ions in this system, and a spectrum which contains several major ion-molecule condensation products seen under longer reaction time conditions. It is known from previous investigations (5) that the major primary species formed from impact of 70 eV electrons on CH_3I include CH_3I^+ (100), I^+ (53), CH_3^+ (28), CH_2I^+ (14), CI^+ (5), CHI^+ (4), and CH_2^+ (4), with relative intensities as given in parentheses. It must be concluded that several of these species have already disappeared by fast ion-molecule reaction with parent, yielding CH_3^+, I^+, CH_2I^+, and CH_3I^+ as the important species under the conditions of the experiment in Figure 27.

Figure 28 was taken under experimental conditions designed to show ion-molecule condensation products in this system, which are formed in reactions of relatively low efficiency. Product species seen include the ether structure ion $CH_3ICH_3^+$ as well as the iodine adduct $CH_3I_2^+$. The parent ion CH_3I^+ still persists with considerable intensity under these conditions.

The time-intensity behavior of major ions investigated in the study is shown in Figures 29, 30, and 31. Figure 29 shows the time decay of parent CH_3I^+ ion, Figure 30 shows both growth and decay of $CH_3ICH_3^+$ and Figure 31 shows growth of $CH_3I_2^+$. Although the dimer $(CH_3I)_2^+$ was seen in qualitative experiments using the TOF mass spectrometer, and has been reported in previous investigations, it is formed with low intensity and was not observable with the ICR instrument.

Quantitative data obtained from the investigations shown in Figures 29 - 31 are given in Table 7. Rate constants were measured for the very rapid loss of CH_3^+ and I^+, with rate constants of 19.9×10^{-10} cm^3 molec.$^{-1}$ s^{-1} and 9.7×10^{-10} cm^3 molec.$^{-1}$ s^{-1} respectively. The large rate constant for the reaction of CH_3^+ with parent is composed of a fast charge transfer process and a much less efficient H^- transfer process, as considered further in the discussion section. The overall rate constant for loss of CH_3I^+ is much slower, having a value of 0.34×10^{-10} cm^3 molec.$^{-1}$ s^{-1}. It was also possible to measure independently the rate of formation of $CH_3ICH_3^+$ and $CH_3I_2^+$, having rate constants of 0.24×10^{-10} and 0.15×10^{-10} cm^3 molec.$^{-1}$ s^{-1}, respectively. As will be seen, there is an approximate balance between rate of formation of these two species and rate of loss of CH_3I^+ precursor. The subsequent decay of $CH_3ICH_3^+$ was found to have a rate constant of 0.09×10^{-10} cm^3 molec.$^{-1}$ s^{-1}.

The reaction pathways for formation of $CH_3ICH_3^+$ and $CH_3I_2^+$ were confirmed using the ICDR (ion cyclotron double resonance) technique and the reactions are as follows

$$CH_3I^+ + CH_3I \longrightarrow I\cdot + CH_3ICH_3^+ \qquad \text{VI-1}$$

$$CH_3I^+ + CH_3I \longrightarrow CH_3\cdot + CH_3I_2^+ \qquad \text{VI-2}$$

2. Discussion

Primary processes in the electron impact ionization of CH_3I include formation of the parent ion, CH_3I^+, as well as the fragment ions CH_3^+, I^+, and CH_2I^+. The product ions, formed as a result of reactions of primary ions with the substrate, are $CH_3I_2^+$ and $(CH_3)_2I^+$, but the dimer $(CH_3I)_2^+$ could not be detected in the ICR instrument even though the analogous ion $(CF_3I)_2^+$ formed from CF_3I^+ was detectable. The set of reactions described below explain some of the gas phase ion chemistry occurring in the CH_3I system.

Major fragment ions CH_3^+ and I^+ disappear by fast reactions with substrate; as suggested previously by Beauchamp (7) a hydride-ion transfer process is a possible route for loss of CH_3^+

$$CH_3^+ + CH_3I \dashrightarrow CH_4 + CH_2I^+ \qquad \text{VI-3}$$

However, the intensity of CH_2I^+ is very low as seen in Fig. 27, whereas the initial intensity of the CH_3^+ peak is reported to be 30% in low pressure electron impact on CH_3I. It does not appear possible that Reaction VI-3 is the main channel for loss of CH_3^+. Since the ionization potential of $CH_3^\cdot$ is somewhat greater than that of the substrate as shown in Table 10, the charge exchange process is possible, and must constitute the main reaction channel

$$CH_3^+ + CH_3I \dashrightarrow CH_3^\cdot + CH_3I^+ \qquad \text{VI-4}$$

Although independent measurements of the rate constant for reactions of CH_3^+ with substrate to form CH_4 + CH_2I^+ and CH_3I^+ + $CH_3^\cdot$ respectively were not made, the rate constant for the former must be quite small. Although the precursor to CH_2I^+(that is, CH_3^+) is initially present with an intensity nearly 30% of the precursor to $CH_3ICH_3^+$ (namely, CH_3I^+), the intensity of CH_2I^+ is almost unobservable compared with $CH_3ICH_3^+$. Since the latter is formed with a measured rate constant of 0.24×10^{-10} cm^3 $molec.^{-1}$ s^{-1}, the rate constant for H^- transition from substrate to CH_3^+ must be even smaller.

It appears that a charge exchange reaction is also the main route for loss of I^+, since I_2^+ was not observed in the product ion spectrum

$$I^+ + CH_3I \text{ ----> } I^\cdot + CH_3I^+ \qquad \text{VI-5}$$

This is not unexpected, since the ionization potential of $I^\cdot$ is 10.451 eV while that of CH_3I is 9.54 eV (98) as shown in Table 10. Hamill and co-workers suggest that an iodine atom transfer may also occur

$$I^+ + CH_3I \text{ ---> } I_2^+ + CH_3 \qquad \text{VI-6}$$

These workers observed I_2^+ in the high pressure mass spectrum of CH_3I using a modified magnetic mass spectrometer, and it was also observed in the present work during studies on CF_3I-CH_3I mixtures. Beauchamp and co-workers

(7) were unable to investigate any two-iodine species due to the limited mass range of their ICR machine. Since I_2^+ is known to be observable with the instrument used in the present work, and is absent in the product ion spectrum from CH_3I, the implication is that the I• atom transfer Reaction VI-6 is too slow to complete with the charge exchange Reaction VI-5. Although I_2^+ was not seen in the present work done in the 10^{-6} torr pressure range, it may be formed with reasonable efficiency in a 3-body process under the much higher pressure conditions used in magnetic sector and TOF instruments.

The fragment ion CH_2I^+ was observed with low intensity in the present work, under short reaction time conditions. Since it was not seen at longer reaction times, it must have some available reaction channel. This species could not be studied in detail because of its low intensity, and because it differed by only one mass unit from the predominant ion CH_3I^+.

Hamill and co-workers (5) suggest that CH_2I^+ is a precursor to I_2^+, which was observed in their work

$$CH_2I^+ + CH_3I \dashrightarrow I_2^+ + C_2H_5^{\bullet} \qquad \text{VI-7}$$

The condensation products $(CH_3)_2I^+$ and $CH_3I_2^+$ are detected as described above. Using ICDR experiments their formation from the parent ion is confirmed.

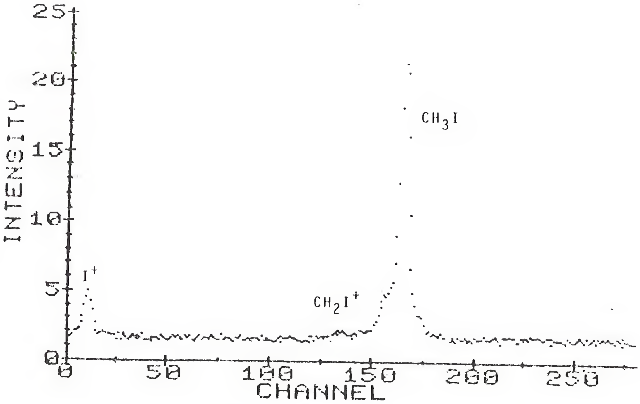

Fig. 27. Mass spectrum of I^+, CH_2I^+ and CH_3I^+ at a pressure of 1.8 x 10^{-6} torr. The spectrum was obtained from a magnetic sweep in 2 min centered at 12.15 kG.

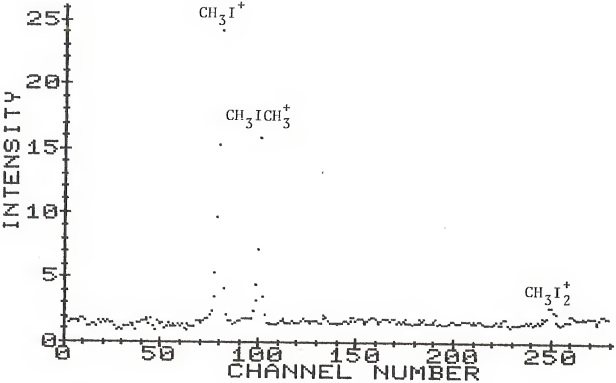

Fig. 28. Mass spectrum of pure CH_3I at 3.8×10^{-6} torr generated by electron impact with 70 eV electrons. The grid was pulsed for 3.5 ms then the ions were detected 50 ms later by a 4.5 ms pulse of 72.47 kHz frequency from the marginal oscillator. The ions were brought into resonance by sweeping the magnetic field from 4 to 14 kG. Each point is the average of 30 experiments.

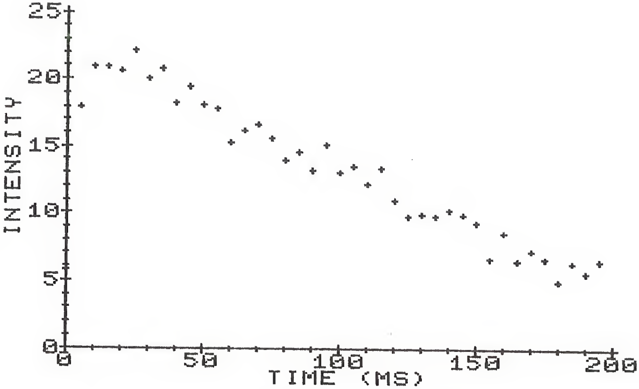

Fig. 29. Ion decay signal showing reaction of CH_3I^+ in pure CH_3I at a pressure of 8.8×10^{-6} torr. Each point is the average of 16 scans. The ions were generated by a 4.5 ms pulse of 70 eV and trapped at a magnetic field of 12 kG and monitored by a 4 ms detect pulse at a resonance frequency of 129.8 kHz.

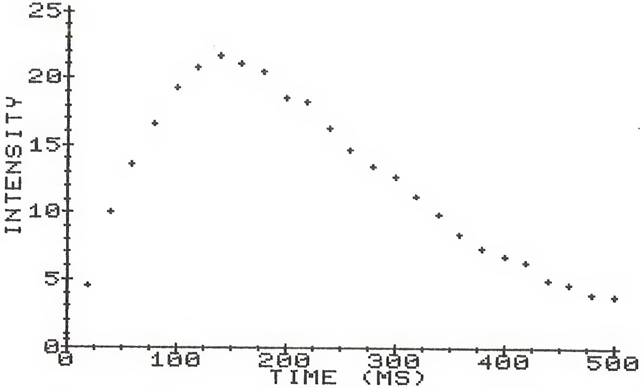

Fig. 30. Ion decay signal showing reaction of $CH_3ICH_3^+$ in pure CH_3I at a pressure of 2.7×10^{-5} torr. Each point is the average of 10 experiments. The ions were generated by 3.5 ms pulse of 70 eV electron impact and trapped at a magnetic field of 12 kG and monitered at a resonance frequency of 117 kHz.

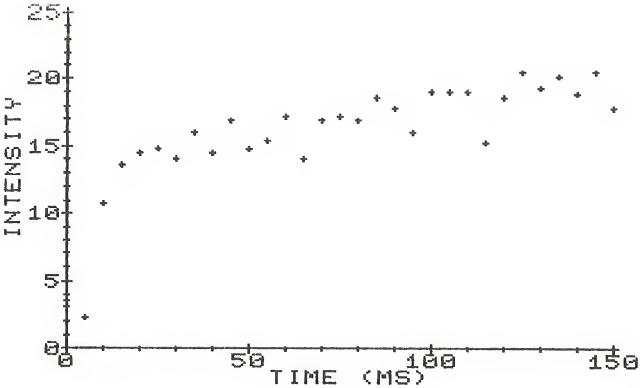

Fig. 31. Ion decay signal showing $CH_3I_2^+$ ions in pure CH_3I at 2.8×10^{-5} torr generated by 5 ms electron impact of 70 eV electrons. Each point is the average of 16 experiments. The ions were trapped at 12.78 kG and detected with a 4.5 ms detect pulse of the marginal oscillator set at 72.47 kHz.

$CH_3I^+ + CH_3I \dashrightarrow I^\cdot + (CH_3)_2I^+$ VI-8

$CH_3I^+ + CH_3I \dashrightarrow CH_3^\cdot + CH_3I_2^+$ VI-9

The $(CH_3)_2I^+$ ion reacts slowly with the substrate with a rate constant of 9×10^{-12} cm^3 $molec.^{-1}s^{-1}$ suggesting that it is collisionally stabilized. It also undergoes a slow decay process

$(CH_3)_2I^+ + CH_3I \dashrightarrow$ products VI-10

The nature of products formed was not determined. The identification of the heavy ion $CH_3I_2^+$ was reported in only one previous investigation (5). It was not seen in an earlier ICR investigation due to the low sensitivity for heavy mass ions of Beauchamp's apparatus (7). For the overall reaction rate constants see Table 7.

The following sections give a brief account of the time-intensity behavior of each of the major ions seen in Figures 27-31, in light of the mechanistic discussion given above.

Mass Spectrum of Pure CH_3I. Figures 27 and 28 show mass spectra of pure CH_3I at two different pressures. In Fig. 27 the mass spectrum was taken at a pressure of 1.6×10^{-6} torr and shows peaks for CH_3I^+, I^+ and CH_2I^+ where the ion intensity of CH_3I^+ is the highest and that of CH_2I^+ the lowest. This indicates that at lower pressures the primary ions CH_3I^+ and I^+ are predominant. In Fig. 28

the mass spectrum was taken at 3.8×10^{-6} torr and the ions identified were CH_3I^+, $(CH_3)_2I^+$ and $CH_3I_2^+$. From this mass spectrum it can be concluded that ion-molecule reactions had taken place as shown in Reactions VI-8 and VI-9.

CH_3I^+. Figure 29 shows the intensity graph of the parent ion , CH_3I^+, as a function of time at a pressure of 8.8×10^{-6} torr. The intensity decreases rapidly which means ion-molecule reactions as shown on Table 7 are consuming the CH_3I^+ ion as soon as it is generated. It is formed both by electron impact and by charge transfer from CH_3^+ and I^+ as discussed above.

$(CH_3)_2I^+$. Figure 30 is the intensity graph of the product ion, $(CH_3)_2I^+$. The intensity of $(CH_3)_2I^+$ increases up to 139 ms and then decreases slowly . This means that $(CH_3)_2I^+$ was formed as shown in Reaction VI-8 and Table 7, but the slow decrease of its intensity after 139 ms must occur as indicated in Reaction VI-10.

$CH_3I_2^+$. Figure 31 shows the time dependence of ion intensity of the product ion, $CH_3I_2^+$, at a relativly high pressure of 1.5×10^{-5} torr. Observation of Fig. 28 indicates that the intensity increases fast intially, and thereafter the intensity grows steadily. There is no evidence for a decayg process which means $CH_3I_2^+$ is a stable ion once it is formed. One channel of its formation must be through Reaction VI-9.

C. CF_3I System

1. Experimental Results

Although ion molecule reaction chemistry of CF_3I had been examined previously in this laboratory (8), it appeared appropriate to reexamine the subject, since several improvements had been made in the operation of the ICR mass spectrometer. These modifications allow improved detection of low intensity species, especially in the higher mass range necessary to observe dimers of CF_3I.

Figure 32 is a partial mass spectrum of CF_3I which shows primary ions CF_2I^+ and CF_3I^+ as well as the condensation product I_2^+. The time dependence of intensities of CF_3I^+ and CF_3^+ ions is shown in Figures 33 and 34, respectively. There is an indication of the build up of intensity of both ions up to about 20 ms, followed by decay into the 100-200 ms range. Figure 37 shows a similar build up of intensity of I_2^+ ion extending to about 40 ms, and a considerably slower rate of decay.

Table 8 records rate constant values for the loss or formation of several ion species studied in this investigation, along with known or postulated reaction pathways. CF_3^+ was found to decay with a rate constant of $2.4 \pm 1.0 \times 10^{-10}$ cm^3 $molec.^{-1}$ s^{-1}. As confirmed by ICDR, about 50

Table 8

Experimental rate constants and ion-molecule reactions in CF_3I system

Reaction	k(exp)[a]	k(ref)	Comments
$CF_3^+ + CF_3I \longrightarrow$ Products	2.4±1.0		
$\longrightarrow CF_4 + CF_2I^+$	1.2	1.68 (8)	ICDR[b]
$\longrightarrow CF_3I^+ + CF_3\cdot$	1.2[c]		
$I^+ + \longrightarrow$ Products	3.1±0.2		
$\longrightarrow I_2^+ + CF_3$	1.1	0.79 (8)	ICDR
$\longrightarrow CF_3I^+ + I\cdot$	2.0[c]	3.9 (96)	
$CF_3I^+ + \longrightarrow$ Products	0.74±0.55		
$\longrightarrow CF_3ICF_3^+ + I$	0.50±0.18		ICDR
$\longrightarrow CF_3I_2^+ + CF_3\cdot$	0.30±0.10	0.03 (8)	
$\longrightarrow (CF_3I)_2^+$	0.18	0.22 (8)	
$CF_2I^+ + \longrightarrow$ Products	0.14		
$I_2^+ + \longrightarrow$ Products	0.15		
$CF_3ICF_3^+ + \longrightarrow$ Products	0.29 ± 0.12		
$CF_3I_2^+ + \longrightarrow$ Products	0.19 ± 0.08		
$(CF_3I)_2^+ + \longrightarrow$ Products	0.14		

a All k's are in cm^3 $molec.^{-1}$ $s^{-1} \times 10^{+10}$.

b ICDR means the reaction channel was verified by ICR double resonance experiments.

c Obtained by difference.

to 100% of this reaction corresponds to a fluoride ion transfer process from parent, forming CF_2^+. The charge transfer reaction is also possible, as discussed later.

The iodine ion I^+ ion appears in a reaction with substrate having a total rate constant of 3.1×10^{-10} cm^3 $molec.^{-1}$ s^{-1}; a reaction channel with rate constant 1.1×10^{-10} cm^3 $molec.^{-1}$ s^{-1}, forming $I_2^+ + CF_3^\cdot$, was identified using ICDR technique. Charge transfer with the substrate is possible, and has been postulated by earlier workers.

The parent ion CF_3I^+ undergoes several condensation reactions with substrate; the combined rate constant for loss of CF_3I^+ was measured as $0.74 \pm 0.55 \times 10^{-10}$ cm^3 $molec.^{-1}$ s^{-1}. Reaction channels leading to $(CF_3I)_2^+$ and $CF_3I_2^+ + CF_3^\cdot$ had been seen earlier; the third reaction channel forming $CF_3ICF_3^+$ was confirmed in the present work by the ICDR technique. Cross sections for these processes are 0.18×10^{-10}, $0.30 \pm 0.10 \times 10^{-10}$, and $0.50 \pm 0.18 \times 10^{-10}$ cm^3 $molec.^{-1}$ s^{-1}, respectively.

Rate constants for decay of several other species were measured, although the reaction pathways were not identified. The species reacting and the corresponding rate constants are as follows: CF_2I^+, 0.14×10^{-10} I_2^+, 0.15^{-10} $CF_3ICF_3^+$, $0.29 \pm 0.12 \times 10^{-10}$ $CF_3I_2^+$, $0.19 \pm 0.08 \times 10^{-10}$ and $(CF_3I)_2^+$, $0.14 \times 10^{-10} cm^3$ $molec.^{-1}$ s^{-1}.

2. Discussion

Ion-molecule reactions in CF_3I had been investigated earlier with an ICR instrument by Beauchamp's group (96) using low pressure conditions unsuitable for observation of condensation products, and also in this laboratory using both TOF and ICR instruments, under relatively high pressure conditions. Reaction pathways which were identified by earlier workers include the following:

$$CF_3^+ + CF_3I \dashrightarrow CF_3I^+ + CF_3\cdot \qquad \text{VI-11}$$

$$CF_3^+ + CF_3I \dashrightarrow CF_2I^+ + CF_4 \qquad \text{VI-12}$$

$$I^+ + CF_3I \dashrightarrow CF_3I^+ + I\cdot \qquad \text{VI-13}$$

$$I^+ + CF_3I \dashrightarrow I_2^+ + CF_3\cdot \qquad \text{VI-14}$$

$$CF_3I^+ + CF_3I \dashrightarrow CF_3I_2^+ + CF_3\cdot \qquad \text{VI-15}$$

$$CF_3I^+ + CF_3I \dashrightarrow (CF_3I)_2^+ \qquad \text{VI-16}$$

In addition to the above, formation of the ether-structure ion was observed for the first time in the present work:

$$CF_3I^+ + CF_3I \dashrightarrow (CF_3)_2I^+ + I\cdot \qquad \text{VI-17}$$

Measurements were also made on the total rate of consumption of CF_3^+ and I^+.

$$CF_3^+ + CF_3I \dashrightarrow \text{products} \qquad \text{VI-18}$$

$$I^+ + CF_3I \dashrightarrow \text{products} \qquad \text{VI-19}$$

There was direct evidence for all of the processes listed above, except for as the charge exchange Reactions VI-11 and VI-13. Occurrence of these processes can be inferred with rate constants of ca. 1.2×10^{-10} for charge exchange of CF_3^+ with parent and ca. 2.0×10^{-10} cm^3 $molec.^{-1}$ s^{-1} for reaction of I^+, since total rate constants for loss of CF_3^+ to form CF_4 and CF_2I^+ and for loss of I^+ to form I_2^+ and CF_3 were less than the total rates of loss of CF_3^+ and I^+, respectively, by the amounts indicated.

Other reaction processes that were monitored are as follows

$$CF_2I^+ + CF_3I \longrightarrow \text{products} \qquad \text{VI-20}$$

$$I_2^+ + CF_3I \longrightarrow \text{products} \qquad \text{VI-21}$$

$$(CF_3)_2I^+ + CF_3I \longrightarrow \text{products} \qquad \text{VI-22}$$

$$CF_3I_2^+ + CF_2I \longrightarrow \text{products} \qquad \text{VI-23}$$

$$(CF_3I)_2^+ + CF_3I \longrightarrow \text{products} \qquad \text{VI-24}$$

The detailed reaction pathway is not known for any of these processes.

The formation of ether-type ions RXR^+ from ion-molecule reactions of alkyl iodides was first observed by Hamill and co-workers (5) for the cases of $CH_3ICH_3^+$ and $C_2H_5IC_2H_5^+$. This reaction type was subsequently studied by other workers. J. L. Beauchamp and his group (7) suggested that the reaction

$$CH_3Cl^+ + CH_3Cl \longrightarrow (CH_3)_2Cl^+ + Cl\cdot \qquad \text{VI-25}$$

occurs, but in less than one in a hundred collisions. Similarly, Reaction VI-17 apparently occurs once in 40 collisions or less. It was observed (99) that both $(CH_3)_2Cl^+$ and CH_4Cl^+ arise from the dimer $(CH_3Cl)_2^+$ with comparable efficiency. Likewise the dimer species $(CF_3I)_2^+$ may be a transient intermediate in formation of $CF_3ICF_3^+$.

$$(CF_3I)_2^+ \text{ ---> } (CF_3)_2I^+ + I\cdot \qquad \text{VI-26}$$

Reaction VI-12 is the reaction of fragment CF_3^+ with the parent with a rate constant of 1.2×10^{-10} cm^3 $molec.^{-1}$ s^{-1} to form a neutral molecule, CF_4, and an ion, CF_2I^+.

$$CF_3^+ + CF_3I \text{ ---> } CF_4 + CF_2I^+ \qquad \text{VI-12}$$

For the reaction above the previously reported rate constant (8) is 1.68×10^{-10} cm^3 $molec.^{-1}s^{-1}$. A decay process for CF_2I^+ was not detected previously using Time-of-Flight mass spectrometry (8) but was found by ICR mass spectrometry with a rate constant of 0.14×10^{-10} cm^3 $mole.^{-1}$ s^{-1}.

$$CF_2I^+ + CF_3I \text{ ---> products} \qquad \text{VI-20}$$

The products for this reaction pathway are not known.

Reaction VI-14 is identified by ICRD experiment and was found to have a rate constant of 1.1×10^{-10} cm^3 $molec.^{-1}s^{-1}$.

$$I^+ + CF_3I \text{ ---> } I_2^+ + CF_3\cdot \qquad \text{VI-14}$$

As mentioned above, the total rate of disappearance of CF_3^+ may not be due to Reaction VI-11 alone but may also involve the charge transfer reaction

$$CF_3^+ + CF_3I \text{ ---> } CF_3I^+ + CF_3^{\cdot} \qquad \text{VI-11}$$

It was suggested earlier (8) that Reaction VI-11 is too endothermic to be detected in an ICR experiment due to the ionization potential difference between CF_3I (10.23 eV) and $CF_3^{\cdot}$ (9.25 eV) (98). However, this process appears to give the best explanation for the difference between the total rate of loss of CF_3^+ and the rate of formation of CF_2I^+.

Reactions VI-15 and VI-16 were observed in the TOF mass spectrometer as well as in the ICR instrument even though detecting these heavy molecules in the ICR is very difficult. The disappearance of the heavy species such as the ether type $(CF_3)_2I^+$, the dimer $(CF_3I)_2^+$ and the iodo-complex $CF_3I_2^+$ occurs at small rate constants compared to the disappearance of CF_3^+, I^+, and CF_2I^+ suggesting that these species are better able to distribute their energy of formation internally and stabilize themselves without recourse to collisional energy transfer with a third body.

As mentioned previously the ether type ions $CF_3ICF_3^+$ and $(C_2F_5)_2I^+$ were not reported previously in studies of CF_3I and C_2F_5I gas phase ion chemistry, but $(CF_3)_2I^+$ was found in the present work during studies of the pure CF_3I

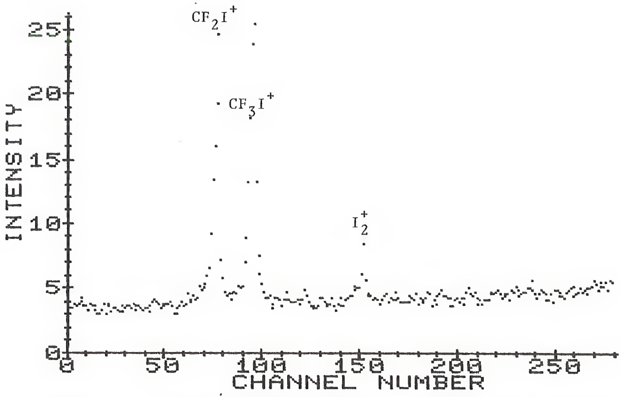

Fig. 32. Mass spectrum of pure CF_3I at a pressure of 1.5 x 10^{-5} torr. Each point is the average of 30 scans. The ions were generated by 5 ms electron impact pulse with 70 eV electrons. The ions were monitored after a 50 ms detect pulse delay then irradiated at 52.4 kHz while the magnetic was swept from 3.5 to 13.5 kG.

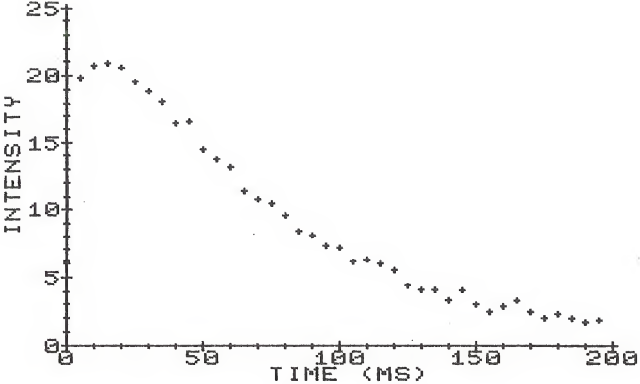

Fig. 33. Ion decay signal showing reaction of CF_3I^+ ions in pure CF_3I at a pressure of 4.8 x 10^{-6} torr. Each point is the average of 10 experiments. The ions were generated by 4.5 ms pulse of 70 eV electrons and monitored by a 5 ms detect pulse from the marginal oscillator set at 93.95 kHz with the magnetic strength being at 12 kG.

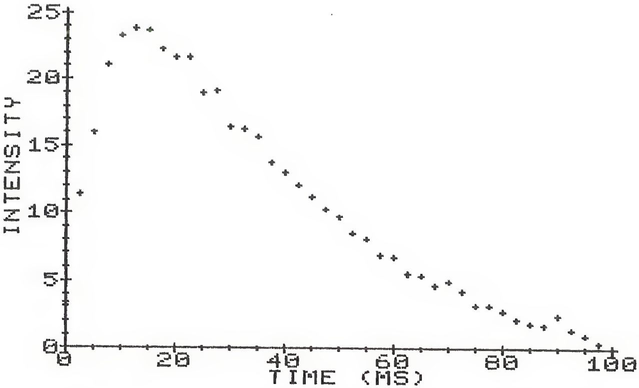

Fig. 34. Ion decay signal showing reaction of CF_3^+ in pure CF_3I at a pressure of 2.0 x 10^{-6} torr. This decay curve is an average of 10 experiments. The ions were generated by 5 ms pulse electron impact of 80 eV electrons and trapped at a magnetic field strength of 12 kG and monitored by a 3 ms detect pulse at a resonance frequency of 267.2 kHz.

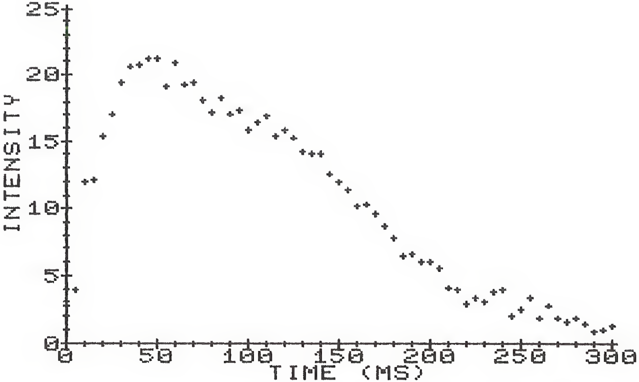

Fig. 35. Ion decay signal showing reaction of $(CF_3)_2I^+$ ions in pure CF_3I at a pressure of 1.4 x 10^{-5} torr and were generated by a 5 ms pulse of 80 eV electrons. The ions were monitored by a 4 ms detect pulse from the marginal oscillator set at 69.55 kHz and with a magnetic field strength of 12 kG. Each point is the average of 19 experiments.

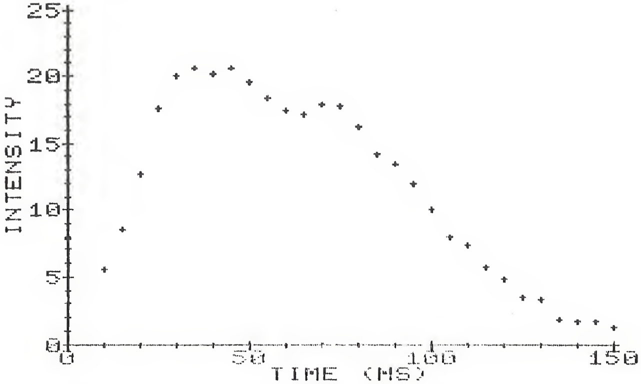

Fig. 36. Ion decay signal showing reaction of $CF_3I_2^+$ ion in pure CF_3I at a pressure of 5.5×10^{-5} torr. Each point is the average of 36 experiments. The ions were generated by a 5 ms pulse of 70 eV electrons and were monitored with a 5 ms detect pulse from the marginal oscillator set at 52.4 kHz and with magnetic yield strength of 11.345 kG.

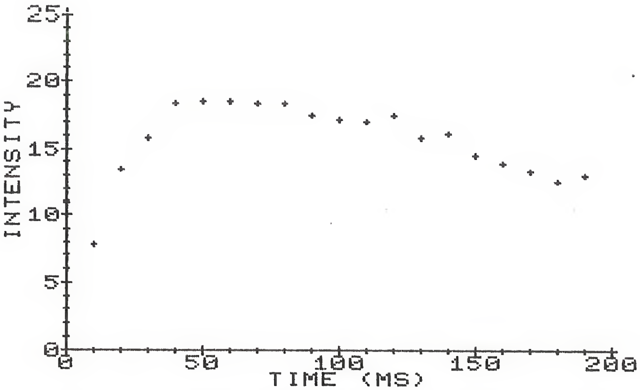

Fig. 37. Ion decay signal showing reaction of I_2^+ ions in pure CF_3I at a pressure of 9.2×10^{-6} torr. Each point is the average of 25 scans. The ions were generated by a 5 ms pulse of 70 eV electrons. The ions were trapped at a magnetic field strength of 12 kG and detected with a 5 ms detect pulse from the marginal oscillator set at a resonance frequency of 72.51 kHz.

system using the ICR instrument as well as in the Bendix TOF instrument during studies of gas phase ion chemistry of the equimolar CH_3I-CF_3I mixture.

The following sections give a brief account of the time-intensity behavior of each of the major ions seen in Figures 31-37, in light of the mechanistic discussion given above.

Mass Spectrum of Pure CF_3I^+. Figure 31 shows a mass spectrum of the pure CF_3I generated by electron impact at 70 ev and a pressure of 1.5×10^{-5} torr. The prominent ions are CF_3I^+, CF_2I^+ and I_2^+, respectively. The ions were monitored after a 50 ms pulse delay. Other ions such as CF_3^+, CF_2I^+, amd I^+ were not observed under these conditions.

$CF_3I^+$and CF_3^+. Figures 33 and 34 shows decay of the signal of CF_3I^+ ions at a pressure of 4.8×10^{-6} torr and that of CF_3^+ at a pressure of 2.0×10^{-6} torr in the pure CF_3I system. In Fig. 30 the CF_3I^+ intensity decreases rapidly and approaches zero after 200 ms. Three channels for its disappearance are shown in Table 8. In the case of CF_3^+ ion the intensity decreases very rapidly after 15 ms. This means, that CF_3^+ ion is very reactive and disappears through Reactions VI-11 and V1-12. These reactions are also shown in Table 8 along with their rate constants.

$(CF_3)_2I^+$ and $CF_3I_2^+$ Figures. 35 and 36 depict time dependent ion decay signals of the ether type ion $(CF_3)_2I^+$ at a pressure of $4x10^{-5}$ torr generated by a 5 ms pulse of 80 eV electrons and that of $CF_3I_2^+$ at a pressure of $5.5x10^{-5}$ generated by a 5 ms pulse of 70 eV electrons in pure CF_3I. The intensity of $(CF_3)_2I^+$ decreases after 50 ms and approaches zero after 300 ms. Although formation of $(CF_3)_2I^+$ according to Reaction V1-17 was confirmed by the ICDR method, the products of its decay(Reaction VI-22) are not known. The rate constants for its formation and disappearance are given in Table 8. The time-intensity dependence of $CF_3I_2^+$ is somewhat unusual. Generally its intensity increases up to 40 ms and then decreases out to 150 ms. However, there is some evidence for onset of a second formation process around 60-70 ms, with an apparently faster decay rate beyond 80 ms. If this behaviour is real, rather than an experimental artifact, its explanation is unknown. Unlike its counterpart $CH_3I_2^+$ in the pure CH_3I system, $CF_3I_2^+$ does not grow throughout the duration of the experiment, but instead reaches a maximum and decays rather rapidly. From this observation it can be concluded that $CF_3I_2^+$ is very reactive while $CH_3I_2^+$ does not react at all. $CF_3I_2^+$ is thought to be formed through Reaction VI-15; the products of its decay Reaction V1-23 are unknown. The rate constant for both reactions are shown in Table 8.

I_2^+. Figure 37 shows the intensity of I_2^+ as a function of time when it was generated at a pressure of 9.2×10^{-6} torr by a 5 ms pulse of 70 eV electrons in pure CF_3I. As is described in Reactions VI-5 and Vl-14, I_2^+ was only seen in the CF_3I system and the equimolar mixture of CF_3I-CH_3I. In the case of pure CH_3I, charge transfer ($I^+ + CH_3I \longrightarrow I\cdot + CH_3I^+$) is much faster than the analogous reaction shown as Reaction VI-14. As it is shown in Fig. 37, the I_2^+ reacts very slowly once it is formed and the intensity never approaches zero within the reaction time shown. Formation of I_2^+ via Reactions VI-14 was confirmed by the ICDR method; details of its decay(Reaction VI-21) are not known.

D. Equimolar Mixtures of CH_3I and CF_3I

1. Experimental Results

The ion-molecule chemistry of CF_3I - CH_3I equimolar mixtures was studied using both ion cyclotron resonance (ICR) and time-of-flight (TOF) instruments. The former has the advantage that reaction channels can be confirmed using the double-resonance technique; but the sensitivity becomes poor as the mass increases, so that certain dimeric species containing two iodine atoms could be studied only by extensive signal averaging. The pressure range is also

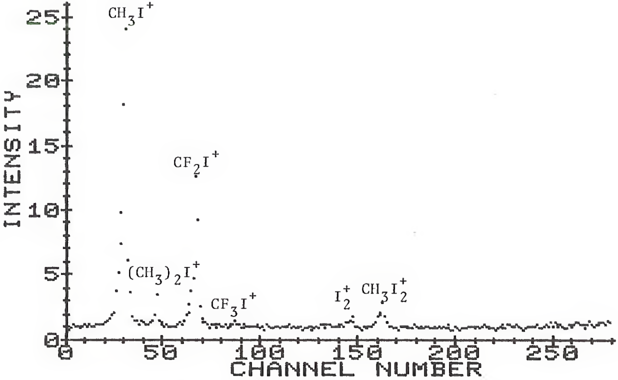

Fig. 38. A mass spectrum of an equimolar mixture of CH_3I and CF_3I at a total pressure of 1.1×10^{-5} torr. The ions were generated by a 5 ms pulse of 70 eV electrons. Each point is the average of 7 experiments. The ions were monitored after a 50 ms delay with a 4.5 ms detect pulse from the marginal oscillator set at 52.35 kHz. The magnet was swept from 4 to 14 kG.

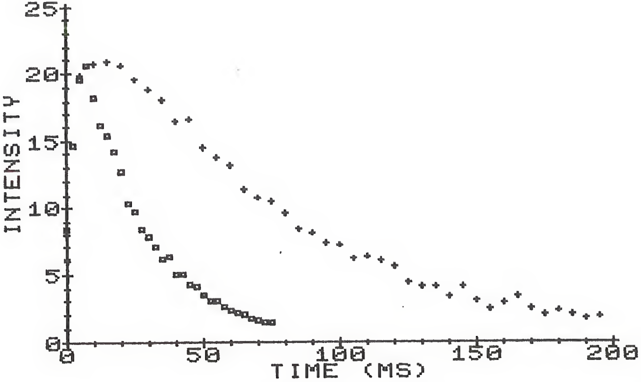

Fig. 39. Ion decay signal showing reaction of pure CF_3I^+ (the plus sign) and in the equimolar mixture of CF_3I and CH_3I (the square signs) where the pressure in the pure case was 4.8×10^{-6} torr and in the mixture the total pressure was 3.8×10^{-6} torr. The CF_3I^+ reacts away very rapidly even in lower pressure mixture due to a very favorable charge transfer reaction to generate CH_3I^+.

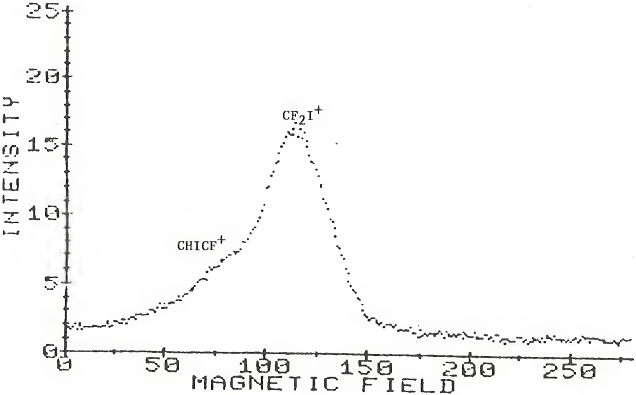

Fig. 40. Mass spectrum of $CHICF^+$ and CF_2I^+ of the equimolar mixture of CH_3I and CF_3I at a total pressure of 1.09×10^{-6} torr. The ions were generated by 5 ms pulse of 70 eV electrons. The ions were monitored after a 50 ms detect pulse from the marginal oscillator set at 87.4 kHz. The magnet was swept from 4 to 14 kG.

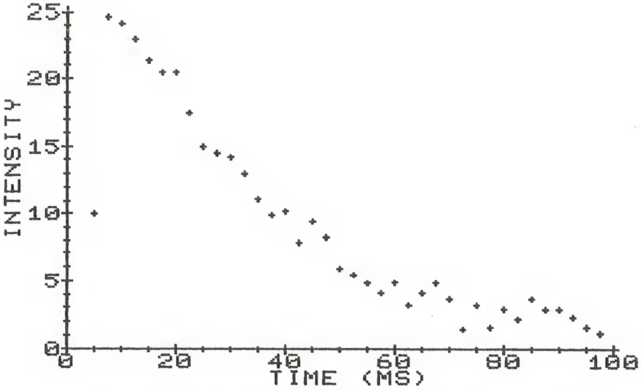

Fig. 41. Ion decay signal showing reaction of I^+ in the equimolar mixtures of CH_3I and CF_3I at a total pressure of 1.6×10^{-6} torr generated by a 5 ms pulse of 70 eV electrons. Each point is the average of 25 experiments. The ions were monitored by a 4 ms pulse from the marginal oscillator set at 148.73 kHz with a magnetic field strength of 12.38 kG.

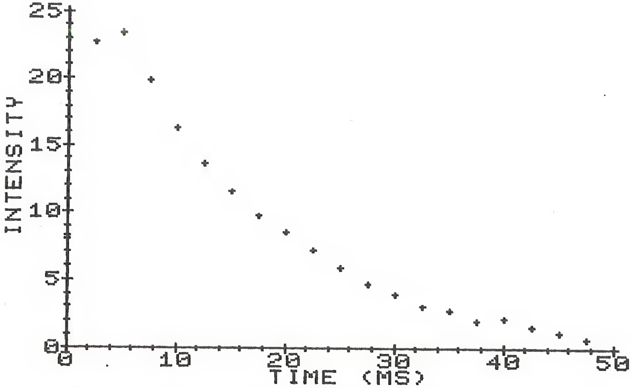

Fig. 42. Ion decay signal showing reaction of CH_3^+ in the equimolar mixture of CH_3I and CF_3I at a total pressure of 1.8×10^{-6} torr generated by a 5 ms pulse of 70 eV electrons. Each point is the average of 25 experiments. The ions were monitored by a 5 ms detect pulse from the marginal oscillator set at 787.26 kHz with a magnetic field strength of 7.7 kG.

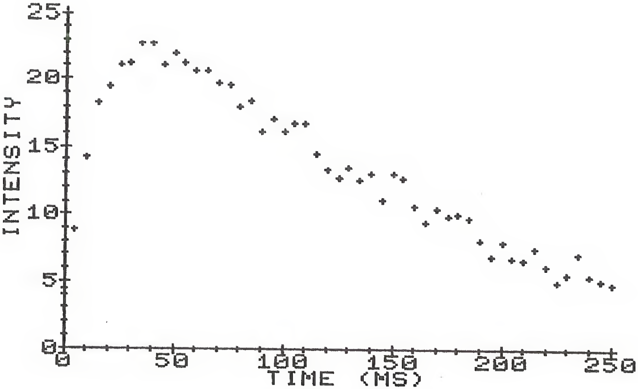

Fig. 43. Ion decay signal showing reaction of CF_2I^+ in an equimolar mixture of CH_3I and CF_3I at a pressure of 1.3×10^{-5} torr generated by a 5 ms pulse of 70 eV electrons. The ions were monitored by a 3 ms detect pulse from the marginal oscillator set at 87.4 kHz and a magnetic field strength of 10.26 kG. Each point is the average of 9 experiments.

limited to about 5×10^{-5} torr or lower, so that processes with a pressure dependence higher than second order can not be studied. Although the TOF instrument has rather poor resolution and is somewhat difficult to adjust in the high pressure mode used for ion-molecule reaction studies, pressures as high as 1 torr can be achieved. It can be used in both a pressure-dependent mode and a time-delay mode up to about 0.150 torr, but the latter could not be used at the higher pressures needed to study some of the low-efficiency condensation processes important in the present work.

Figures made from the ICR data taken for an equimolar mixture of CH_3I-CF_3I are shown in Figs. 29 to 43. All the ICR data figures show ion intensities as a function of time. Figures 44 to 52 show data taken as a function of pressure with the TOF instrument, while Fig. 44 shows results of a limited study using the TOF instrument in the time-delay mode. The ICR results are described below, followed by the data from the TOF instrument. Due to the complexity of the system it will be appropriate to make some refernce to the reaction scheme in the process of reporting the data, but a full account is reserved for the discussion section.

Mass Spectrum of a 1:1 mixture of CH_3I-CF_3I. The mass spectrum of the equimolar mixture was taken as shown in Fig. 38 at a total pressure of 1.1×10^{-5} torr. The ions were generated by a 5 ms pulse of 70 eV electrons. The ions were monitored after a 50 ms delay with a 4.5 ms detect pulse from the marginal oscilator which was set at 52.35 kHz. The ions which were identified, listed in order of decreasing intensity, are as follows: CH_3I^+, CF_2I^+, $CH_3I_2^+$, $(CH_3I)_2I^+$, and I_2^+. Figures 28 and 31 will show that CH_3I^+ and $(CH_3)_2I^+$ are major ions in the case of the CH_3I system, while $CH_3I_2^+$ is a minor product. In the case of pure CF_3I, CF_2I^+ and CF_3I^+ have the highest intensities, while I_2^+ is a minor specie. Certain species such as $(CH_3)_2I^+$, CF_3I^+, and I_2^+, which are of major importance in the pure systems, are of rather low intensity in the mixture. It nevertheless appears that many of the ion-molecule reaction channels which are seen in the two pure substances also play an important role in the case of the mixture.

$\underline{CF_3I^+}$. Figure 39 is an ion decay graph showing reactions of CF_3I^+ in the pure CF_3I system as well as in the mixture of CH_3I-CF_3I. As can be observed in the figure, CF_3I^+ is very reactive in the mixture compared to its behaviour in the pure system. Similarily it was shown in the mass spectrum of the equimolar mixture of CH_3I-CF_3I in Fig. 38 that the CF_3I^+ intensity is almost nonexistent. From both these observations it can be concluded that the charge transfer reaction to generate CH_3I^+, as shown in Reaction VI-27, is a dominant channel for consumption of

$CH_3I + CF_3I^+ \dashrightarrow CH_3I^+ + CF_3I$ VI-27

CF_3I^+ compared to other reaction channels in the mixture. Also, from the rate constant for Reaction VI-2 as given in Table 9, the reaction is faster than the other reaction channels.

CF_2I^+ and $CHICF^+$. In Fig. 40 the peak due of CF_2I^+ is very intense while that of $CHICF^+$ is very weak. In the case of the pure CF_3I system as well as in the mixture, the mass spectral intensity of CF_2I^+ is strong as is shown in Figs. 32 and 38. The formation and disappearance of CF_2I^+ can be accounted for through reaction channels as indicated in Reactions VI-12, VI-20, VI-23 and Table 8.

$I^+$and CH_3^+. The time dependent ion decay graph depicted in Figs. 41 and 42 for I^+ and CH_3^+ in the equimolar mixture system were taken at pressures of $1.6x10^{-6}$ and $1.8x10^{-6}$ torr respectively and were generated by a 5 ms pulse of 70 eV electrons. By comparing the two figures it can be concluded that the CH_3^+ ion decays very fast and its intensity approaches zero after 48 ms while I^+ decays at a slower rate than CH_3^+ and approaches zero after 98 ms. As described earlier in this chapter, the I^+ ion was seen in pure CF_3I and the 1:1 mixture systems but was not detected in thepure CH_3I system. Therefore, I^+ must be generated in CF_3I, as well as in the CH_3I-CF_3I systems as one of the primary fragment ions. The reason why it was not seen in the CH_3I system must be a charge transfer reaction as described in Reaction VI-5. Another route for I^+ disappearance could be production of I_2^+ through Reaction VI-14. Reaction schemes with rate constants are shown in Tables 7, 8 and 9 for I^+, CH_3^+ and other ions.

CF_2I^+. In Fig. 43 the time dependent ion decay signal showing reactions of CF_2I^+ in the equimolar mixture of CH_3I-CF_3I was generated at pressure of 1.3×10^{-5} torr by 70 eV electrons. As indicated in the mass spectra of pure CF_3I and the 1:1 mixture , the intensity of CF_2I^+ is quite high. From Fig. 43 it can be observed that the signal grows up to 30 ms and then decreases until 250 ms without approaching zero. One of the routes of its formation can be through Reaction VI-12 where a neutral product, CF_4, is expected to be produced. The CF_2I^+ ion might decay through Reactions VI-20 and VI-23 to form products which were not identified.

2. Time-of-Flight Results

Several graphs showing ion intensities as a function of pressure, obtained from the TOF instrument are presented in Figs. 45 through 52. From these experimetal studies the small CF^+ ion and mixed product ions such as $CF_3ICH_3^+$, $CF_2ICH_2^+$ and $CF_3I_2CH_3^+$ were identified. Another product which could not be detected in the ICR but was seen

Table 9

Experimental rate constants and ion-molecule reactions in the equimolar CH_3I-CF_3I system

Reactions	k(exp)[a]	Comments
$CH_3^+ + CF_3I \dashrightarrow CH_3F + CF_2I^+$	10.0	ICDR[b]
CH_3^+ + RI[c] --> product	45.8	TOF[d]
CH_3I^+ + RI --> product	9.88	TOF
$CF_3I^+ + CH_3I \dashrightarrow CF_3I + CH_3I^+$	6.7	ICDR
$CF_3^+ + CH_3I \dashrightarrow CF_3H + CH_2I^+$	3.0 ± 1.2	ICDR
CF_3^+ + RI --> product	4.0	TOF
I^+ + RI --> product	10.3	ICDR
CF^+ + RI --> product	37.5	TOF
CF_2I^+ + RI --> product	0.22	ICDR

a All k's are in cm^3 $molec.^{-1}$ s^{-1} x 10^{+10}.

b ICDR means the reaction channel was verified by ICR double resonance experiments.

c RI means CH_3I or CF_3I.

d TOF means Time Of Flight mass spectrometer.

Table 10
Rate constants determined from pressure–intensity data in the equimolar CH_3I–CF_3I system using the Time-of-Flight instrument

Ions		k(Relative)	k(Literature)[b]	Ref.
I^+	dec.(0.001–0.012)	14.0	9.7±2.8; 3.1±0.2; 10.3[c] 2.85	ICR[d] (8)
CH_3^+	dec.(0.004–0.012)	30.0		
CH_3^+	dec.(0.017–0.032)	7.7	19.9±1.2; 10.0[c]	ICR
CH_3I^+	dec.(0.014–0.028)	3.1	0.34±0.12	ICR
$(CH_3)_2I^+$	dec.(0.17–0.27)	0.44		
$(CH_3I)_2^+$	dec.(0.005–0.03)	0.44		
CFI^+ (?e)	dec.(0.002–0.006)	10.0		
CF^+	dec.(0.001–0.022)	12.0		
CF_2^+	inc.(0.02–0.025)	9.5		
CF_3^+	dec.(0.001–0.025)	3.3	2.4±1.0; 3.0±1.2[c] 2.46	ICR (8)
CF_2I^+	inc.(0.001–0.037)	1.5	1.68	(8)
CF_2I^+	dec.(0.04–0.23)	0.55	0.14; 0.22(b)	ICR
CF_3I^+	dec.(0.006–0.034)	3.1	0.74±0.55; 6.7(b) 1.36	ICR (8)
$(CF_3)_2I^+$	dec.(0.1–0.2)	0.1	0.29±0.12	ICR
$CF_2I_2^+$	dec.(0.024–0.034)	1.4		
$CF_2I_2^+$	inc.(0.01–0.17)	0.34		
$CF_3I_2^+$	dec.(0.2–0.37)	0.11		
$(CF_3I)_2^+$	inc.(0.17–0.4)	0.06	0.14 0.22	ICR (8)
$CH_2ICF_2^+$	dec.(0.12–0.4)	0.15		
$CH_3ICF_3^+$	dec.(0.008–0.028)	0.04		

---

[a] Rate Constants in cm^3 $molec.^{-1}$ s^{-1} as calculated by equation $\ln[I^+]/[I_o^+] = k_{abs}[n/v]t$ are 10 times the values listed and all the pressures in paretheses are in torr.

[b] Values are from pure CF_3I and CH_3I systems unless indicated.

[c] These values were obtained from the 1:1 mixtures.

[d] ICR experiments from this work.

[e] Ion has same mass number as $(CH_3)_2I^+$ but it appeared at very low pressure where $(CH_3)_2I^+$ is unlikely to appear.

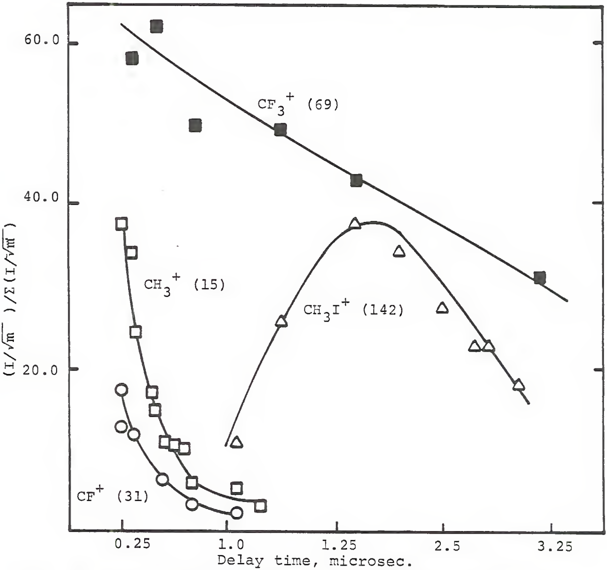

Fig. 44. Normalized ion intensities as a function of delay time in the TOF mass spectrometry of 1:1 mixture of CF_3I-CH_3I system at 25°C.

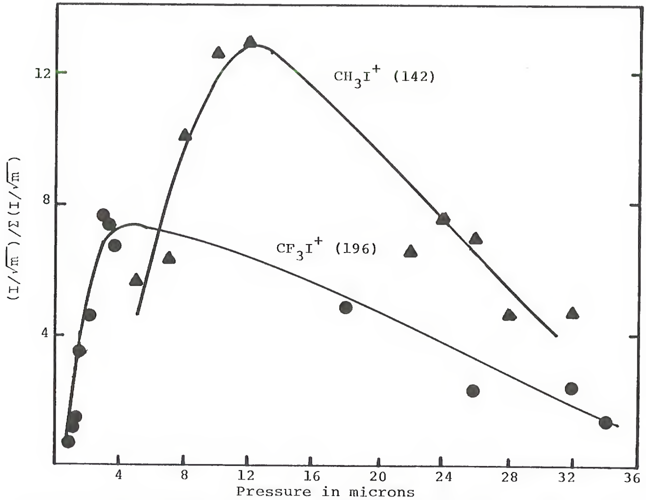

Fig. 45. Normalized ion intensities as a function of pressure in TOF mass spectrometry of 1:1 mixture of CF_3I-CH_3I systems at 25°C.

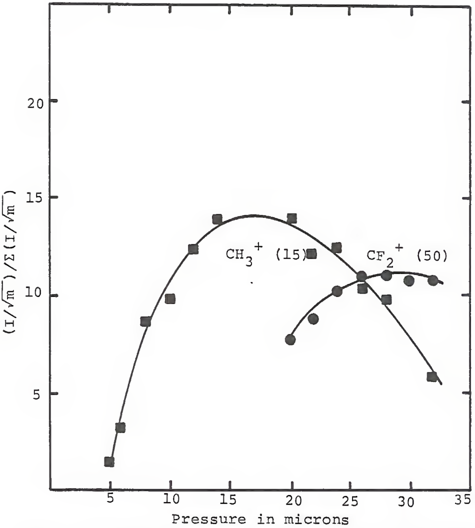

Fig. 46. Normalized ion intensities as a function of pressure in the in the TOF mass spectrometry of 1:1 mixture of CF_3I-CH_3I system at 25°C.

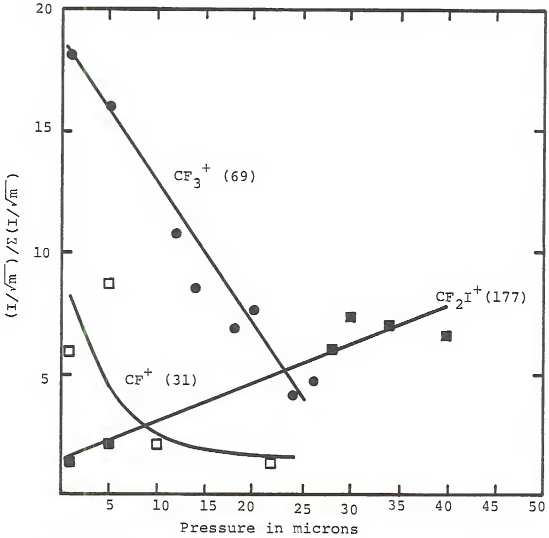

Fig. 47. Normalized ion intensities as a function of pressure in the TOF mass spectrometry of 1:1 mixture of CF_3I-CH_3I system at 25°C.

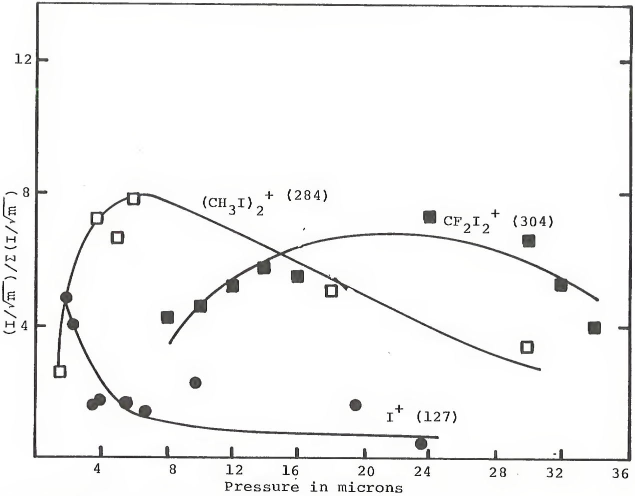

Fig. 48. Normalized ion intensities as a function of pressure in the TOF mass spectrometry of 1:1 mixture of CF_3I-CH_3I system at 25°C.

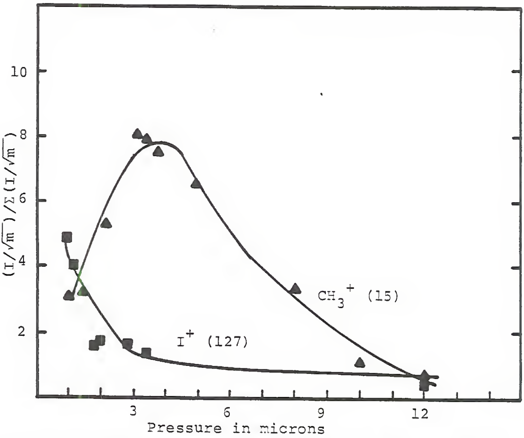

Fig. 49. Normalized ion intensities as a function of pressure in the TOF mass spectrometry of 1:1 mixture of CF_3I-CH_3I system at 25°C.

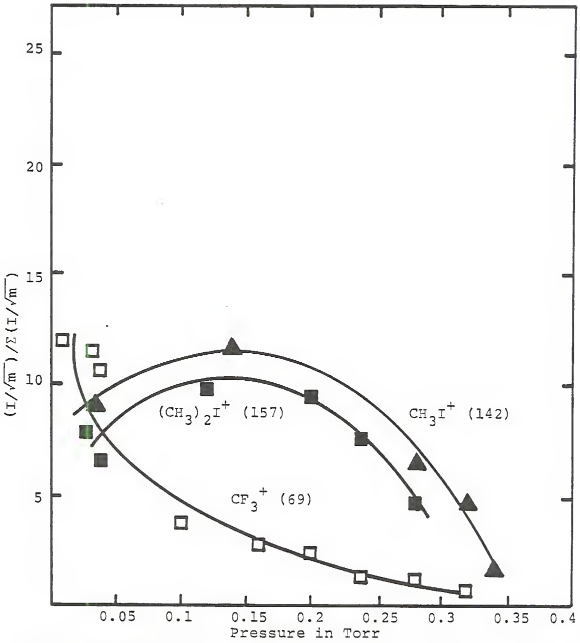

Fig. 50. Normalized ion intensities as a function of pressure in the TOF mass spectrometry of 1:1 mixture of CF_3I-CH_3I system at 25°C.

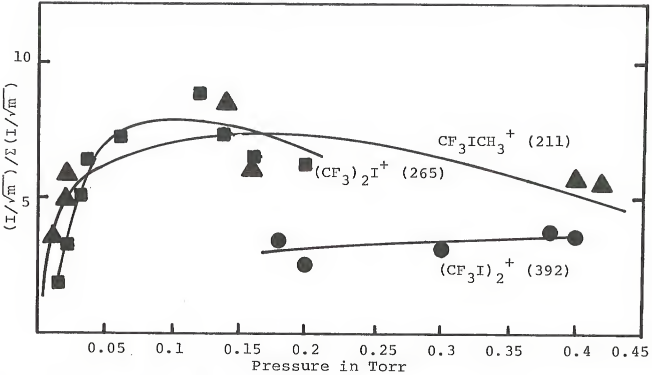

Fig. 51. Normalized ion intensities as a function of pressure in the TOF mass spectrometry of 1:1 mixture of CF_3I-CH_3I system at 25°C.

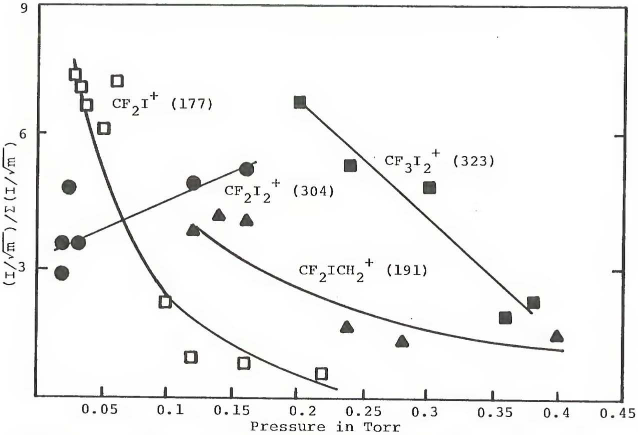

Fig. 52. Normalized ion intensities as a function of pressure in the TOF mass spectrometryof 1:1 mixture of CF_3I-CH_3I system at 25°C.

in the TOF, is $(CH_3)_2I_2^+$ as shown in Fig. 48. The mixed products pressure dependent graphs are shown in Figs. 51 and 52 An explanation of why the mixed products and $(CH_3)_2I_2^+$ (both in the 1:1 mixture and pure CH_3I) could not be seen in the ICR is given in the following discussion section.

Square-root-corrected intensities, of parent ion CH_3I^+ and some fragment ions such as CF_3^+, CH_3^+, CF^+ in the high pressure TOF mass spectrometry of CH_3I-CF_3I equimolar mixture are plotted as a function of delay time in microseconds as shown in Fig. 44. The reason for carrying out the square-root corrections is explained in section 3 of this discussion. Intensities of CH_3^+ and CF_3^+, and CF^+ decrease with delay time. The CH_3I^+ intensity increases from 0.7 microsec. up to 1.5 microsec. and thereafter it decreases rapidly. The rate constant for CH_3^+ reaction with substrates in the equimolar CH_3I-CF_3I system using the TOF instrument was calculated to be 45.8×10^{-10} cm^3 $molec.^{-1}$ s^{-1} ; this value is about four times larger compared to the value obtained from the ICR machine. The ICR value represents only one of several possible reaction channels, while the TOF value is a sum of rate constants over all possible channels. Figure 44 shows that the intensity of CF^+ as well as that of CH_3^+ falls rapidly and approaches zero. The CF^+ rate constant was evaluated to be 37.5×10^{-10} cm^3 $molec.^{-1}$ s^{-1}. This rate constant indicates that CF^+ is a very reactive species and also could have many reaction pathways. Data shown in Figs. 36-43 were also taken in a time delay mode, but on the ICR rather than the TOF instrument.

Most of the data taken on the CF_3I-CH_3I system with TOF instrument were measured as a function of pressure, using the continuous ionization mode. Figures 45 to 52 show the variation of normalized ion intensities as a function of pressure in microns. In Fig. 45 the CF_3I^+ intensity increases from 1.0 to 4.0 microns, then decreases rapidly. In Fig. 48 the I^+ intensity decreases sharply from 1.0 micron up to 3.0 micron and then levels off. In Fig. 45 the CH_3I^+, and CF_3I^+ intensities are shown as a function of pressure. Figure 50 shows that at high pressure of substrates the intensities of one of the parent CH_3I^+ the ether type product $(CH_3)_2I^+$ and the fragment ion, CF_3^+, all decrease rapidly in the pressure range 0.05 to 0.35 torr. As shown in Fig. 52 shows the intensity behavior of the ions CF_2I^+, $CF_2I_2^+$, $CF_3I_2^+$ and $CH_2ICF_2^+$ at high pressure; the latter three are not observable under low pressure conditions. bit higher than background pressure.

When the data shown in Figures 45-52 were evaluated by the method described in the Experimental section in Chapter II, resulting rate constants were invariably sustantially larger than literature values, or values determined in the present work using the ICR instrument. It is apparent that equation VI-6 underestimates the residence time ,t. Using the literature values for several of the processes measured, it was found by back calculation that typical residence times were more nearly 15 rather than 1.5 microseconds.

This discrepancy could have several physical causes including effects of space charge, collisions with ambient molecules, nonrectilinear paths, paths not colinear with the line- of-sight to the ion exit slit, and longer paths due to ions born on the far side of the electron beam. In addition, the moderately intense negative charge region caused by the electron beam may constitute a "quasi-ground". The result is that most of the potential drop (20 volts total) due to the backing plate occurs between the backing plate and the region of the electron beam, with relatively slight additional potential drop between that point and the exit slit.

It is not unreasonable that the cumulative effect of these several factors could be a 10-fold increase in residence time. Additionally, there is independent evidence of the longer actual residence times obtained in early experiments using the same TOF instrument operating in the time delay mode. In those investigations, it was frequently possible to take data using a time delay between ion formation and ion extraction of as much as 12 microseconds; this would not be possible if, in fact, all ions had escaped from the source within 1.5 microseconds.

For the reasons described, rate constants calculated using equation II-4 above with the t value obtained from the equations VI-6 were divided by 10; these values are recorded in Table 10. It is seen that reasonable agreement with literature values (within a factor of 2 to 3) is obtained in most cases for which literature values are available. Rate constants for the other processes, where no relevant literature values exist may be relied upon with the same degree of uncertainty.

The rate constant for loss of CH_3^+ in the pressure-intensity study was evaluated to be 7.7×10^{-10} cm^3 molec.$^{-1}$ s^{-1} in the pressure range 0.017-0.032 torr as shown in Fig. 46. This value is less than the values calculated from the ICR (time-intensity data) by a factor of 1.3 for the equimolar CH_3I-CF_3I system and 2.6 for the pure CH_3I system as shown in Table 10. In addition to the rate constant shown in Table 10, a lower pressure(0.004-0.012 torr) value was found to be 30.0×10^{-10} cm^3 molec.$^{-1}$ s^{-1}. This rate constant is higher by a factor of 3 than that obtained for the 1:1 mixture from the ICR instrument and 1.5 times higher than that in the pure CH_3I system. The rate constants evaluated from the ICR data are for single reaction channels while those from the TOF machine are for all possible reaction channels.

One of the important discoveries in this system is the identification of $(CF_3)_2I^+$ which was not reported previously (8). It is seen both in the TOF and in the ICR instrument although signal averaging was needed to detect in the ICR. Additonally, the dimers $(CH_3I)_2^+$ and $(CF_3I)_2^+$ were detected at a high pressure by the TOF instrument. The species $(CF_3I)_2^+$ was also detected in the ICR instrument, but $(CH_3I)_2^+$ could not been seen.

3. Discussion

The gas phase radiolysis (3) and photolysis of equimolar mixtures of CH_3I-CF_3I were investigated in this laboratory. End product identification and analysis following gamma radiolysis showed a variety of cross-products such as CF_3H, CH_3CF_3, and CF_2CH_2. Although CH_3F was also identified as a product in the photolysis of the mixtures at a relatively high pressure (100 torr of each substrate), the yield is extremely small and difficult to measure. Therefore involvement of ion-molecule reactions in the formation of cross-products during radiolysis was suggested (3). The gas phase ion chemistry, radiation chemistry, and photochemistry of pure CH_3I and pure CF_3I as well as the radiation and photochemistry of the 1:1 mixtures were described previously (1,2,3,14).

As a result of electron impact in the TOF instrument, ions were seen which derived from CH_3I only, from CF_3I

only, and from both reactants. The first product group includes CH_3^+, CH_3I^+, $CH_3I_2^+$, $(CH_3)_2I^+$, and $(CH_3I)_2^+$. Ions derived from the fluorocarbon parent include CF^+, CF_2^+, CF_3^+, CF_2I^+, CF_3I^+, $CF_2I_2^+$, $CF_3I_2^+$, the ether type ion $(CF_3)_2I^+$, and the dimer ion $(CF_3I)_2^+$. Cross-products arising from both substrates include $CH_3ICF_3^+$, $CH_2ICF_2^+$, and $CHICF^+$, in addition to the species I^+. It was possible to take data on ion intensities of all of these species as a function of pressure in the ion source. Other species were present and were observed on the display oscilloscope, although data could not be recorded because of short lifetimes (e.g., CH^+ and CH_2^+), low intensity (I_2^+, $CF_3I_2CH_3^+$, $CHICF^+$), or limited resolution ($CH_3I_2^+$). Some of these species were studied successfully with the ICR instrument, however.

Using an ion cyclotron resonance mass spectrometer, several fragment ions were seen, as well as CH_3I^+, CF_3I^+, $CF_3I_2^+$ and $(CF_3I)_2^+$. All of these ions were also seen in the TOF instrument.

A brief description of the reactions characteristic of the mixture is given below. Properties of the two pure systems are also considered for comparison.

The ion-molecule reaction scheme for CH_3I-CF_3I mixtures will, in general, include all of the processes seen in pure CH_3I and CF_3I, plus additional reactions characteristic of the mixtures. The former reactions are listed in Tables 7 and 8, respectively. Contributions of processes involving reaction of CF_3I^+ upon CF_3I substrate are somewhat diminished, however, due to the efficient charge exchange reaction

$$CH_3I + CF_3I^+ \text{--->} CH_3I^+ + CF_3I \qquad \text{VI-27}$$

This process is energetically favorable due to the difference in ionization potentials between CH_3I (9.54 eV) and CF_3I (10.23 eV). The rate constant for reaction VI-27 was measured as 6.7×10^{-10} cm^3 $molec.^{-1}$ s^{-1}. Occurrence of this process was confirmed using the ICDR technique.

As mentioned above, some of the neutral cross-products seen in the gamma radiolysis of the equimolar mixtures of CH_3I-CF_3I could be accounted through ion-molecule reactions seen in the present work. An example is seen in the case of formation of CF_3H. Using the ICR instrument, the CF_3^+ ion is found to react with substrate CH_3I with a rate constant of $3.0 \pm 1.2 \times 10^{-10}$ cm^3 $molec.^{-1}$ s^{-1}. The equation is presumed to be

$$CF_3^+ + CH_3I \text{--->} CF_3H + CH_2I^+ \qquad \text{VI-28}$$

It is found in the ICR instrument that the I^+ ion undergoes the same reaction observed in the pure CH_3I and CF_3I systems, reacting via charge exchange with CH_3I and producing I_2^+ with the CF_3I.

$$I^+ + CH_3I \text{--->} CH_3I^+ + I\cdot \qquad \text{VI-5}$$

$$I^+ + CF_3I \dashrightarrow CF_3 + I_2^+ \qquad \text{VI-14}$$

While there is no evidence on this point, it is interesting to speculate that there could be an alternate route to I_2^+ according to the reaction

$$CH_3I^+ + CF_3I \dashrightarrow CH_3CF_3 + I_2^+ \qquad \text{VI-29}$$

This could be one of the ways of forming CF_3CH_3 (and subsequently its decomposition product CF_2CH_2) in the radiolysis of gas phase CF_3-CH_3I mixtures.

The cross-product ions seen at high pressure in the TOF instrument were $CH_3ICF_3^+$ and $CH_2ICF_2^+$; production of these ions was studied as a function of pressure. There was also limited evidence supporting formation of $CHICF^+$. Due to the low pressure operation of the ICR instrument and since at this low pressure the charge transfer reaction is dominant, the absence of these cross-products and especially $CH_3ICF_3^+$ should not be surprising.

Reactions of the primary ions, CH_3I^+, CH_3^+, CF_2I^+, and I^+ to form various products such as $(CH_3)_2I^+$, $(CF_3)_2I^+$, $(CH_3I)_2^+$, $(CF_3I)_2^+$, $CH_3I_2^+$, $CF_3I_2^+$, CF_2I^+ will be very much like the chemistry seen in pure CH_3I and CF_3I. However, the production of I_2^+ can occur only through I^+ reacting with substrate CF_3I since in reaction with CH_3I the preferred reaction channel is charge transfer. In the ICR instrument the charge transfer reaction between CF_3I^+ and CH_3I

$$CF_3I^+ + CH_3I \longrightarrow CF_3I + CH_3I^+ \qquad \text{VI-27}$$

was verified using the ICDR experiment and the reaction is very fast. The alternative reactions of the primary ion CF_3I^+ (which is the source for the production of the reaction products $CF_3I_2^+$, $(CF_3)_2I^+$ and $(CF_3I)_2^+$) are too slow to compete effectively with the faster charge transfer reaction channel. Due to this channel, these products were not seen in the equimolar mixture experiment using the ICR. According to the ICR experiment, the gas phase ion chemistry of the CH_3I-CF_3I systems is dominated by reactions of CH_3I. Under the much higher pressure conditions of the TOF experiment, however, many product ions from CF_3I not observable with the ICR instrument, could be observed and measured as a function of pressure.

The rate constant for loss of the primary ion CH_3^+ in the mixtures has a value which can be accounted for by reaction with CH_3I substate only, as studied using the pure compound. However, it is not possible to exclude a somewhat slower reacation with fluorocarbon substrate, such as

$$CH_3^+ + CF_3I \longrightarrow CH_3I + CF_3^+ \qquad \text{VI-30}$$

A more interesting reaction channel would be transfer of F^-

ion in the process

$$CH_3^+ + CF_3I \longrightarrow CH_3F + CF_2I^+ \qquad \text{VI-31}$$

Again, although there is no evidence supporting this process, its occurrence cannot be excluded.

The cross-product ions $CH_3ICF_3^+$ and $CH_2ICF_2^+$ were seen in the TOF instrument; possible routes for their formation are

$$CH_3^+ + CF_3I \longrightarrow CF_3ICH_3^+ \qquad \text{VI-32}$$

$$CF_3^+ + CH_3I \longrightarrow CF_3ICH_3^+ \qquad \text{VI-33}$$

Subsequently, the $CF_3ICH_3^+$ ion may have sufficient excess internal energy to lose HF to form $CH_2ICF_2^+$.

$$CH_3ICF_3^+ \longrightarrow CH_2ICF_2^+ + HF \qquad \text{VI-34}$$

Another cross-product ion which was seen in the TOF was the species $CH_3I_2CF_3^+$; unfortunately it was not observable using the ICR instrument. It could be accounted through the reaction

$$CH_3I^+ + CF_3I \longrightarrow CH_3I_2CF_3^+ \qquad \text{VI-35}$$

$$CF_3I^+ + CH_3I \longrightarrow CF_3I_2CH_3^+ \qquad \text{VI-36}$$

$$\longrightarrow CF_3I + CH_3I^+ \qquad \text{VI-37}$$

The reaction channels confirmed using the ICR instrument for the three systems are presented in Tables 7 , 8 and 9.

E. Summary

The gas phase ion chemistry of pure CH_3I and pure CF_3I and an equimolar mixture of the two was studied using the

ICR instrument; in addition the equimolar mixture was studied in the TOF instrument as a function of pressure. Ion-molecule reaction pathways in the two pure compounds are very similar. The formation of neutral products such as CH_4, CF_4, CF_3H, CH_3F and CH_3CF_3 seems very possible in the ion molecule reactions determined in this study. Cross product ions such as $CH_3ICF_3^+$, $CH_2ICF_2^+$ and $CH_3I_2CF_3^+$ were observable in the TOF instrument as a function of pressure. They detected in the ICR for the reason that the charge transfer rate from CF_3I^+ to CH_3I is very fast.

APPENDIX I

IDENTIFICATION OF PHOTOLYSIS PRODUCTS

The inorganic products formed in the photolysis of pure CH_3I, pure CF_3I and an equimolar mixtures of both were HF, HI and I_2. These compounds were identified using potentiometric titration using fluoride and iodide selective electrodes and absorption spectroscopy.

All the organic products were identified by their gas chromatographic retention times. The chromatograms for the three systems are shown in Figures 53, 54 and 55, respectively.

Fig. 53. Gas chromatogram of photolyzed CH_3I (helium gas flow rate of 30ml/min. on 9ft x 0.25" O.D. x 0.020" wall stainless steel column packed with 60/80 mesh silica gel.)

Peak identification

1. CH_4
2. C_2H_6
3. C_2H_4
4. C_4H_{10}
5. C_3H_6
6. i-C_5H_{12}
7. n-C_5H_{12}
8. C_4H_8
9. CH_2I_2

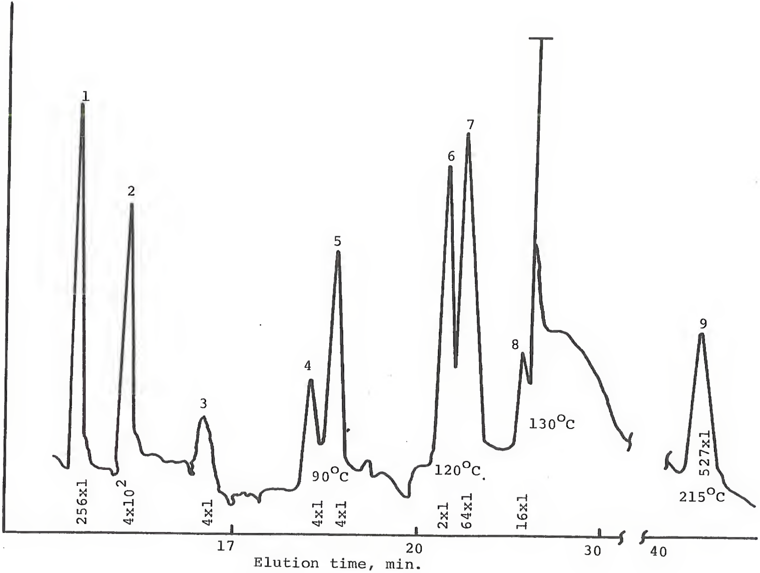
1
2
3
4
5
6
7
8
9
256x1
4x10²
4x1
4x1
4x1
90°C
2x1
64x1
120°C
16x1
130°C
527x1
215°C
17
20
30
40
Elution time, min.

Fig. 53.

Fig. 54. Gas chromatogram of photolyzed CF_3I (helium gas flow rate of 30 ml/min. on 9ft x 0.25" O.D. x 0.020" wall stainless steel column packed with 60/80 mesh silica gel.)

Peak identification

1. C_2F_6
2. C_2F_4
3. C_3F_8
4. C_2F_5I
5. $C_2F_4I_2$
6. $C_2F_2I_2$

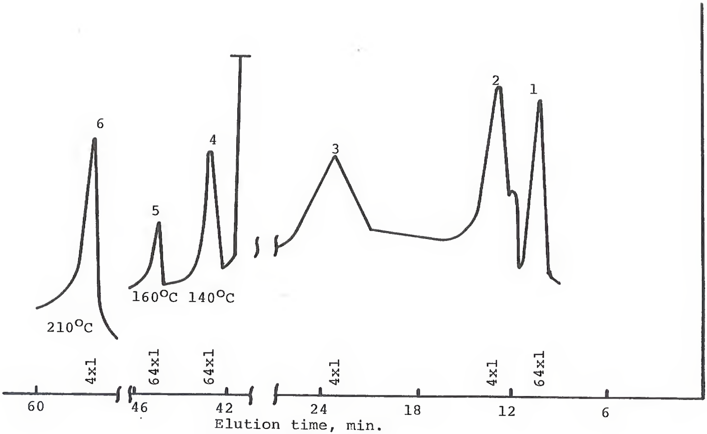
6
4
5
3
2
1
210°C
160°C
140°C
4x1
64x1
64x1
4x1
4x1
64x1
60
46
42
24
18
12
6
Elution time, min.

Fig. 54.

Fig. 55. Gas chromatogram of photolyzed equimolar mixture of CF_3I-CH_3I (helium gas flow rate of 30 ml/min. 6 m x 0.25" O.D. x 0.020" wall stainless steel column packed with 30% SE-30 on 60/80 mesh chromosorb W (non acid wash) plus 4.6 m (same O.D. like the SE-30) column packed with 40/50 mesh silica gel.

Peak identification

1. CH_4
2,3. C_2H_6+C_2F_6
4. C_2H_4
5. CF_3H
6. 1,1-CF_2CH_2
7. 1,1,1-CF_3CH_3
8. C_2F_5I
9. CH_2I_2

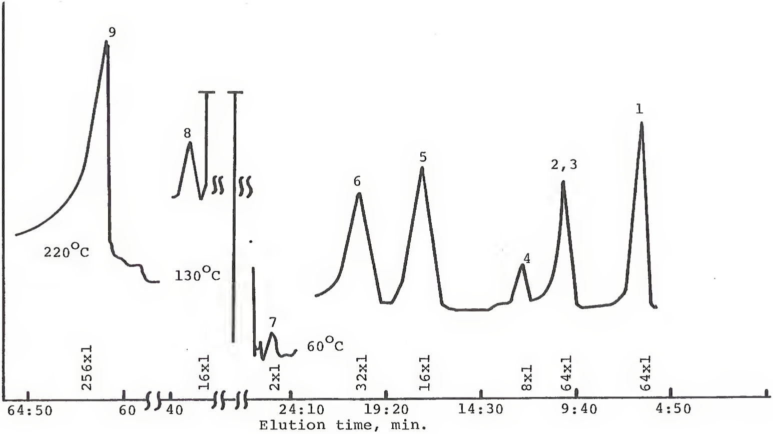
9
8
1
5
2,3
6
4
7
220°C
130°C
60°C
256x1
16x1
2x1
32x1
16x1
8x1
64x1
64x1
64:50
60
40
24:10
19:20
14:30
9:40
4:50
Elution time, min.

Fig. 55.

APPENDIX II

IONIZATION POTENTIALS

The ionization potentials of $I^{\cdot}$, $CH_3{}^{\cdot}$, $CF_3{}^{\cdot}$, CH_3I and CF_3I are presented in Table 11.

Table 11

Ionization Potentials

Name of Compound	Ionization Potentials (eV)[a]
$I\cdot$	10.451
CF_3I	10.21
$CH_3\cdot$	9.83
CH_3I	9.54
$CF_3\cdot$	9.25

---

[a] Reference (98).

REFERENCES

1. J. Marie Donovan and R.J. Hanrahan, "The Radiation Chemistry of Methyl Iodide in the Gas Phase", Int. J. Radiat. Phys. Chem., 3, 491 (1971).

2. T. Hsieh and R.J. Hanrahan, "Gas Phase Radiation Chemistry of Trifluoromethyl Iodide", Rad. Phys. Chem., 12, 153 (1978).

3. D. Teclemariam and R.J. Hanrahan, "Gas Phase Radiolysis of CF_3I-CH_3I Mixtures", Radiat. Phys. Chem., 19, 443 (1982).

4. R. N. Schindler and M. H. J. Wijnen, "The Gas Phase Radiolysis of Ethyl Iodide", Z. Physik Chem. Neue Floge, 38, 285 (1963).

5. E.D. Pottie, R. Barker, and W.H. Hamill, "Ion-Molecule Reactions of Methyl and Ethyl Iodides", Radiat. Res., 10, 644 (1959).

6. L. W. Sieck and R. Gordon, Jr, "Formation of Association Ions in the Photoionization of Alkyl Halides", Int. J. Chem, Kinetics, 5, 445 (1973).

7. J. L. Beauchamp, D. Holtz, S.D. Woodgate, and S. L. Patt, "Thermochemical Properties and Ion-Molecule Reactions of the Alkyl Halies in the Gas Phase by Ion Cyclotron Resonance Spectroscopy", J. Am. Chem. Soc., 94, 27-98 (1972).

8. T. Hsieh, John R. Eyler, and R.J. Hanrahan, "Ion-Molecule Reactions in Trifluoromethyl Iodide and Pentafluoroethyl Iodide", Intern. J. Mass Spec. Ion Physics, 28, 113 (1978).

9. J.V.V. Kasper and G. C. Pimentel, "Atomic Iodine Photochemical Laser", Appl. Phys. Letters, 11, 231 (1964).

10. J.V.V. Kasper and G. O. Pimentel, "Iodine Atom Laser Emission in Alkyl Iodide Photolysis", J. Chem. Phys., 43, 1827 (1965).

11. G. A. Skorbogatov and V. M. Simirnov, "Chemical Reactions Occurring in Kasper-Pimentel Perfluoroalkyl Iodide Laser", Zhurnal Obshehei Khimii, 41, 1411 (1971), Available in English, Translation from Consultants Bureau Inc.

12. R. Srinirasn and J. R. Lankard, "The Role of $CF_3\cdot$ Radicals in the Photochemical Iodine Laser", J. Phys. Chem., 78, 951 (1974).

13. A. Costell, Juan in Figuera, M. Martin, and L. Valle, "Influence of Photochemistry of CH_3I Photodissocitation Laser Performance", J. of Photochemistry, 12, 235 (1980).

14. J. R. Dacey, "The Photolysis of Trifluoromethyl-Iodide", Discuss. Faraday Soc., 14, 84 (1953).

15. H. Okabe,"Photochemistry of Small Molecule", pp. 302-3, John Wiley and Sons, New York, 1976.

16. V. L. Talroze, M. N. Larichev, etal, "Mass-Spectra Study of CF_3I and C_3F_7I Photolysis", J. Chem. Phys., 64, 3138 (1976).

17. T. Donohue and J. R. Wiesenfield, "Photodissociation of Alky Iodides", J. Chem. Phys., 63, 3130 (1975).

18. E.W.R. Steacie "Atomic and Free Radical Reactions", Reinhold, New York, 1946.

19. Noyes and Leighton, "The Photochemistry of Gases", Reinhold, New York, 1946.

20. T. Hsieh, Ph.D. Dissertation, The Radiation Chemistry and Mass Spechometry of Trifluoromethyl Iodide and Pentafluoromethyl Iodide in the Gas Phase, University of Florida, 1976.

21. (a). I. Mcalpine and H. Sutcliffe, "The Radiolysis of Trifluoro Iodomethane in the Gas Phase", J. Phy. Chem. 73, 3215 (1969). (b). I. McAipine and H. Sutcliffe, "The Radiolysis of Gaseous Trifluoromethane in the Presence of Nitric Oxide", J. Phys. Chem., 74, 849 (1970).

22. P.G. Shah, D.R. Stranks, and R. Cooper, "The Radiolysis of Gaseous Triflurometnyl Iodide", Am. J. Chem., 23, 253 (1970).

23. R.A. Fass and J.E. Willard, "Hydrogen Abstraction by Hot CF_3 Radicals", J. Chem. Phys., 52, 1874, (1970).

24. T. Ogawa, G.A. Carlson, and G.O. Pimentel, "Reaction Rate of Trifluoro Methyl Radicals by Rapid scan Infrared Spectroscopy", J. Phys. Chem., 74, 2090 (1970).

25. D. Porret and C.F. Goodeve, "The Continuous Absorption Spectrum of Methyl Iodide", Proc. Roy. Soc. London Ser., A165, 31 (1938).

26. D. Porret and C.F. Goodeve, "The Continuous Absorption Spectrum of Alkyl Bromides and Their Quantal Interpretation", Proc. Roy. Soc. London Ser., A165, 31 (1938).

27. M. Ito, P.C. Huang, and E.M. Kosower,"Electron Abosrption Spectra of Iodo- and Bromethanes", Trans. Faraday Soc., 57,1662 (1961).

28. S.J. Riley and K.B. Wilson,"Excited Fragments From Excited Molecules: Energy Partitioning in the Photodissociation of Alkyl Iodides", Faraday Discuss. Chem. Soc., 53, 132(1972).

29. R.D. Schultz and H.A. Taylor, "Photolysis of Methyl Iodide", J. Chem. Phys., 18,194 (1950).

30. F.P. Hudson, R.R. Williams, Jr. and W.H. Hamil, "Moderation of Hot Methyl Radicals in Photolysis of Methyl Iodide", J. Chem. Phys., 21,1894 (1953).

31. R.B. Martin and W.A. Noyes, Jr., "Photochemical Studies. XLVIII. The Reaction of Methyl Radicals with Oxygen", J. Am. Chem. Soc., 75 4183 (1953).

32. G.M. Harris and J.E. Willard, "Photochemical Reactions in the System Methyl Iodide-Iodine-Methane; The Reaction $C^{14}H_3\cdot + CH_4 \dashrightarrow C^{14}H_4 + CH_3\cdot$", J. Am. Chem. Soc., 76, 4678 (1954).

33. R.D. Souffie, R.R. Williams, Jr., and W.H. Hamill, "Hot Radical Reactions in the Photolysis of Methyl Iodide Vapour", J. Am. Chem. Soc., 78, 917 (1956).

34. J.E. Willard,"Radiation Chemistry and Hot Atom Chemistry", Am. Rev. Phys. Chem., 6, 141 (1955).

35. Richard d. Doepker and P. Ausloos, "Gas-Phase Photolysis of Methyl Iodide Reactions of Hot Methyl Radicals with Added Organic Compounds", J. Chem. Phys., 41, 1865 (1964).

36. C.C. Chou, P. Angelberger and S. Rowland, "Methylene Reaction in Photolytic Systems Involving Methyl iodide", J. Phys. Chem., 75, (16),(1971).

37. B.M. Mahan, and R. Mandal, "Vacuum Ultra-Violet Photolysis of Methane", J. Chem. Phys., 37, 207 (1963).

38. G. Herzberg, "Electronic Spectra of Polyatomic Molecules", D. VaNostrand Co., Inc., Princeton, N.J., p. 448 (1967).

39. M.E. Jacox and D.E. Milligan, "Matrix-Isolation Study of the Vacuum Ultra-Violet Photolysis of Methyl Chloride and Methylene Chloride. Infrared and Ultra-Violet Spectra of the Free Radicals $CCl\cdot$, $H_2CCl\cdot$, and $CCl_2:$", J. Chem. Phys., 53, 2688 (1970).

40. M.E. Jacox and D.E. Milligan, "Matrix-Isolation Study of the Vacuum Ultra-Violet Photolysis Methyl Fluoride. The Infrared Spectra of the Free Radicals $CF\cdot$, $HCF:$, and $H_2CF\cdot$", J. Chem. Phys., 50, 3252(1969).

41. T.F. Hunter and K.S. Kristjansson, "Optoacoustic Method of Measuring Reaction Rates of the Radicals $CH_3\cdot$, $CD_3\cdot$, $C_2H_5\cdot$, and $CH_2I\cdot$ with $I\cdot$ and I_2", J. Chem. Soc. Faraday Trans, 2, 78, 2067 (1982).

42. F.R. Majer and J.P. Simons, "Photochemical Processes in Halogenated Compounds", Adv. Photochemistry, 2, 137 (1964).

43. L. F. Fiser and M. Fieser, Regents for Organic Syntheses, John Wiley & Sons, New York, 1967, p. 17

44. A.J. Frank, Ph.D. Dissertation, The Radiation Chemistry and Photochemistry of Ethyl Bromide in the Gas Phase, Univ. of Florida, (1975).

45. E.C.Y. Inn and Y. Tanaka, "Ozone Chemistry and Technology", in Advances in Chemistry Series, 12, American Chemical Society, Washington D.C., 1959, p. 263.

46. B.J. Huebet and R.M. Martin, "Gas Phase for Ultraviolet Absorption Spectrum of Hydrogen Bromide and Hydrogen Iodide", J. Phys. Chem., 72, (8) 3046 (1968).

47. S.L. Baugheum and S.R. Leone, "Photofragmentation Infrared Emission Studies of Vibrationally Excited Free Radicals CH_3• and CH_2I•", J. Chem. Phys., 72 (12), 6531 (1980).

48. W.H. Pence, S.L. Baughecum and S.R. Leone, "Laser UV Photofragmentation of Hologenated Molecules. Selective Bond Dissociation and Wavelength-Specific quantum Yields for excited I ($^2P_{1/2}$) and Br ($^2P_{1/2}$) Atoms", J. Phys. Chem., 85, 3844 (1981).

49. H. Okabe, "Photochemistry of Small Molecules", A Wiley-Interscience Publication, John Wiley and Sons, 1978 p. 64.

50. R.M. Martin and J.E. Willard, "Reactions of Photochemically Produced Hot Hydrogen Atoms in the Photolysis of HI at 184.9 nm", J. Chem. Phys., 40, 2999 (1964).

51. C.A. Kennedy, Ph.D. Dissertation, "Effects of Free Radical Scavengers in the Radiolysis of Systems Containing Perfluoracycloxane", University of Florida, 1969.

52. E. Rabinowitch and W.C. Wood, "The Extinct Ion Coefficients of Iodine and Other Hologens ", Trans. Faraday soc., 32, 540 (1963).

53. C.A. Goy and H.O. Pritchard, "Pressure Dependence of the Visible Iodine Bond", J. Mole. Spectroscopy, 12, 38 (1964).

54. E. Heckle and P.F. Marsh, "Titration of Subnanomole Quantities of Fluoride Ions in Polar Nonaqueous Solvents", Anal. Chem., 44, 2347 (1972).

55. J.H. Futrell, T.D. Teirman, F.P. Abramson, and C.D. Miller, "Modification of a Time-of-Flight Mass Spectrometer for Investigation of Ion-Molecule Reactions at Elevated Pressured", Rev. Sci. Inst., 39, 340 (1968).

56. M.B. Fallagatter and R.J. Hanrahan, "High Pressure Mass Spectrometry of Simple Hydrocarbon and Alkyl Halide Systems Using Pulsed and Continuous Ionization", Paper No. 145, 158th ACS National Meeting, New York, N.Y., 1969.

57. A.R. Ravishankara, Ph.D. Dissertation, The Photolysis, Radiolysis and Mass Spectrommetry of 1,1,2,2- Tetrafluorocycle Butane, University of Florida, 1975.

58. E. Heckel and R.J. Hanrahan, "Ion-Molecule Reactions in the System CF_4-CH_4 and CF_4-C_2H_6", J. Chem. Phys., 62, 1027 (1975).

59. M.B. Fallgatter and Hanrahan, "SPC-12 Mass Spectrometer Routines: Real Time Data Acquisition and Data Reduction for Bendix Mass Spectrometrs", Available from COSMIC Library, Univ. of Georgia, No. COS-02260 (1970).

60. J.M.S. Henis, "Ion Cyclotron Resonance Spectrometry", in "Ion-Molecule Reactions", Ed. J.L. Franklin, Plenum Press, New York, 1972, p. 395.

61. H. Hartmann,"Ion Cyclotron Resonance Spectroscopy", Topics Curr. Chem., 43, 57 (1973).

62. T.J. Buckley, Ph.D. Dissertation Development and Application of a Microcomputer Based Data Acquisition System for an Ion Cyclotron Resonance Mass Spectrometer, University of Florida, 1982.

63. K.P. Wanczek, "Dynamic Mass Spectrometery", Eds. D. Price and J.F.J. Todd, vol. 6, chapter 2, Heyeden, Philadelphia, 1981.

64. J. L. Beauchamp, "Ion Cyclotron Resonance Spectroscopy", Ann. Rev. Phys. Chem., 22, 527 (1971).

65. R.T. McIver, "A Solid State Marginal Oscillator for Pulsed Ion Cyclotron Resonance Spectroscopy", Rev. Sci. Instrement, 44,1071 (1973).

66. T. E. Sharp, J.R. Eyler, and E.Li, "Traped-Ion Motion in Ion Cyclotron Resonance Spectroscopy", Int. J. Mass Spectrom. and Ion Phys., 9, 421 (1972).

67. R.J. McIver, Fr. and R.C. Dunbar, "Pulse Ion Cyclotron Double Resonance for the Study of Ion-Molecule Reactions", Int. J. Mass Spectom. and Ion Phys., 7, 471 (1971).

68. C.C. Goode, A.J. Ferrer-Correia and K.R. Jenning, "The Interpretation of Double Resonance Signals in Ion Cyclotron Resonance Mass Spectrometry", Int. J. Mass Spectrom. Ion Phys, 5, 229 (1970).

69. Barocal Model 1023 Electronic Manometer with Model 523H-15 Pressure Head and 525 Thermal Base, CGS Datametrics, Watertown, Ma.

70. A.H. Young and J.E. Willard, "Radiolytic and Photo Chemical Decomposition and Exchange in Liquid and Gaseous CCl3Br", J. Phys. Chem., 66, 271 (1962).

71. W. West and L. Schlessinger, "The Mechanism of the Photodecomposition of Methyl and Ethyl Iodides", J. Am. Chem. Soc., 60, 961 (1938).

72. S. W. Benson, "The Foundations of Chemical Kinetics", p. 399. McGraw-Hill Book Company, New York, 1960.

73. Bonhoeffer and Farcas, Z. Physik. Chem., 132, 235 (1928).

74. J. R. Bates and R. Spence, "The Oxidation of Free Alkyl Groups. Photoxidation of Gaseous Methyl Iodide", J. AM. Chem. Soc., 53, 1689 (1931).

75. G. J. Maines and D. Lewis, "The Flash Photolysis of Methyl Iodide", J. Phys. Chem., 74, 1694 (1970).

76. G. Schmitt and F. J. Comer, "Photolysis of CH_2I_2 and 1,1-$C_2H_4I_2$ at 300 nm", J. of Photochemistry, 14, 107 (1980).

77. L.H. Gevantman and R.R. Williams, Jr., "Detection and Identification of Free Radicals in the Radiolysis of Alkanes and Alkyl Iodides", J. Phys. Chem., 56, 569 (1952).

78. P. T. McTigue and A. S. Buchanan, "The Photolysis of Methyl Iodide in the Presence of Metals", Trans. Faraday Soc., 55, 1153 (1959).

79. T. Iredale and E. R. McCartney, "The Quantum Yield in the Photo-Reaction between Methyl Iodide and Nitric Oxide", J. AM. Chem. Soc., 68, 144 (1946).

80. G.S. Laurence, "Thermal and Photochemical Exchange of Ioding with Trifluonsmethyl Iodide", Trans. Faraday Soc., 63, 1155 (1967).

81. J.C. Amphlett and E. Whittle, "Reactions of Trifluoromethyl Radicals with Iodine and Hydrogen Iodide", Trans. Faraday Soc., 63, 2695 (1967).

82. A.A. Filyukov, V.B. Mitrofanov and Mishchenko, Khim. Vys. Energ., 10, 35 (1976).

83. R.C. Petry and R.H. Schuler, "The Radiolysis of Liquid Methyl Iodide", J. Am. Chem. Soc., 75, 3796 (1953).

84. H.A. Gillis, R.R. Williams, Jr., and W.H. Hamil, "Ionic and Free Radical Processes in the Radiolysis of Liquid Methyl and Ethyl Iodides", J. Am. Chem. Soc., 83, 17 (1961).

85. D.D.Davis, J.F. Schmidt, C.M. Neeley and R.J. Hanrahan, "Effects of Wavelength in the Gas Phase Photolysis of Carbon Tetrachloride", J. Phys. Chem., 79, 11 (1975).

86 B. deB. Darwent "Bond Dissociation Energies in Simple Molecules", National Bureau of Standard, NSRDS-NBS 31 p. 33 (1970).

87. E.W.R. Steacie, "Atomic and Free Radical Reactions," 2nd Ed., ACS Monograph #125, Reinhold, New York, 1954.

88. W.G. Alcock and Whittle, "Reactions of Trifluoromethyl Radicals with Organic Halides", Trans. Faraday Soc., 61, 244 (1965).

89. B.D. Neely and H. Carmichael, "Kinetic Isotope Effects in the Dehydrofluorination of Chemically Activated 1,1,1- Trifluoroethane,"J. Phys. Chem., 73, 307 (1973).

90. M. D. Scanlon and R. J. Hanrahan, "The Radiation Chemistry of Mixtures of Ethane and Hexafluoroethane in the Gas Phase", Radiat. Phys. Chem., 17, 87 (1981).

91. C. L. Kibby and R. E. Weston, "Differences in the Reactivities of Trifluoromethyl and Methyl Radicals by Photodissociation", 90, 1085 (1968).

92. M.Vanpee and F. Grad, "La Photolyse du Cetene en Presence de Methane,"Bull. Chem. Soc., 60, 206 (1951).

93. J.A. Bell and G.B. Kistiakowsky, "The Reactions of Methylene. VI. The Addition of Methylene to Hydrogen and Methane," J. Am. Chem. Soc., 84, 3417 (1962).

94. D. Teclemariam, Ms. Thesis, The Radiation Chemistry of Methyl Iodide and Trifluoromethyl Iodide Equimolar Mixtures in Gas Phase, University of Florida, 1978.

95. J.M.S. Henis, M.D. Loberg, and M.J. Welch, "Ion-Molecule Reactions in Methyl Cations and Halide Transfer Reactions", J. Am. Chem. Soc., 96, 1665 (1974).

96. D.W. Berman and J.L. Beauchamp,"Ion Cyclotron Resonance and Photoionization Investigation of the Thermochemistry and Reactions of Ions Derived from CF_3I" Int. J. Mass Spectrom. and Ion Phys., 39, 47 (1981).

97. L.W.Sieck, J.Res of N.B.S. A. Phys. and Chem., 81A, 267, (1977).

98. H.M. Rosenstock, K. Draxal, B.W. Steiner, and J.T. Herron, J. Phys. Chem. Ref., Data Suppl., 1, 6 (1977).

99. C.E. Klots, "VanDer Waals Molecules-Linking the Gas and Liquid Phases", Radiat. Phys. Chem., 20, 51 (1982).

BIOGRAPHICAL SKETCH

Dawit Teclamarian was born in Wasdemba in Senhit province, Eritrea, on January 12, 1951. He finished elementary, middle and high school in Wasdemba, Keren and Asmara (Eritrean capital). He recieved the Bachelor of Science in chemistry from the Faculty of Science, Hailesselase I University in June, 1971. From 1971 to 1973 he taught in a high school in Addis Ababa, the Ethiopian capital. From 1973 to August 1975 he served as a graduate assistant in the Department of Chemistry, Hailesselase I University.

He entered graduate school at the University of Florida in September, 1975, to work toward the Master of Science degree under AID sponsorship and graduated in September, 1978. He later pursued the Ph.D. program holding research assistantships in the Department of Chemistry, University of Florida.

Dawit Teclemariam is married to Mikela Okubai and is the father of two daughters, Eri and Lula and a son, Yobeal.

I certify that I have read this study and that in my opinion it conforms to acceptable standards of scholarly presentation and is fully adequate, in scope and quality, as a dissertation for the degree of Doctor of Philosophy.

Robert J. Hanrahan, Chairman
Professor of Chemistry

I certify that I have read this study and that in my opinion it conforms to acceptable standards of scholarly presentation and is fully adequate, in scope and quality, as a dissertation for the degree of Doctor of Philosophy.

M. Luis Muga
Professor of Chemistry

I certify that I have read this study and that in my opinion it conforms to acceptable standards of scholarly presentation and is fully adequate, in scope and quality, as a dissertation for the degree of Doctor of Philosophy.

Phillip M. Achey

Phillip M. Achey
Professor of Microbiology
and Cell Science

I certify that I have read this study and that in my opinion it conforms to acceptable standards of scholarly presentation and is fully adequate, in scope and quality, as a dissertation for the degree of Doctor of Philosophy.

Willis B. Person

Willis B. Person
Professor of Chemistry

I certify that I have read this study and that in my opinion it conforms to acceptable standards of scholarly presentation and is fully adequate, in scope and quality, as a dissertation for the degree of Doctor of Philosophy.

Williams Weltner, Jr.
Professor of Chemistry

This dissertation was submitted to the Graduate Faculty of the Department of Chemistry in the College of Liberal Arts and Sciences and to the Graduate Council, and was accepted as partial fulfillment of the requirements for the degree of Doctor of Philosopy.

April 1984

Dean for Graduate Studies
and Research